Electronic Supplementary Material (ESI) for Organic & Biomolecular Chemistry.

Supporting Information

Biocatalytic approach to chiral fluoroaromatic scaffolds

Irena Dokli,[a] Zlatko Brkljača,[b] Petra Švaco,[a] Lixia Tang,[c] Višnja Stepanić[a] and Maja Majerić Elenkov[a]

[a] Ruđer Bošković Institute, Bijenička c. 54, Zagreb 10000, Croatia

[b] Selvita Ltd., 10000 Zagreb, Croatia

[c] University of Electronic Science and Technology, No.4, Section 2, North Jianshe Road, Chengdu, China

Contents

Materials

Starting materials, reagents and solvents were purchased from commercial sources and used as received without further purification. 2-(2-(Trifluoromethyl)phenyl)oxirane (**1k**), 2-(3-(trifluoromethyl)phenyl)oxirane (**1l**), 2-(4-(trifluoromethyl)phenyl)oxirane (**1m**) and corresponding azido alcohols (**2k**-**2m, 3k-3m**) were prepared as reported earlier.[1]

General procedure for the synthesis of substrates

Epoxides **1b**–**1e** were prepared according to a literature procedure.[3] Trimethylsulfonium iodide or trimethylsulfoxonium iodide (20 mmol) were dissolved in dry DMSO (15 mL) under argon. Sodium hydride (20 mmol, 60% dispersion in mineral oil) or KO*t*Bu (20 mmol) was added and the mixture was stirred for 20 minutes. Solution of aldehyde or ketone (12 mmol) in DMSO (20 mL) was added dropwise and the reaction mixture was stirred for 2-20 h until completion. Water was added (80 mL) and the mixture was extracted with EtOAc (3 x 100 mL). Combined organic extracts were washed with water (2 x 100 mL) and brine (100 mL), dried over Na_2SO_4, filtered and concentrated under reduced pressure. Crude epoxides were purified by Kugelrohr distillation under reduced pressure (2 mbar, 90 - 140 °C) or silicagel column chromatography (*n*-hexane/EtOAc = 95/5).

2-(2-Fluorophenyl)oxirane (1a)[4]

Prepared according to general procedure and isolated after distillation in 57% yield.

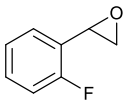

^{1}H NMR (300 MHz, $CDCl_3$) δ 2.79 (dd, J = 5.6, 2.6 Hz, 1H), 3.17 (dd, J = 5.6, 4.1 Hz, 1H), 4.12-4.17 (m, 1H), 7.01-7.08 (m, 1H), 7.09-7.19 (m, 2H), 7.20-7.31 (m, 1H). ^{13}C NMR (75 MHz, $CDCl_3$) δ 47.0 (d, $^3J_{C\text{-}F}$ = 6.3 Hz), 50.5, 115.2 (d, $^2J_{C\text{-}F}$ = 20.9 Hz), 124.3 (d, $^4J_{C\text{-}F}$ = 3.6 Hz), 124.9 (d, $^2J_{C\text{-}F}$ = 12.7 Hz), 125.9 (d, $^3J_{C\text{-}F}$ = 3.8 Hz), 129.4 (d, $^3J_{C\text{-}F}$ = 8.2 Hz), 161.6 (d, $^1J_{C\text{-}F}$ = 246 Hz).

2-(3-Fluorophenyl)oxirane (1b)[5]

Prepared according to general procedure and isolated after distillation in 49% yield.

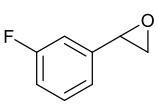

^{1}H NMR (300 MHz, $CDCl_3$) δ 2.76 (dd, J = 5.5, 2.5 Hz, 1H), 3.15 (dd, J = 5.5, 4.1 Hz, 1H), 3.86 (dd, J = 4.1, 2.5 Hz, 1H), 6.93-7.04 (m, 2H), 7.05-7.11 (m, 1H), 7.26-7.36 (m, 1H). ^{13}C NMR (75 MHz, $CDCl_3$) δ 51.3, 51.8 (d, $^4J_{C\text{-}F}$= 2.2 Hz), 112.2 (d, $^2J_{C\text{-}F}$ = 22.6 Hz), 115.1 (d, $^2J_{C\text{-}F}$ = 21.2 Hz), 121.3 (d, $^4J_{C\text{-}F}$ = 2.9 Hz), 130.1 (d, $^3J_{C\text{-}F}$ = 8.3 Hz), 140.4 (d, $^3J_{C\text{-}F}$ = 7.5 Hz), 163.1 (d, $^1J_{C\text{-}F}$ = 246 Hz).

2-(2-Fluorophenyl)-2-methyloxirane (1d)[6]

Prepared according to general procedure and isolated after distillation in 58% yield.

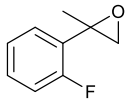

^{1}H NMR (600 MHz, $CDCl_3$) δ 1.68 (s, 1H), 2.82 (d, J = 5.3 Hz, 1H), 2.96 (d, J = 5.3 Hz, 1H), 7.03 (ddd, J = 10.5, 8.2, 1.2 Hz, 1H), 7.12 (td, J = 7.5, 1.1 Hz, 1H), 7.24-7.29 (m, 1H), 7.41 (td, J = 7.5, 1.8 Hz, 1H). ^{13}C NMR (151 MHz, $CDCl_3$) δ 23.1 (d, $^4J_{C\text{-}F}$ = 2.6 Hz), 54.9, 55.3, 115.3 (d, $^2J_{C\text{-}F}$ = 21.2 Hz), 124.1 (d, $^4J_{C\text{-}F}$ = 3.4 Hz), 127.8 (d, $^3J_{C\text{-}F}$ = 4.3 Hz), 128.7 (d, $^2J_{C\text{-}F}$ = 14.5 Hz), 129.3 (d, $^3J_{C\text{-}F}$ = 7.9 Hz), 160.4 (d, $^1J_{C\text{-}F}$ = 247 Hz).

2-(3-Fluorophenyl)-2-methyloxirane (1e)

Prepared according to general procedure and isolated after distillation in 76% yield.

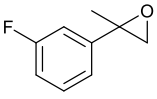

^{1}H NMR (300 MHz, $CDCl_3$) δ 1.71 (d, J = 0.8 Hz, 3H), 2.77 (dd, J = 5.4, 0.8 Hz, 1H), 2.98 (d, J = 5.4 Hz, 1H), 6.96 (tdd, J = 8.3, 2.6, 1.0 Hz, 1H), 7.06 (ddd, J = 10.1, 2.6, 1.7 Hz, 1H), 7.14 (ddd, J = 7.8, 1.6, 1.0 Hz, 1H), 7.30 (td, J = 7.9, 5.8 Hz, 1H). ^{13}C NMR (75 MHz, $CDCl_3$) δ 21.5, 56.3 (d, $^4J_{C\text{-}F}$ = 2.2 Hz), 57.1, 112.4 (d, $^2J_{C\text{-}F}$ = 22.6 Hz), 114.4 (d, $^2J_{C\text{-}F}$ = 21.1 Hz), 121.0 (d, $^4J_{C\text{-}F}$ = 3.0 Hz), 129.9 (d, $^3J_{C\text{-}F}$ = 8.3 Hz), 144.0 (d, $^3J_{C\text{-}F}$ J = 7.2 Hz), 163.0 (d, $^1J_{C\text{-}F}$ = 245 Hz). ^{19}F NMR (282 MHz, $CDCl_3$) δ -111.4 (m, 1F). HRMS (MALDI) *m/z*, ([M]$^-$): calcd. for C_9H_9FO: 153.0637, found: 153.0634.

2-(4-Fluorophenyl)-2-methyloxirane (1f)[7]

Prepared according to general procedure and isolated after distillation in 70% yield.

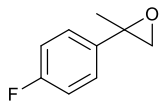

^{1}H NMR (300 MHz, $CDCl_3$) δ 1.70 (d, J = 0.8 Hz, 3H), 2.76 (dd, J = 5.4, 0.8 Hz, 1H), 2.96 (d, J = 5.4 Hz, 1H), 6.94-7.08 (m, 2H), 7.26-7.39 (m, 2H). ^{13}C NMR (75 MHz, $CDCl_3$) δ 21.9, 56.4, 57.0, 115.2 (d, $^2J_{C\text{-}F}$ = 21.7 Hz), 127.1 (d, $^3J_{C\text{-}F}$ = 8.2 Hz), 137.0 (d, $^4J_{C\text{-}F}$ = 3.2 Hz), 162.2 (d, $^1J_{C\text{-}F}$ = 246 Hz).

2-(2,6-Difluorophenyl)oxirane (1g)[8]

Prepared according to general procedure and isolated after distillation in 32%.

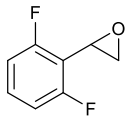

^{1}H NMR (300 MHz, $CDCl_3$) δ 3.12-3.17 (m, 1H), 3.31 (dd, J = 5.4, 2.8 Hz, 1H), 4.04 (dd, J = 4.3, 2.8 Hz, 1H), 6.83-6.94 (m, 2H), 7.18-7.37 (m, 1H). ^{13}C NMR (75 MHz, $CDCl_3$) δ 44.7 (t, $^4J_{C\text{-}F}$ = 3.6 Hz), 47.2 (t, $^3J_{C\text{-}F}$ = 4.0 Hz), 111.3–112.1 (m), 113.0 (t, $^2J_{C\text{-}F}$ = 16.3 Hz), 130.1 (t, $^3J_{C\text{-}F}$ = 10.6 Hz), 162.1 (dd, $^1J_{C\text{-}F}$ = 251 Hz, $^3J_{C\text{-}F}$ = 7.5 Hz).

2-(2,4-Difluorophenyl)oxirane (1h)

Prepared according to general procedure and isolated after distillation in 53% yield.

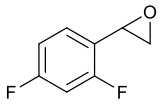

^{1}H NMR (300 MHz, $CDCl_3$) δ 2.77 (dd, J = 5.5, 2.6 Hz, 1H), 3.16 (dd, J = 5.5, 4.0 Hz, 1H), 4.07-4.11 (m, 1H), 6.77-6.90 (m, 2H), 7.15 (td, J = 8.4, 6.3 Hz, 1H). ^{13}C NMR (151 MHz, $CDCl_3$) δ 46.7 (d, $^3J_{C\text{-}F}$ = 5.5 Hz), 50.3, 103.7 (t, $^2J_{C\text{-}F}$ = 25.1 Hz), 111.6 (dd, $^2J_{C\text{-}F}$ = 21.5 Hz, $^4J_{C\text{-}F}$ = 3.7 Hz), 120.9 (dd, $^2J_{C\text{-}F}$ = 13.2 Hz, $^4J_{C\text{-}F}$ = 3.8 Hz), 126.9 (dd, $^3J_{C\text{-}F}$ = 9.8 Hz, $^3J_{C\text{-}F}$ = 5.4 Hz), 161.6 (dd, $^1J_{C\text{-}F}$ = 250 Hz, $^3J_{C\text{-}F}$ = 12.0 Hz), 162.5 (dd, $^1J_{C\text{-}F}$ = 249 Hz, $^3J_{C\text{-}F}$ = 11.9 Hz). ^{19}F NMR (282 MHz, $CDCl_3$) δ -108.8 (m, 1F), -115.5 (m, 1F). HRMS (MALDI) *m/z*, ([M]$^-$): calcd. for $C_8H_6F_2O$: 156.0387, found: 156.0389.

2-(3,4-Difluorophenyl)oxirane (1i)

Prepared according to general procedure and isolated after distillation in 54% yield.

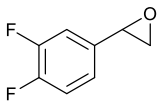

^{1}H NMR (600 MHz, $CDCl_3$) δ 2.73 (dd, J = 5.4, 2.5 Hz, 1H), 3.14 (dd, J = 5.4, 4.0 Hz, 1H), 3.80-3.88 (m, 1H), 6.99-7.11 (m, 2H), 7.14 (dt, J = 10.0, 8.2 Hz, 1H). ^{13}C NMR (151 MHz, $CDCl_3$) δ 51.3, 51.4 (d, $^4J_{C\text{-}F}$ = 1.7 Hz), 114.3 (d, $^2J_{C\text{-}F}$ = 18.2 Hz), 117.4 (d, $^2J_{C\text{-}F}$ = 17.5 Hz), 121.7 (dd, $^3J_{C\text{-}F}$ = 6.5 Hz, $^4J_{C\text{-}F}$ =3.8 Hz), 134.8 (dd, $^3J_{C\text{-}F}$ = 5.7 Hz, $^4J_{C\text{-}F}$ = 3.5 Hz), 150.2 (dd, $^1J_{C\text{-}F}$ = 248 Hz, $^2J_{C\text{-}F}$ = 12.7 Hz), 150.6 (dd, $^1J_{C\text{-}F}$ = 248 Hz, $^2J_{C\text{-}F}$ 12.9 Hz). ^{19}F NMR (282 MHz, $CDCl_3$) δ -135.7 (m, 1F), -136.8 (m, 1F). HRMS (MALDI) *m/z*, ([M]$^-$): calcd. for $C_8H_6F_2O$: 156.0387, found: 156.0382.

2-(2,4,5-Trifluorophenyl)oxirane (1j)

Prepared according to general procedure and isolated after silicagel column chromatography in 33% yield.

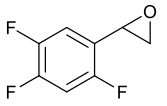

^{1}H NMR (600 MHz, $CDCl_3$) δ 2.72 (dd, J = 5.5, 2.5 Hz, 1H), 3.18 (dd, J = 5.5, 4.0 Hz, 1H), 4.07–4.10 (m, 1H), 6.94 (td, J = 9.7, 6.4 Hz, 1H), 6.99 (ddd, J = 10.5, 8.7, 6.6 Hz, 1H). ^{13}C NMR (151 MHz, $CDCl_3$) δ 46.3 (d, $^3J_{C\text{-}F}$ = 5.0 Hz), 50.6, 105.5 (dd, $^2J_{C\text{-}F}$ = 27.6 Hz, $^2J_{C\text{-}F}$ = 20.9 Hz), 113.8 (dd, $^2J_{C\text{-}F}$ = 20.9 Hz, $^3J_{C\text{-}F}$ = 5.3 Hz), 121.7-121.8 (m), 147.3 (ddd, $J_{C\text{-}F}$ = 249, 12.6, 3.5 Hz), 149.6 (ddd, $J_{C\text{-}F}$ = 252, 15.0, 12.2 Hz), 156.3 (ddd, $J_{C\text{-}F}$ = 246, 8.8, 2.0 Hz). ^{19}F NMR (282 MHz, $CDCl_3$) δ -121.2 (m, 1F), -132.3 (m, 1F), -140.4 (m, 1F). HRMS (MALDI) *m/z*, ([M]$^-$): calcd. for $C_8H_5F_3O$: 174.0292, found: 174.0290.

General procedure for the synthesis of racemic azido alcohols

Racemic alcohols **2a**-**2e** and **3a**-**3e** were synthetized by NH_4Cl-mediated ring-opening of the corresponding epoxides with NaN_3 following a procedure given in the literature.[9]

*General procedure for the synthesis of racemic azido alcohols **2a-2e** and **3a-3e**.* To a solution of epoxide **1a**-**1e** (1 mmol) in methanol (15 mL), ammonium chloride (3 mmol) and sodium azide (3 mmol) were added. Reaction mixture was stirred 3-16 h at 65 °C. Mixture was diluted with ethyl acetate (10 mL), water was added (10 mL), and the mixture was extracted with

ethyl acetate (3 x 10 mL). Combined organic extracts were dried over Na_2SO_4, filtered and concentrated under reduced pressure. A mixture of regioisomers **2/3** were obtained. Column chromatography (SiO_2; hexane/EtOAc, 9 : 1) furnished the pure azido alcohols.

2-Azido-1-(2-fluoro-phenyl)-ethanol (2a)[10]

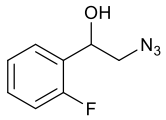

^{1}H NMR (300 MHz, $CDCl_3$) δ 2.45 (d, J = 4.0 Hz, 1H), 3.46 (dd, J = 12.5, 7.7 Hz, 1H), 3.54 (dd, J = 12.4, 3.5 Hz, 1H), 5.17-5.22 (m, 1H), 7.01-7.07 (m, 1H), 7.19 (td, J = 7.4, 0.7 Hz, 1H), 7.26-7.34 (m, 1H), 7.53 (td, J = 7.6, 1.3 Hz, 1H). ^{13}C NMR (151 MHz, $CDCl_3$) δ 56.8, 67.6, 115.4 (d, $^2J_{C\text{-}F}$ = 21.5 Hz), 124.5 (d, $^4J_{C\text{-}F}$ = 3.6 Hz), 127.4 (d, $^3J_{C\text{-}F}$ = 3.8 Hz), 127.5, 129.7 (d, $^3J_{C\text{-}F}$ = 8.2 Hz), 159.5 (d, $^1J_{C\text{-}F}$ = 246 Hz).

2-Azido-2-(2-(fluoro)phenyl)ethanol (3a)[10]

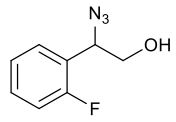

^{1}H NMR (300 MHz, $CDCl_3$) δ 2.04 (s, 1H), 3.72-3.85 (m, 2H), 5.04 (dd, J = 8.0, 4.3 Hz, 1H), 7.07-7.13 (m, 1H), 7.17-7.21 (m, 1H), 7.30-7.35 (m, 1H), 7.41 (td, J = 7.4, 1.3 Hz, 1H). ^{13}C NMR (151 MHz, $CDCl_3$) δ 61.3 65.3, 115.8 (d, $^2J_{C\text{-}F}$ = 21.6 Hz), 123.5 (d, $^2J_{C\text{-}F}$ = 13.9 Hz), 124.6 (d, $^3J_{C\text{-}F}$ = 3.7 Hz), 128.4 (d, $^4J_{C\text{-}F}$ = 3.4 Hz), 130.2 (d, $^3J_{C\text{-}F}$ = 8.3 Hz), 160.1 (d, $^1J_{C\text{-}F}$ = 247 Hz).

2-Azido-1-(3-fluoro-phenyl)-ethanol (2b)[10]

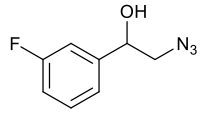

^{1}H NMR (600 MHz, $CDCl_3$) δ 2.49 (d, J = 3.5 Hz, 1H), 3.45 (d, J = 6.0 Hz, 2H), 4.84-4.89 (m, 1H), 6.97-7.04 (m, 1H), 7.09-7.14 (m, 2H), 7.33 (td, J = 7.9, 5.8 Hz, 1H). ^{13}C NMR (151 MHz, $CDCl_3$) δ 57.9, 72.8 (d, $^4J_{C\text{-}F}$ = 1.7 Hz), 112.9 (d, $^2J_{C\text{-}F}$ = 22 Hz), 115.2 (d, $^2J_{C\text{-}F}$ = 21 Hz), 121.5 (d, $^4J_{C\text{-}F}$ = 2.8 Hz), 130.3 (d, $^3J_{C\text{-}F}$ = 8.2 Hz), 143.1 (d, $^3J_{C\text{-}F}$ = 6.9 Hz), 163.5 (d, $^1J_{C\text{-}F}$ = 247 Hz).

2-Azido-2-(3-(fluoro)phenyl)ethanol (3b)[10]

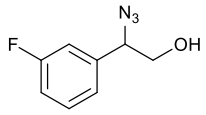

^{1}H NMR (600 MHz, $CDCl_3$) δ 1.71 (dd, J = 7.3, 5.5 Hz, 1H), 3.32 (ddd, J = 11.7, 8.3, 5.5 Hz, 1H), 3.36 (ddd, J = 11.7, 7.7, 4.5 Hz, 1H), 4.27 (dd, J = 7.9, 4.3 Hz, 1H), 6.64-6.67 (m, 2H), 3.72 (d, J = 7-7 Hz, 1H), 6.97 (td, J = 7.9, 5.8 Hz, 1H). ^{13}C NMR (151 MHz, $CDCl_3$) δ 65.9, 66.7, 113.7 (d, $^2J_{C\text{-}F}$ = 23 Hz), 115.2 (d, $^2J_{C\text{-}F}$ = 21 Hz), 122.3 (d, $^4J_{C\text{-}F}$ = 3.7 Hz), 130.0 (d, $^3J_{C\text{-}F}$ = 7.7 Hz), 138.3 (d, $^3J_{C\text{-}F}$ = 5.8 Hz), 162.4 (d, $^1J_{C\text{-}F}$ = 247 Hz).

2-Azido-1-(4-fluorophenyl)ethanol (2c)[11]

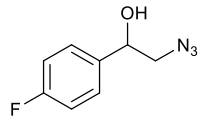

^{1}H NMR (600 MHz, $CDCl_3$) δ 2.47 (d, J = 3.3 Hz, 1H), 3.42 (dd, J = 12.6, 4.2 Hz, 1H), 3.44 (dd, J = 12.6, 7.9 Hz, 1H), 4.84-4.86 (m, 1H), 7.06 (t, J = 8.5 Hz, 2H), 7.34 (dd, J = 8.5, 5.3 Hz, 2H). ^{13}C NMR (151 MHz, $CDCl_3$) δ 58.1, 72.7, 115.6 (d, $^2J_{C\text{-}F}$ = 22 Hz), 127.6 (d, $^3J_{C\text{-}F}$ = 7.6 Hz), 136.3 (d, $^4J_{C\text{-}F}$ = 2.3 Hz), 162.6 (d, $^1J_{C\text{-}F}$ = 247 Hz).

2-Azido-2-(4-(fluoro)phenyl)ethanol (3c) [6,12]

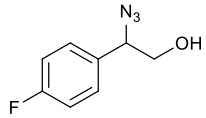

^{1}H NMR (600 MHz, $CDCl_3$) δ 2.09 (t, J = 6.2 Hz, 1H), 3.69-3.75 (m, 2H), 4.65 (dd, J = 7.6, 5.3 Hz, 1H), 7.08 (t, J = 8.5 Hz, 2H), 7.31 (dd, J = 5.3 Hz, 2H). ^{13}C NMR (151 MHz, $CDCl_3$) δ 66.4, 67.1, 115.9 (d, $^2J_{C\text{-}F}$ = 20.7 Hz), 128.9 (d, $^3J_{C\text{-}F}$ = 7.5 Hz), 132.1 (d, $^4J_{C\text{-}F}$ = 3.3 Hz), 162.8 (d, $^1J_{C\text{-}F}$ = 248 Hz).

1-Azido-2-(2-fluorophenyl)propan-2-ol (2d)

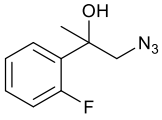

^{1}H NMR (300 MHz, $CDCl_3$) δ 1.62 (d, J = 1.0 Hz, 3H), 2.55 (d, J = 1.5 Hz, 1H), 3.59 (dd, J = 12.3, 0.6 Hz, 1H), 3.82 (d, J = 12.3 Hz, 1H), 7.03 (ddd, J = 12.2, 8.1, 1.2 Hz, 1H), 7.18 (td, J = 7.6, 1.3 Hz, 1H), 7.25-7.33 (m, 1H), 7.63 (td, J = 8.0, 1.8 Hz, 1H). ^{13}C NMR (75 MHz, $CDCl_3$) δ 25.9 (d, $^4J_{C\text{-}F}$ = 3.8 Hz), 60.4 (d, $^4J_{C\text{-}F}$ = 5.1 Hz), 73.7 (d, $^3J_{C\text{-}F}$ = 4.2 Hz), 116.0 (d, $^2J_{C\text{-}F}$ = 23.8 Hz), 124.4 (d, $^4J_{C\text{-}F}$ = 3.2 Hz), 127.6 (d, $^3J_{C\text{-}F}$ = 4.2 Hz), 129.5 (d, $^3J_{C\text{-}F}$ = 8.9 Hz), 131.2 (d, $^2J_{C\text{-}F}$ = 12.3 Hz), 159.3 (d, $^1J_{C\text{-}F}$ = 245 Hz).

^{19}F NMR (282 MHz, $CDCl_3$) δ -111.9 (s, 1F). HRMS (MALDI) *m/z*, ($[M]^+$): calcd. for $C_9H_{10}FN_3O$: 195.0808, found: 195.0810.

1-Azido-2-(3-fluorophenyl)propan-2-ol (2e)[13]

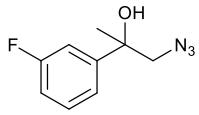

^{1}H NMR (600 MHz, $CDCl_3$) δ 1.57 (s, 3H), 2.37 (s, 1H), 3.45 (d, *J* =12.5 Hz, 1H), 3.58 (d, *J* = 12.2 Hz, 1H), 6.98 (tdd, *J* = 8.2, 3.4, 0.9 Hz, 1H), 7.18-7.21 (m, 2H), 7.34 (td, *J*= 8.0, 5.7 Hz, 1H). ^{13}C NMR (151 MHz, $CDCl_3$) δ 27.1, 61.9, 74.3, 112.3 (d, $^2J_{C\text{-}F}$ = 22.8 Hz), 114.4 (d, $^2J_{C\text{-}F}$ = 20.6 Hz), 120.4 (d, $^4J_{C\text{-}F}$ = 2.2 Hz), 130.0 (d, $^3J_{C\text{-}F}$ = 7.3 Hz), 147.4 (d, $^3J_{C\text{-}F}$ = 6.3 Hz), 162.3 (d, $^1J_{C\text{-}F}$ = 248 Hz).

2-Azido-2-(3-fluorophenyl)propan-1-ol (3e)

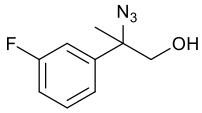

^{1}H NMR (600 MHz, $CDCl_3$) δ 1.72 (s, 3H), 1.81 (dd, *J* = 7.3, 5.8 Hz, 1H), 3.64 (dd, *J* = 11.3, 7.3 Hz, 1H), 3.71 (dd, *J* = 11.6, 6.0 Hz, 1H), 7.02 (tdd, *J* = 8.3, 2.6, 1.0 Hz, 1H), 7.15-7.17 (m, 1H), 7.20-7.22 (m, 1H), 7.37 (td, *J* = 7.9, 5.9 Hz, 1H). ^{13}C NMR (151 MHz, $CDCl_3$) δ 21.4, 67.4, 70.5, 113.4 (d, $^2J_{C\text{-}F}$ = 23 Hz), 114.9 (d, $^2J_{C\text{-}F}$ = 20.5 Hz), 121.5 (d, $^4J_{C\text{-}F}$ = 2.4 Hz), 130.2 (d, $^4J_{C\text{-}F}$ = 8.5 Hz), 143.5 (d, $^3J_{C\text{-}F}$ = 6.9 Hz), 162.9 (d, $^1J_{C\text{-}F}$ = 246 Hz). ^{19}F NMR (282 MHz, $CDCl_3$) δ -110.2 (m, 1F). HRMS (MALDI) *m/z*, ($[M]^+$): calcd. for $C_9H_{10}FN_3O$: 195.0808, found: 195.0810.

1-Azido-2-(4-fluorophenyl)propan-2-ol (2f)[9]

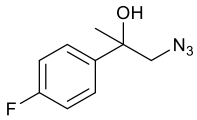

^{1}H NMR (600 MHz, $CDCl_3$) δ 1.56 (s, 3H), 2.28 (s, 1H), 3.43 (d, *J* = 12.0 Hz, 1H), 3.56 (d, *J* = 12.3 Hz, 1H), 7.03-7.06 (m, 2H), 7.40-7.44 (m, 2H). ^{13}C NMR (151 MHz, $CDCl_3$) δ 26.7, 61.6, 73.7, 114.7 (d, $^2J_{C\text{-}F}$ = 21 Hz), 126.2 (d, $^3J_{C\text{-}F}$ = 7.5 Hz), 139.9 (d, $^4J_{C\text{-}F}$ = 3.2 Hz), 161.6 (d, $^1J_{C\text{-}F}$ = 247 Hz).

2-Azido-2-(3-fluorophenyl)propan-1-ol (3f)

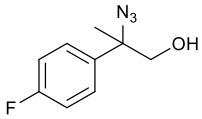

^{1}H NMR (600 MHz, $CDCl_3$) δ 1.72 (s, 3H), 1.82 (dd, *J* = 7.5, 6.2 Hz, 1H), 3.61 (dd, *J* = 11.3, 7.5 Hz, 1H), 3.69 (dd, *J* = 11.5, 5.7 Hz, 1H), 7.05-7.09 (m, 2H), 7.39-7.43 (m, 2H). ^{13}C NMR (151 MHz, $CDCl_3$) δ 21.5, 67.3, 70.6, 115.6 (d, $^2J_{C\text{-}F}$ = 21.8 Hz), 127.8 (d, $^3J_{C\text{-}F}$ = 8.1 Hz), 136.6 (d, $^4J_{C\text{-}F}$ = 3.3 Hz), 162.3 (d, $^1J_{C\text{-}F}$ = 247 Hz). ^{19}F NMR (282 MHz, $CDCl_3$) δ -112.7 (s, 1F). HRMS (MALDI) *m/z*, ($[M]^+$): calcd. for $C_9H_{10}FN_3O$: 195.0808, found: 195.0810.

2-Azido-1-(2,6-difluorophenyl)ethanol (2g)[8]

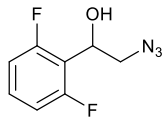

^{1}H NMR (600 MHz, $CDCl_3$) δ 2.57 (dt, *J* = 7.7, 2.2 Hz, 1H), 3.50 (dd, *J* = 12.4, 4.2, 1H), 3.82 (dd, *J* = 12.4, 8.4 Hz, 1H), 5.25 (td, *J* = 7.5, 4.8 Hz, 1H), 6.90-6.94 (m, 2H), 7.29 (tt, *J* = 8.3, 6.3, 1H). ^{13}C NMR (151 MHz, $CDCl_3$) δ 55.7 (t, $^4J_{C\text{-}F}$ =1.8 Hz), 65.8 (t, $^3J_{C\text{-}F}$ = 2.4 Hz), 112.0 (dd, $^2J_{C\text{-}F}$ = 21.9 Hz, $^4J_{C\text{-}F}$ = 4.3 Hz, 2C), 115.9 (t, $^2J_{C\text{-}F}$ = 16.6 Hz), 130.9 (t, $^3J_{C\text{-}F}$ = 10.5 Hz), 161.2 (dd, $^1J_{C\text{-}F}$ = 250 Hz, $^3J_{C\text{-}F}$ = 7.8 Hz, 2C).

2-Azido-2-(2,6-difluorophenyl)ethanol (3g)

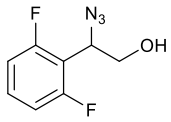

^{1}H NMR (600 MHz, $CDCl_3$) δ 2.03 (dd, *J* = 7.9, 5.0 Hz, 1H), 3.81 (ddd, *J* = 12.0, 7.8, 4.6, 1H), 4.07-4.12 (m, 1H), 5.10 (dd, *J* = 9.0, 4.7 Hz, 1H), 6.92-6.97 (m, 2H), 7.32 (tt, *J* = 8.3, 6.3, 1H). ^{13}C NMR (151 MHz, $CDCl_3$) δ 58.5, 63.7 (t, $^3J_{C\text{-}F}$ = 3.0 Hz), 112.0 (dd, $^2J_{C\text{-}F}$ = 21.9 Hz, $^4J_{C\text{-}F}$ = 4.3 Hz, 2C), 112.1 (t, $^2J_{C\text{-}F}$ = 17.3 Hz), 130.7 (t, $^3J_{C\text{-}F}$ = 10.5 Hz), 161.2 (dd, $^1J_{C\text{-}F}$ = 250 Hz, $^3J_{C\text{-}F}$ = 7.8 Hz, 2C). ^{19}F NMR (282 MHz, $CDCl_3$) δ -112.7 (s, 2F). HRMS (MALDI) *m/z*, ($[M]^+$): calcd. for $C_8H_7F_2N_3O$: 199.0557, found: 199.0550.

2-Azido-1-(2,4-difluorophenyl)ethan-1-ol (2h)[14]

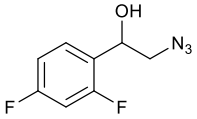

^{1}H NMR (600 MHz, $CDCl_3$) δ 2.36 (d, *J* = 4.0 Hz, 1H), 3.38 (dd, *J* = 12.5, 7.7 Hz, 1H), 3.45 (dd, *J* = 12.5, 3.6 Hz, 1H), 5.07-5.10 (m, 1H), 6.73 (ddd, *J* = 10.8, 8.8, 2.5 Hz, 1H), 6.85 (m, 1H), 7.45 (td, *J* = 8.3, 6.3 Hz, 1H). ^{13}C NMR (151 MHz, $CDCl_3$) δ 55.8, 66.2, 102.8 (t, $^2J_{C\text{-}F}$ = 25.3 Hz), 110.7 (dd, $^2J_{C\text{-}F}$ =

21.2 Hz, $^{4}J_{C\text{-}F}$ = 4.6 Hz), 122.5 (dd, $^{2}J_{C\text{-}F}$ = 12.6 Hz, $^{4}J_{C\text{-}F}$ = 3.4 Hz), 127.5 (dd, $^{3}J_{C\text{-}F}$ = 9.7 Hz, $^{3}J_{C\text{-}F}$ = 5.4 Hz), 158.5 (dd, $^{1}J_{C\text{-}F}$ = 248 Hz, $^{3}J_{C\text{-}F}$ = 12.2 Hz), 161.7 (dd, $^{1}J_{C\text{-}F}$ = 249 Hz, $^{3}J_{C\text{-}F}$ = 12.2 Hz).

2-Azido-2-(2,4-difluorophenyl)ethan-1-ol (3h)

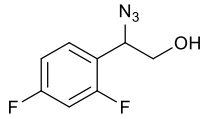

^{1}H NMR (600 MHz, $CDCl_3$) δ 2.04 (dd, J = 7.4, 5.4 Hz, 1H), 3.74 (ddd, *J* = 11.6, 7.7, 5.3 Hz, 1H), 3.81 (ddd, *J* = 11.4, 7.2, 4.1 Hz, 1H), 4.98 (dd, *J* = 7.9, 3.9 Hz), 6.85 (ddd, *J* = 10.3, 8.7, 2.6 Hz), 6.91-6.95 (m, 1H), 7.40 (td, *J* = 8.3, 6.3 Hz, 1H). ^{13}C NMR (151 MHz, $CDCl_3$) δ 60.8, 65.4, 104.2 (t, $^{2}J_{C\text{-}F}$ = 26.3 Hz), 111.9 (dd, $^{2}J_{C\text{-}F}$ = 21.4 Hz, $^{4}J_{C\text{-}F}$ = 3.6 Hz), 119.7 (dd, $^{2}J_{C\text{-}F}$ = 13.9 Hz, $^{4}J_{C\text{-}F}$ = 3.6 Hz), 129.4 (dd, $^{3}J_{C\text{-}F}$ = 9.6 Hz, $^{3}J_{C\text{-}F}$ = 5.1 Hz), 160.2 (dd, $^{1}J_{C\text{-}F}$ = 250 Hz, $^{3}J_{C\text{-}F}$ = 12.5 Hz), 162.9 (dd, $^{1}J_{C\text{-}F}$ = 250 Hz, $^{3}J_{C\text{-}F}$ = 12.5 Hz). ^{19}F NMR (282 MHz, $CDCl_3$) δ -107.5 (m, 1F), -112.4 (m, 1F). HRMS (MALDI) *m/z*, ($[M]^+$): calcd. for $C_8H_7F_2N_3O$: 199.0557, found: 199.0550.

2-Azido-1-(3,4-difluorophenyl)ethan-1-ol (2i)

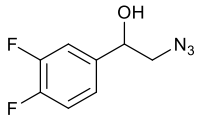

^{1}H NMR (600 MHz, $CDCl_3$) δ 2.49 (bs, 1H), 3.43 (d, *J* = 1.9 Hz, 1H), 3.44 (s, 1H), 4.84 (t, *J* = 5.8 Hz, 1H), 7.07-7.09 (m, 1H), 7.16 (dt, *J* = 10.0, 8.3 Hz, 1H), 7.23 (ddd, *J* = 9.8, 7.7, 2.1 Hz, 1H). ^{13}C NMR (151 MHz, $CDCl_3$) δ 57.9, 72.2, 115.1 (d, $^{2}J_{C\text{-}F}$ = 18.0 Hz), 117.5 (d, $^{2}J_{C\text{-}F}$ = 17.3 Hz), 121.9 (dd, $^{3}J_{C\text{-}F}$ = 6.1 Hz, $^{4}J_{C\text{-}F}$ = 3.5 Hz), 137,5 (t, $^{3}J_{C\text{-}F}$ = 4.2 Hz), 150.1 (dd, $^{1}J_{C\text{-}F}$ = 249 Hz, $^{2}J_{C\text{-}F}$ = 13.7 Hz), 150.3 (dd, $^{1}J_{C\text{-}F}$ = 249 Hz, $^{2}J_{C\text{-}F}$ = 13.0 Hz). ^{19}F NMR (282 MHz, $CDCl_3$) δ -135.0 (m, 1F), -136.6 (m, 1F). HRMS (MALDI) *m/z*, ($[M]^+$): calcd. for $C_8H_7F_2N_3O$: 199.0557, found: 199.0555.

2-Azido-2-(3,4-difluorophenyl)ethan-1-ol (3i)

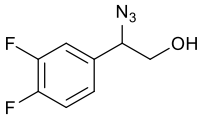

^{1}H NMR (600 MHz, $CDCl_3$) δ 2.10 (t, *J* = 5.7 Hz, 1H), 3.68-3.77 (m, 2H), 4.63 (dd, *J* = 7.7, 4.4 Hz), 7.06-7.09 (m, 1H), 7.17-7.21 (m, 2H). ^{13}C NMR (151 MHz, $CDCl_3$) δ 66.3, 66.6, 116.3 (d, $^{2}J_{C\text{-}F}$ = 18.0 Hz), 117.8 (d, $^{2}J_{C\text{-}F}$ = 17.0 Hz), 123.3 (dd, $^{3}J_{C\text{-}F}$ = 6.3, 4.0 Hz), 133.4 (t, $^{3}J_{C\text{-}F}$ = 4.2 Hz), 150.3 (dd, $^{1}J_{C\text{-}F}$ = 250 Hz, $^{2}J_{C\text{-}F}$ = 12.4 Hz), 150.4 (dd, $^{1}J_{C\text{-}F}$ = 249 Hz, $^{2}J_{C\text{-}F}$ = 12.4 Hz). ^{19}F NMR (282 MHz, $CDCl_3$) δ -134.4 (m, 1F), -135.6 (m, 1F). HRMS (MALDI) *m/z*, ($[M]^+$): calcd. for $C_8H_7F_2N_3O$: 199.0557, found: 199.0560.

2-Azido-1-(2,4,5-trifluorophenyl)ethan-1-ol (2j)

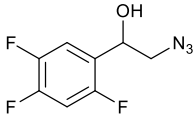

^{1}H NMR (600 MHz, $CDCl_3$) δ 2.47 (d, *J* = 3.8 Hz, 1H), 3.41 (dd, *J* = 12.8, 7.9 Hz, 1H), 3.54 (dd, *J* = 12.5, 3.3 Hz, 1H), 5.13-5.15 (m, 1H), 6.92 (td, *J* = 9.6, 6.1 Hz, 1H), 7.38-7.43 (m, 1H). ^{13}C NMR (151 MHz, $CDCl_3$) δ 56.7, 66.7, 105.5 (dd, $^{2}J_{C\text{-}F}$ = 27.6 Hz, $^{2}J_{C\text{-}F}$ = 21 Hz), 115.7 (dd, $^{2}J_{C\text{-}F}$ = 20.1 Hz, $^{3,4}J_{C\text{-}F}$ = 5.2 Hz), 124.1 (dt, $^{2}J_{C\text{-}F}$ = 15.6 Hz, $^{3}J_{C\text{-}F}$ = 4.2 Hz), 147.1 (ddd, $^{1}J_{C\text{-}F}$ = 246 Hz, $^{2}J_{C\text{-}F}$ = 13.6 Hz, $^{4}J_{C\text{-}F}$ = 3.7 Hz), 149.7 (ddd, $^{1}J_{C\text{-}F}$ = 252 Hz, $^{3}J_{C\text{-}F}$ = 14.1 Hz, $^{4}J_{C\text{-}F}$ = 12.7 Hz), 155.0 (ddd, $^{1}J_{C\text{-}F}$ = 245 Hz, $^{3}J_{C\text{-}F}$ = 9.2 Hz, $^{4}J_{C\text{-}F}$ = 2.6 Hz). ^{19}F NMR (282 MHz, $CDCl_3$) δ -119.0 (s, 1F), -132.1 (m, 1F), -139.9 (s, 1F). HRMS (MALDI) *m/z*, ($[M]^+$): calcd. for $C_8H_6F_3N_3O$: 217.0463, found: 217.0460.

2-Azido-2-(2,4,5-trifluorophenyl)ethan-1-ol (3j)

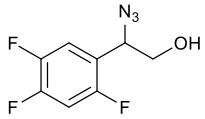

^{1}H NMR (600 MHz, $CDCl_3$) δ 1.99 (bs, 1H), 3.69-3.73 (m, 1H), 3.82-3.85 (m, 1H), 4.96 (dd, *J* = 7.6, 4.1 Hz, 1H), 6.97 (td, *J* = 9.6, 6.4 Hz, 1H), 7.26-7.30 (m, 1H). ^{13}C NMR (151 MHz, $CDCl_3$) δ 60.3, 65.3, 105.9 (dd, $^{2}J_{C\text{-}F}$ = 27.8 Hz, $^{2}J_{C\text{-}F}$ = 21.0 Hz), 116.5 (dd, $^{2}J_{C\text{-}F}$ = 20.6 Hz, $^{3}J_{C\text{-}F}$ = 5.4 Hz), 120.3 (dt, $^{2}J_{C\text{-}F}$ = 15.9 Hz, $^{3,4}J_{C\text{-}F}$ = 4.5 Hz), 147.1 (ddd, $^{1}J_{C\text{-}F}$ = 246 Hz, $^{2}J_{C\text{-}F}$ = 12.4 Hz, $^{4}J_{C\text{-}F}$ = 3.3 Hz), 150.0 (ddd, $^{1}J_{C\text{-}F}$ = 252 Hz, $^{2}J_{C\text{-}F}$ = 14.2 Hz, $^{3}J_{C\text{-}F}$ = 12.3 Hz), 154.2 (ddd, $^{1}J_{C\text{-}F}$ = 244 Hz, $^{2}J_{C\text{-}F}$ = 9.0 Hz, $^{4}J_{C\text{-}F}$ = 2.3 Hz). ^{19}F NMR (282 MHz, $CDCl_3$) δ -118.1 (s, 1F), -130.9 (m, 1F), -139.3 (s, 1F). HRMS (MALDI) *m/z*, ($[M]^+$): calcd. for $C_8H_6F_3N_3O$: 217.0463, found: 217.0465.

Determination of enantiomeric excess and absolute configuration

Determination of enantiomeric excesses (*ee's*) was performed under conditions described in Tables S1 and S2.

Table S1 Chiral GC analysis of substrates.

Compound	Column	Conditions	Retention time / min
1a	CP Chirasil-DEX CB	100 °C, isothermal	5.4 (*R*) / 5.6 (*S*)
1b	CP Chirasil-DEX CB	100 °C, isothermal	6.6 (*R*) / 6.8 (*S*)
1c	Lipodex E	100 °C, isothermal	3.4 (*S*) / 3.9 (*R*)
1d	Lipodex E	100 °C, isothermal	2.4 (*R*) / 2.6 (*S*)
1e	Lipodex E	100 °C, isothermal	3.6 (*R*) / 3.7 (*S*)
1f	beta-DEX 225	100 °C, isothermal	7.3 (*S*) / 7.5 (*R*)
1g	CP Chirasil-DEX CB	100 °C, isothermal	6.2 (*R*) / 6.6 (*S*)
1h	CP Chirasil-DEX CB	100 °C, isothermal	4.8 (*R*) / 5.4 (*S*)
1i	CP Chirasil-DEX CB	100 °C, isothermal	7.2 (*R*) / 7.7 (*S*)
1j	CP Chirasil-DEX CB	100 °C, isothermal	4.5 (*R*) / 5.0 (*S*)
1k	Hydrodex G-DiMOM	100 °C, isothermal	2.9 (*R*) / 3.0 (*S*)
1l	CP Chirasil-DEX CB	100 °C, 1 °C/min to 110 °C	8.3 (*R*) / 8.5 (*S*)
1m	CP Chirasil-DEX CB	120 °C, isothermal	3.9 (*R*) / 4.1 (*S*)

Table S2 Chiral GC/HPLC analysis of products.

Comp.	Method	Column	Conditions	Retention time / min
2a	HPLC	Chiralpak IC-3	0.75% 2-PrOH, 254 nm, 1 ml/min, 30 °C	19.4 (*R*) / 19.9 (*S*)
2b	GC	CP Chirasil-DEX CB	100 °C 10 min, 15 °C/min to 180 °C, 5 min	17.9 (*R*) / 18.0 (*S*)
2c	HPLC	Chiralpak IC-3	1% 2-PrOH, 210 nm, 1 ml/min, 30 °C	17.6 (*R*) / 18.8 (*S*)
2d	GC	CP Chirasil-DEX CB	1% 2-PrOH, 210 nm, 1 ml/min, 30 °C	8.3 (*R*) / 8.9 (*S*)
2e	GC	Lipodex E	100 °C 10 min, 15 °C/min to 180 °C, 5 min	17.3 (*R*) / 17.4 (*S*)
2f	HPLC	Chiralpak AD-3	2% 2-PrOH, 210 nm, 1 ml/min, 30 °C	17.2 (*R*) / 18.2 (*S*)
2g	HPLC	Chiralpak IC-3	1% 2-PrOH, 210 nm, 1 ml/min, 30 °C	20.1 (*R*) / 24.4 (*S*)
2h	GC	CP Chirasil-DEX CB	100 °C 10 min, 15 °C/min to 180 °C, 5 min	17.0 (*R*) / 17.2 (*S*)
2i	GC	CP Chirasil-DEX CB	100 °C 10 min, 15 °C/min to 180 °C, 5 min	18.2 (*R*) / 18.5 (*S*)
2j	GC	CP Chirasil-DEX CB	100 °C 10 min, 15 °C/min to 180 °C, 5 min	17.1 (*S*) / 17.7 (*R*)
1k	HPLC	Chiralpak AD-3	1% 2-PrOH, 220 nm, 1 ml/min, 30 °C	25.4 (*R*) / 28.1 (*S*)
1l	HPLC	Chiralpak IC-3	0.75 % 2-PrOH, 220 nm, 1 mL/min, 25 °C	18.3 (*R*) / 20.4 (*S*)
1m	HPLC	Chiralcel OJ-3	2.5% 2-PrOH, 220 nm, 1 ml/min, 30 °C	13.3 (*R*) / 14.6 (*S*)

Calculation of enantioselectivity, enzymatic conversion and regioselectivity

E values were calculated from ee_p and ee_s according to formula:[16]

$$E = \ln[(1 - ee_s)/(1 + ee_s/ee_p)]/\ln[(1 + ee_s)/(1 + ee_s/ee_p)]$$

Enzymatic (intrinsic) conversions were calculated from ee_p and ee_s according to formula:[17]

$$c = ee_s / (ee_s + ee_p)$$

Regioselectivities were calculated by using formula:

$$\beta\text{-regioselectivity} = \beta / (\alpha + \beta)$$

Intrinsic regioselectivities were calculated using the same formula with substracted values of spontaneous chemical activity.

Biocatalysis with HheC-M4

Table S3 Azidolysis of epoxides **1a**-**1j** catalysed by HheC-M4.[a]

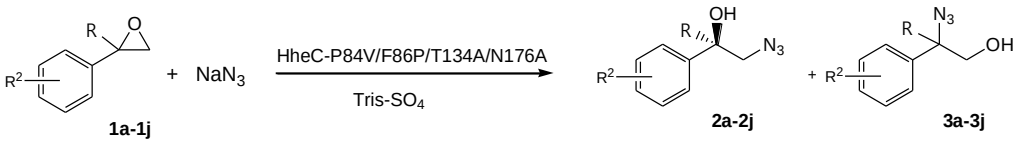

1a-1j **2a-2j** **3a-3j**

Entry	Substrate	t (h)	Conversion (%)	ee **1** (%)[b]	Product **2**	ee **2** (%)[c]	Ratio **2** : **3**	*E*
1	**1a**	1	46	55 (*R*)	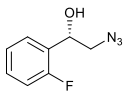	48 (*S*)	87 : 13	5
2	**1b**	1	38	50 (*R*)	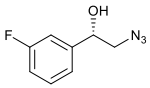	83 (*S*)	95 : 5	18
3	**1c**	1	18	13 (*R*)	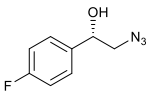	59 (*S*)	68 : 32	4
4	**1d**	1	24	22 (*R*)	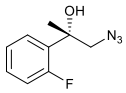	70 (*S*)	98 : 2	7[e]
5	**1e**	1	48	87 (*R*)	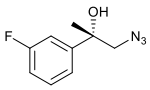	95 (*S*)	100 : 0	111
6	**1f**	1	29	36 (*R*)	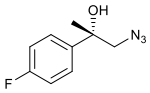	88 (*S*)	75 : 25	22
7	**1g**	1	47	82 (*R*)	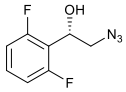	92 (*S*)	92 : 8	61
8	**1h**	1	33	2 (*R*)	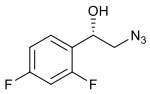	4 (*S*)	93 : 7	1
9	**1i**	1	17	14 (*R*)	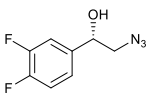	69 (*S*)	94 : 6	6
10	**1j**	1	39	24 (*R*)	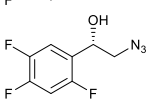	38 (*S*)	92 : 8	3

[a] Reaction conditions: **1a-1j** (2 mM), NaN_3 (3 mM), 250 μL HHDH, Tris-SO_4 buffer (2 mL, 0.5 M, pH 7.0), 5% DMSO, total volume 2.5 mL. [b] determined by GC. [c] determined by GC or HPLC.

Molecular dynamics simulations

All-atom molecular dynamics (MD) simulations of tetramer of P84V/F86P/T134A/N176A mutant of the enzyme HheC (HheC-M4 variant) in aqueous solution were performed by GROMACS 2021.[18] The simulations were prepared and propagated according to previously described protocol for HheC.[19] The X-ray conformation of WT HheC in the complex with (*R*)-*p*-nitrostyrene oxide (*p*-NO_2-SO) downloaded from Protein Data Bank (PDB ID 1ZMT) is used as the starting structure.[18,20] The mutant HheC-M4 was parameterized using AMBER ff14SB force field.[21] The tetramer was immersed in the rectangular box with 80000 water molecules and sodium and chloride ions were added to each simulated system to simultaneously neutralize the net charge of the simulation boxes and to account for ionic strength. Water molecules and salt ions were described by the standard TIP3P water model and via parameters developed by Cheatham III et al. (ion parameters used in AMBER force fields), respectively.[22] The simulation box was minimized using steepest descent algorithm (5000 steps) and subsequently relaxed for 10 ns at T = 298 K (NVT ensemble) with the time step of 2 fs, Berendsen thermostat (time constant for temperature coupling set at 1 ps), with position restraints on all heavy atoms of the protein imposed (500 kJ mol^{-1} nm^{-2}). Furthermore, the system was equilibrated at 298 K (NPT ensemble), with Berendsen thermostat to maintain temperature (time constant for temperature coupling set at 1 ps), Berendsen barostat to maintain constant pressure of 1 bar (time constant for pressure coupling set to 5.0 ps) for 10 ns with the 2 fs time step, and with the weak position restraints on the equivalent set of atoms (100 kJ mol^{-1} nm^{-2}). Finally, production runs were propagated for 500 ns. The production simulation without any restraints was propagated in NPT ensemble, with Nose-Hoover thermostat incorporated to maintain temperature at 298 K (time constant for temperature coupling of 1 ps), whereas Parrinello-Rahman barostat was used to maintain constant pressure of 1 bar (time constant for pressure coupling set to 5.0 ps). Long-range electrostatic interactions beyond a 1.2 nm cutoff were taken into account via the particle mesh Ewald method and periodic boundary conditions in all three directions were used.[23] Using the same conditions, two replicas of M4 variant were propagated for 400 ns with the starting structure corresponding to the conformation extracted at t = 50 ns from primary simulation. The extracted structure was equilibrated using Berendsen barostat in duration of 1 ns, whereby starting velocities of the prepared systems were randomly generated following Boltzmann distribution, constituting different starting points in respective phase spaces. In the subsequent analyses the first 100 ns of all simulations were disregarded. The analyses of root mean square deviation (RMSD), root mean square fluctuation (RMSF), principal component analysis (PCA), contact analysis (hbond) and Jarvis-Patrick clustering were done using GROMACS 2021.[18] The PCA and Jarvis-Patrick clustering were obtained by aggregation of all subunits of the HheC-M4 tetramer extracted each 10 ns (4000 in total), accounting in total for 1μs simulation time. Contact analysis (all contacts and only hydrogen bonds) was performed including heavy atoms of 23 amino acid residues forming binding sites in HheC and HheC-M4 enzymes, and at most 6 Å away from the 1ZMT ligand.

The binding site conformations of the HheC-M4 variant for subsequent molecular docking were determined by performing Jarvis-Patrick clustering on all atoms encapsulated with 5 Å sphere around the 1ZMT substrate placed near the catalytic residues Ser132 and Tyr 145. The Jarvis-Patrick clustering was performed by incorporatin RMSD distance matrix with 20 closest neighbours considered. The 58 clusters were obtained from which the seven most populated clusters, each having more than 5% of all conformations (7 analysed clusters taken together represent 80.4% of the entire set of analysed structures), were considered in molecular docking. The clustering for catalytic site of HheC was performed in analogous manner.

Molecular docking

Molecular docking calculations were performed using software package GOLD.[24] For the HheC (wild-type), the calculations were carried out by exploring the binding site conformation of HheC in the complex with its substrate (*R*)-*p*-NO_2-SO available in the Protein Data Bank (PDB) crystal structure with PDB code 1ZMT.[20] All water molecules were removed. The binding site was defined as all atoms lying within 15 Å radius from the 1ZMT ligand (*R*)-*p*-NO_2-SO. The ChemPLP fitness function was used as a scoring function along with default values of all other program parameters. By using PDB structure 1ZMT,

molecular docking in the substrate binding site of HheC successfully reproduced the experimental binding pose of the substrate (*R*)-*p*-NO_2-SO.[19] The molecular docking for the mutant HheC-M4 was performed using the conformations corresponding to the representative structures of the clusters determined by Jarvis-Patrick clustering (structures closest to the centroids of the respective clusters), populated with more than 5% of all conformations and having the mutual position of the catalytic residues S132 and Y145 close to those in the HheC 1ZMT structure, i.e., arranged in a geometry for the catalysis of the target reaction. This is in accordance with "conformational selection" approach in which it is assumed that a ligand binds selectively to one of these pre-existing conformations of the protein in its unbound state.[25] The binding poses and corresponding binding scores (Table S4) which have been in the best agreement with the observed experimental results, were obtained by using the representative structure of the most populated Jarvis-Patrick cluster (31.3% of the conformation space), that is in the conformation of the catalytic site which is most likely to be adopted by the HheC-M4 enzyme.

The docking was performed by adding the pharmacophore constraint including important hydrogen bond interactions of the catalytic amino acid residues 132 and Y145 with the oxirane oxygen atom of the studied SOs. In such a way, the docking was biased towards poses with interactions essential for the catalysis. Given a compound, binding poses with such hydrogen bond(s) are rewarded. The sphere radius cut-off of 3.5 Å was placed on the oxygen atoms of hydrogen bond donating hydroxyl groups of both S132 and Y145 residues.

The systems were visualized using software packages VMD and PyMOL.[26,27] 2D diagrams of ligand-protein interactions were generated via LigPlot+ v. 2.2.5.[28]

Computational analysis

Overall, the structure of the HheC tetramer as well as its flexibility are largely conserved by introduction of P84V/F86P/T134A/N176A mutations, as demonstrated by comparison of RMSF values between HheC-M4 and HheC tetramers (Figure S1).[19] Secondary elements were retained and structures of the tetrameric subunits (Figure S2), as well as whole tetramers (not shown) were not changed considerably. In comparison with the HheC, amino acid residues most affected by the mutations are the ones found in the vicinity of the mutated residue 134, and also in regions of the protein which have already been noticed as the most flexible regions of HheC.[19]

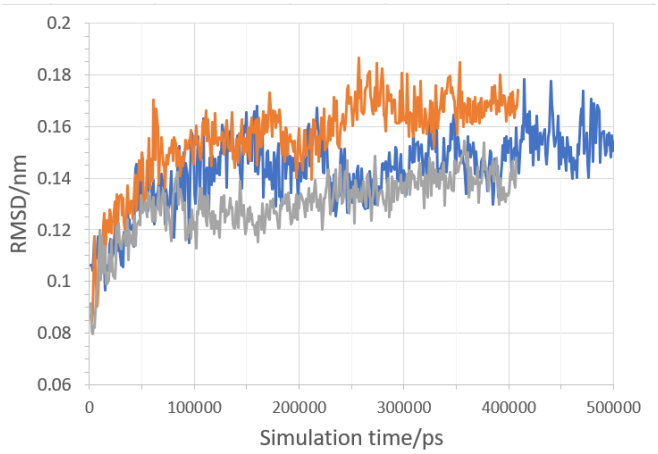

Fig. S1 RMSD for the three MD simulations performed for the tetramer of the mutant variant HheC-M4 (blue - primary simulation, orange - replica 1, grey - replica 2). The RMSD values were calculated considering all atoms. All three MD simulations properly converged. The average RMSD value between two time points from the three trajectories is 1.5 Å. The RMSD values for the HheC tetramer were reported previously.[19]

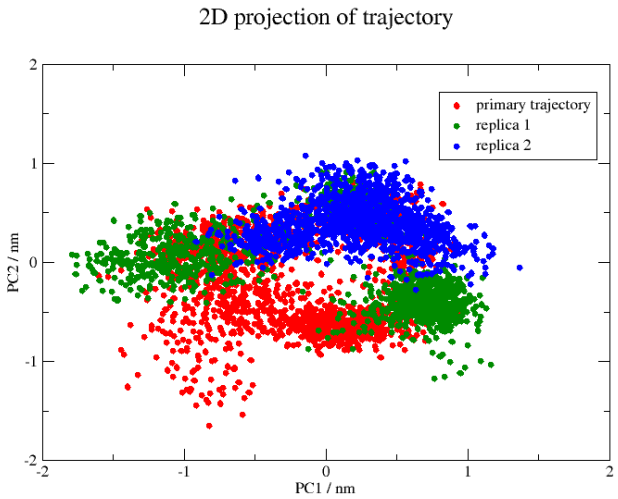

Fig. S2 The PCA plot illustrates the conformational similarity of the subunits of HheC-M4 variant. The PCA plot was calculated with coordinates of Cα atoms of all subunits for the HheC-M4 tetramer in the three simulated systems. The first two common principal components PC1 and PC2 explain 30 % of variance.

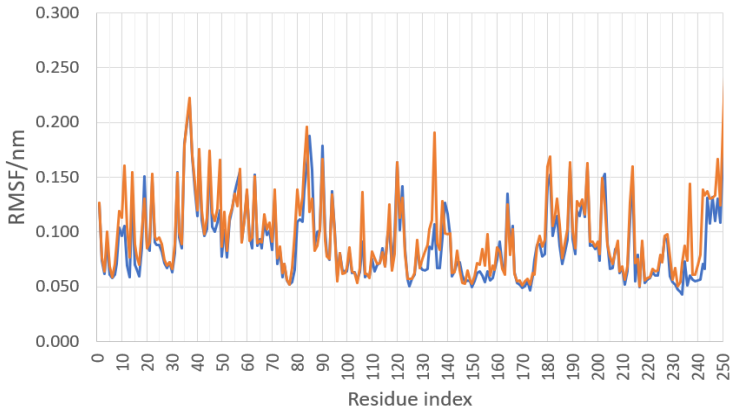

Fig. S3 The residue flexibility is not changed considerably with quadruple mutation P84V/F86P/T134A/N176A in HheC. RMSF values were obtained as the average fluctuation of all atoms of equivalent residues in the four subunits for HheC (blue) and M4 variant (from three simulations, orange) tetramers.

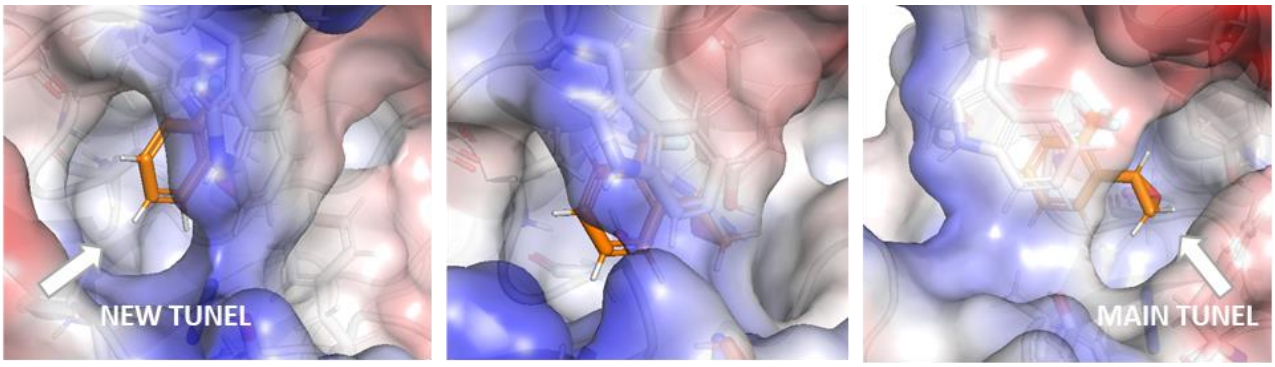

Fig. S4 Three perspectives to binding of (*S*)-**1k** into HheC-4M represented by electrostatic surface (blue positively and red negatively charged parts). The two tunnels lead to the catalytic residues S132 and Y145.

The hydrophobic character of the new pocket enables sterically challenging (*S*)-enantiomers of SOs **1d**, **1e**, **1g** and **1k** to be positioned close to the catalytic S132 and Y145, with terminal Cβ atom nicely oriented towards the nucleophilic binding site which is essential for the S_N2 reaction. Regardless of the substitution pattern, the phenyl ring of these derivatives is placed into the new binding site making the favorable π-π interactions with the residue W139. For comparison, while phenyl ring of associated *R*-enantiomers is predicted to be placed in a similar manner, the orientation of their reactive Cβ atom in such a position is less favorable for the target reaction, which aborts or reduces their catalytic activity.

Table S4 ChemPLP scores for the best predicted binding poses of sterically challenging SOs and 1ZMT ligand *p*-NO_2-SO enantiomers into the most populated catalytic site conformation of HheC-M4. The larger score implies better binding. If a score predicted by GOLD satisfies one and/or two pharmacophore constraints, then a constraint term DE(con) is 10/20.

Compound	Score	DE(con)
(*S*)-*p*-NO_2-SO	67.39	20
(*R*)-*p*-NO_2-SO	63.62	20
(*R*)-**1d**	63.61	20
(*S*)-**1d**	63.01	20
(*R*)-**1g**	57.07	10
(*S*)-**1g**	62.9	20
(*R*)-**1e**	68.09	20
(*S*)-**1e**	70.27	20
(*R*)-**1k**	73.69	20
(*S*)-**1k**	67.8	20

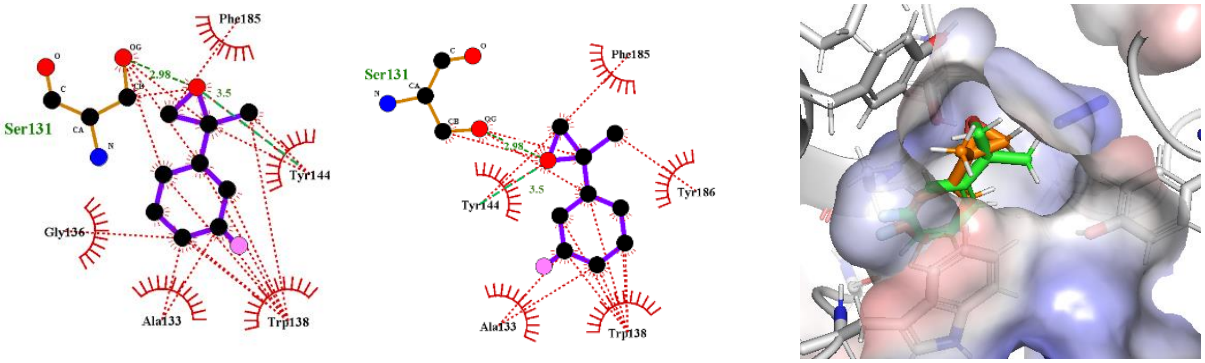

Fig. S5 From left to right: 2D representations of LigPlot favorable interactions of (*S*)-**1e** and (*R*)-**1e** with HheC-M4 (residue number should be increased by one) and their binding within new binding site of HheC-M4.

M4-WT	12PHE	82PHE	83ALA	84PRO	85GLU	86PHE	131THR	132SER	133ALA	134THR	135PRO	139TRP	142LEU	145TYR	149ARG	174GLY	175PRO	176ASN	177TYR	178LEU	185TYR	186PHE	187TYR
12PHE	0	4.43962	0.00647	0.3037	0	0	-1.9932	-3.9884	0.1389	-0.0933	-0.0075	-0.1242	0	0.7422	-3.1406	-0.2599	-6.8895	-1.2054	0.24304	8.8023	-7.218	-12.047	-0.476
82PHE		0	-5.538	52.3583	-4.1922	2.95522	0.35654	0.73254	0.00025	0.00075	0	-0.0343	-1.937	-10.295	3.97462	0	0.20659	0.00349	0	0.00699	7.057	6.0339	0.00624
83ALA			0	-11.907	0.0978	-1.7546	0	0	0	0	0	-0.0072	-0.295	-2.8764	-0.1864	0	0	0	0	0	-6.028	-4.8145	0
84PRO				0	28.715	-48.244	0	0.14951	0.0005	0.036	0	2.18505	17.7332	48.332	0.84878	0	0	0.00025	0	0	-8.8345	6.0821	0.11228
85GLU					0	-7.632	0	0	0	0	0	0.03668	11.5321	4.336	0	0	0	0	0	0	1.21881	0.2984	0
86PHE						0	0	0	0	0	0	-0.0594	52.7306	9.1364	0	0	0	0	0	0	-1.1834	-0.4777	-0.005
131THR							0	0.36	0.86085	2.13534	0.3542	0.12002	0	1.13088	5.343	-6.2726	0.7996	-0.492	0	0.01573	0	-0.2243	0
132SER								0	0.1089	-28.642	-23.385	2.22391	-0.5633	4.6301	10.056	-4.1751	-0.3617	-19.403	0.01504	7.4E-06	-0.0124	-5.2397	-0.2721
133ALA									0	-25.703	-6.1601	7.68157	0.06888	1.13669	1.43359	-1.61	0.9703	-24.827	1.01219	0.00125	0	-0.0289	0.19709
134THR										0	-16.561	-92.078	-30.917	-8.2193	9.6582	1.81893	-2.8678	-48.855	-1.4092	0	-0.0025	-4.5472	-4.098
135PRO											0	0.07948	-10.775	-20.146	-20.483	2.37433	-0.1728	-0.5823	0	0	0	-0.0149	0
139TRP												0	-32.956	-2.1829	3.46715	0.00798	0.5445	-36.901	-3.2847	-0.0209	-0.3423	-18.159	-10.381
142LEU														-9.057	-0.0887	0	0	-1.6913	0.00299	0	-0.4809	-2.611	-0.0021
145TYR															-3.805	0.00075	0.33932	-0.6313	0	0	-5.2439	-9.5958	0.0095
149ARG																0.2109	-0.3019	-0.1716	0	0.0005	0.2744	-1.9155	0
174GLY																	0.4477	-1.3459	0	-0.031	0	0.001	0
175PRO																		-8.4067	-0.389	-6.673	0.00025	-0.5828	-0.9644
176ASN																			-49.223	0.7307	0	-2.4765	-30.106
177TYR																				3.3761	0	-0.503	-11.023
178LEU																					0.19924	1.8892	-2.8188
185TYR																						0.353	-0.8461
186PHE																							2.227
187TYR																							

Fig. S6 Difference between total number of contacts in HheC-M4 and in the reference HheC. The mutated residues are coloured yellow. The absolute differences greater than or equal to 9 are coloured green.

Table S5 The pairs of considered amino acids with the largest time averaged differences in the number of hydrogen bonds in HheC-M4 in reference to WT HheC.

amino acid 1	amino acid 2	M4-WT difference
131Thr	132Ser	0.068259
132Ser	134Thr/Ala	-0.613072
133Ala	176Asn/Ala	-0.231343
145Tyr	149Arg	0.23386
176Asn/Ala	177Tyr	-0.253731
176Asn/Ala	187Tyr	-0.557214
82Phe	145Tyr	-0.32485798
82Phe	84Val	0.189122
84Pro/Val	145Tyr	0.203842
85Glu	86Phe/Pro	-0.40796

NMR Spectra

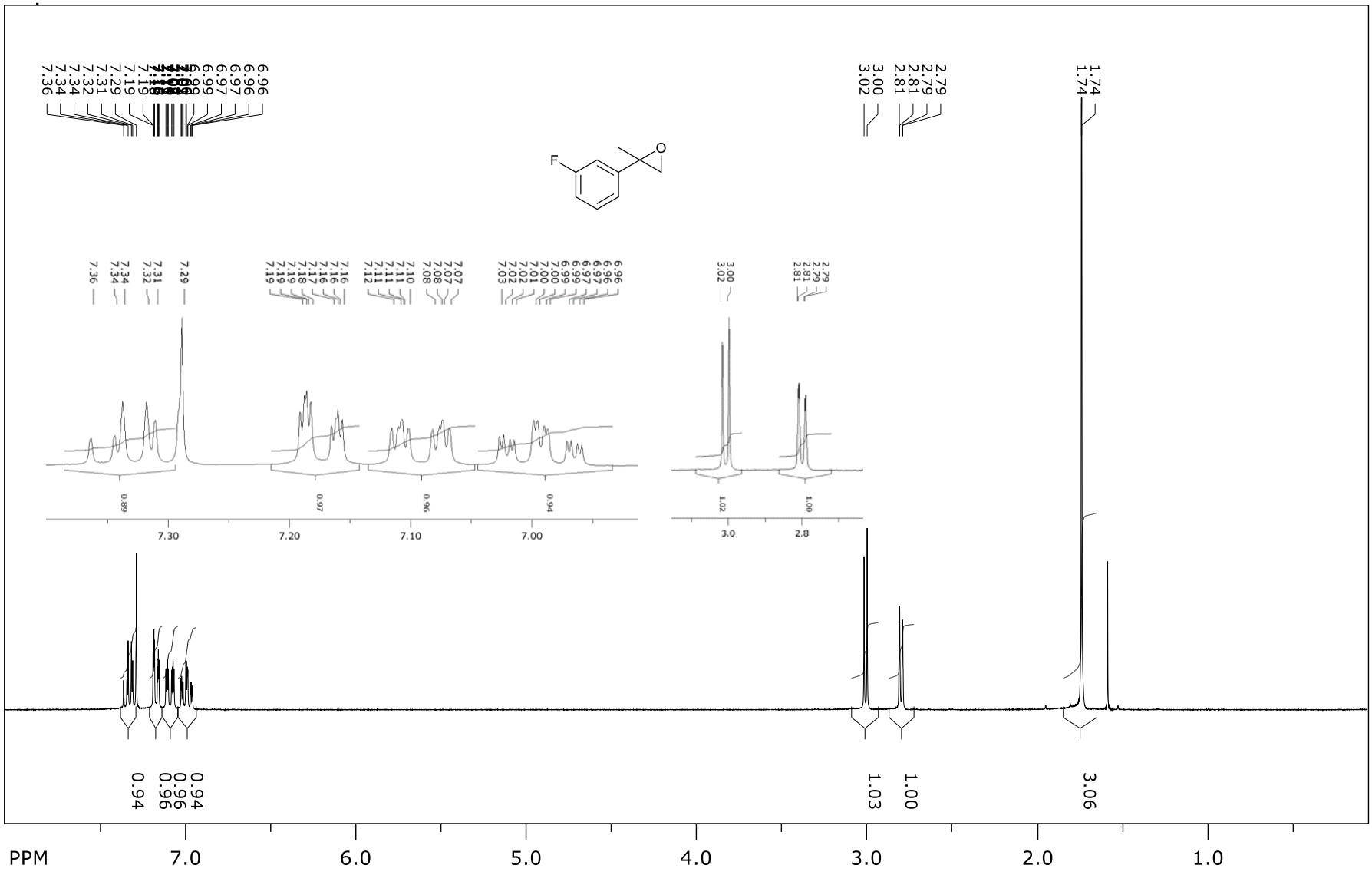
F
O
7.36
7.34
7.34
7.32
7.31
7.29
7.19
6.99
6.97
6.96
3.02
3.00
2.81
2.79
1.74
0.89
0.97
0.96
0.94
1.02
1.00
7.30
7.20
7.10
7.00
3.0
2.8
0.94
0.96
0.96
0.94
1.03
1.00
3.06
PPM
7.0
6.0
5.0
4.0
3.0
2.0
1.0

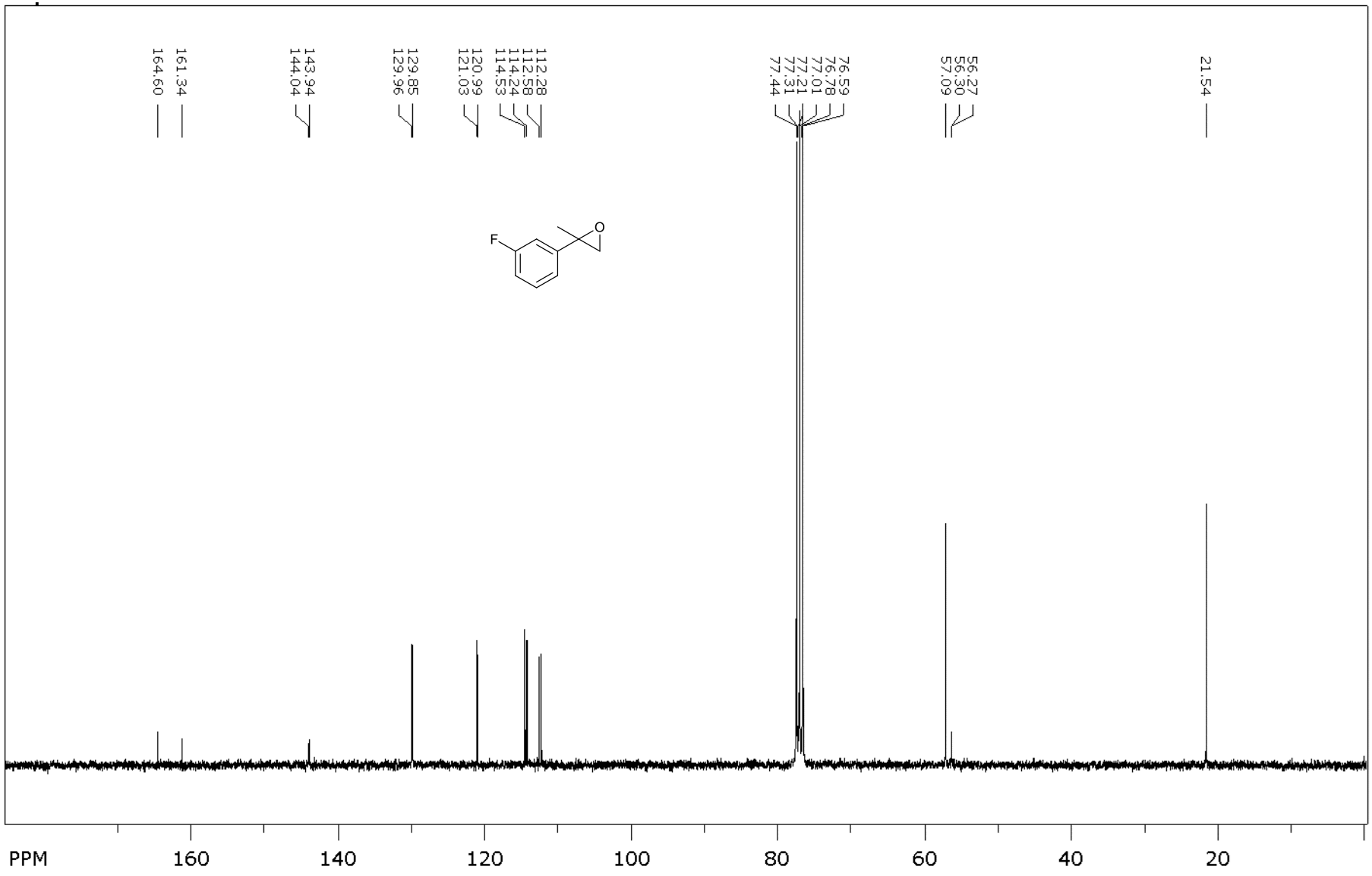
164.60
161.34
144.04
143.94
129.96
129.85
121.03
120.99
114.53
114.24
112.58
112.28
77.44
77.31
77.21
77.01
76.78
76.59
57.09
56.30
56.27
21.54
F
O
PPM
160
140
120
100
80
60
40
20

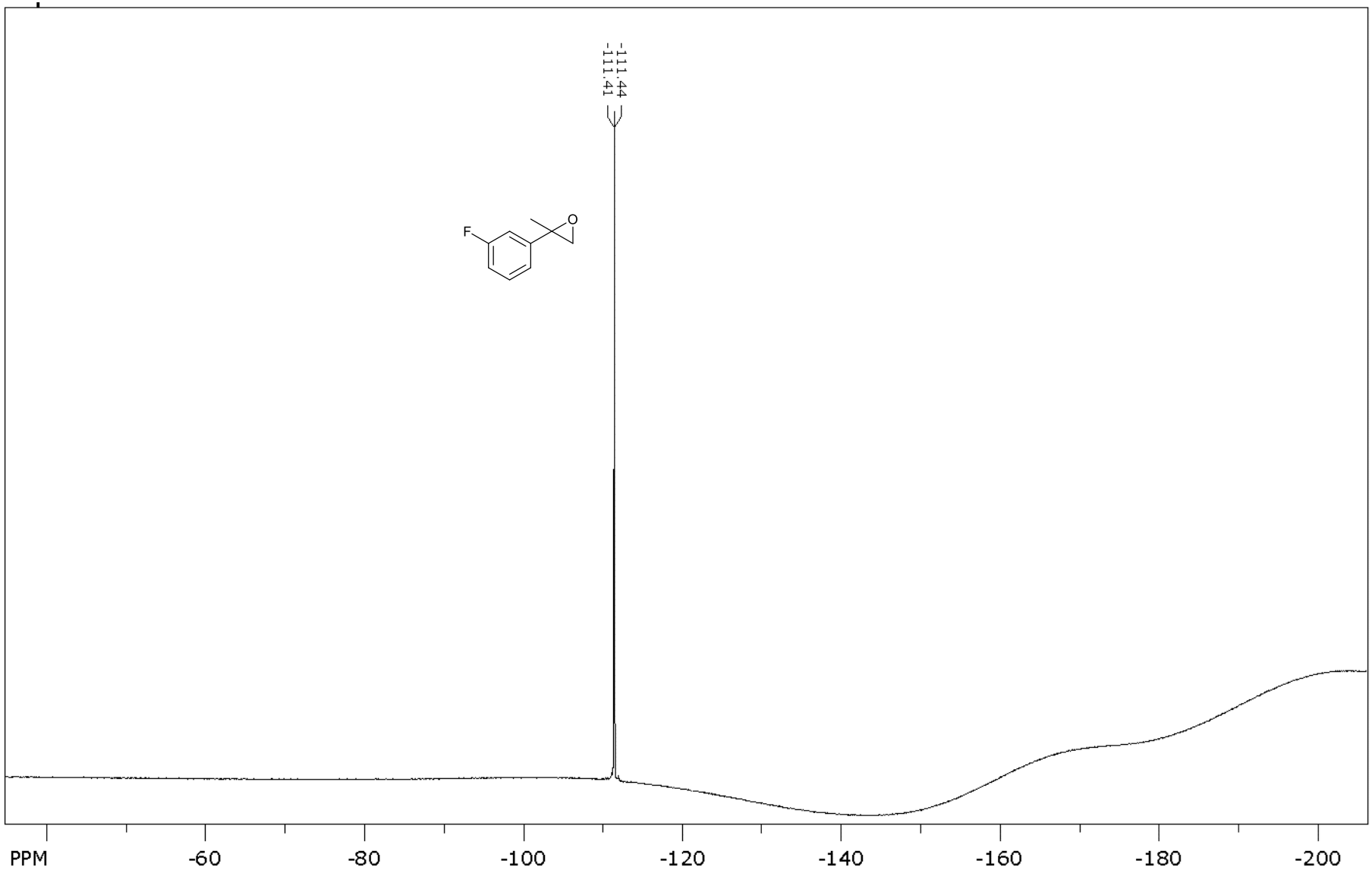
-111.44
-111.41
F
O
PPM
-60
-80
-100
-120
-140
-160
-180
-200

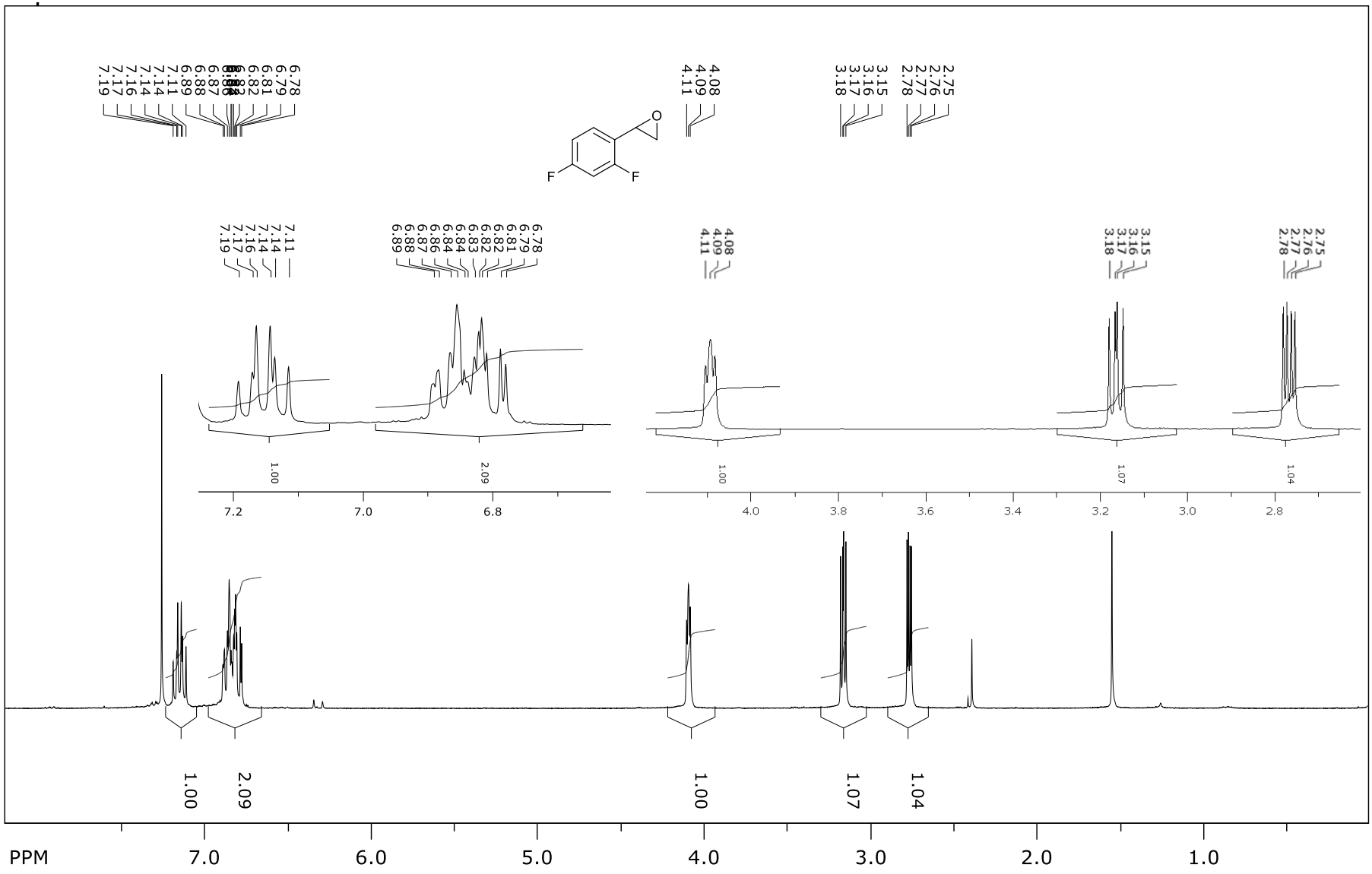
7.19
7.17
7.16
7.14
7.14
7.11
6.89
6.88
6.87
6.82
6.81
6.79
6.78
4.11
4.09
4.08
3.18
3.17
3.16
3.15
2.78
2.77
2.76
2.75
F
F
O
1.00
2.09
1.00
1.07
1.04
7.2
7.0
6.8
4.0
3.8
3.6
3.4
3.2
3.0
2.8
PPM
7.0
6.0
5.0
4.0
3.0
2.0
1.0

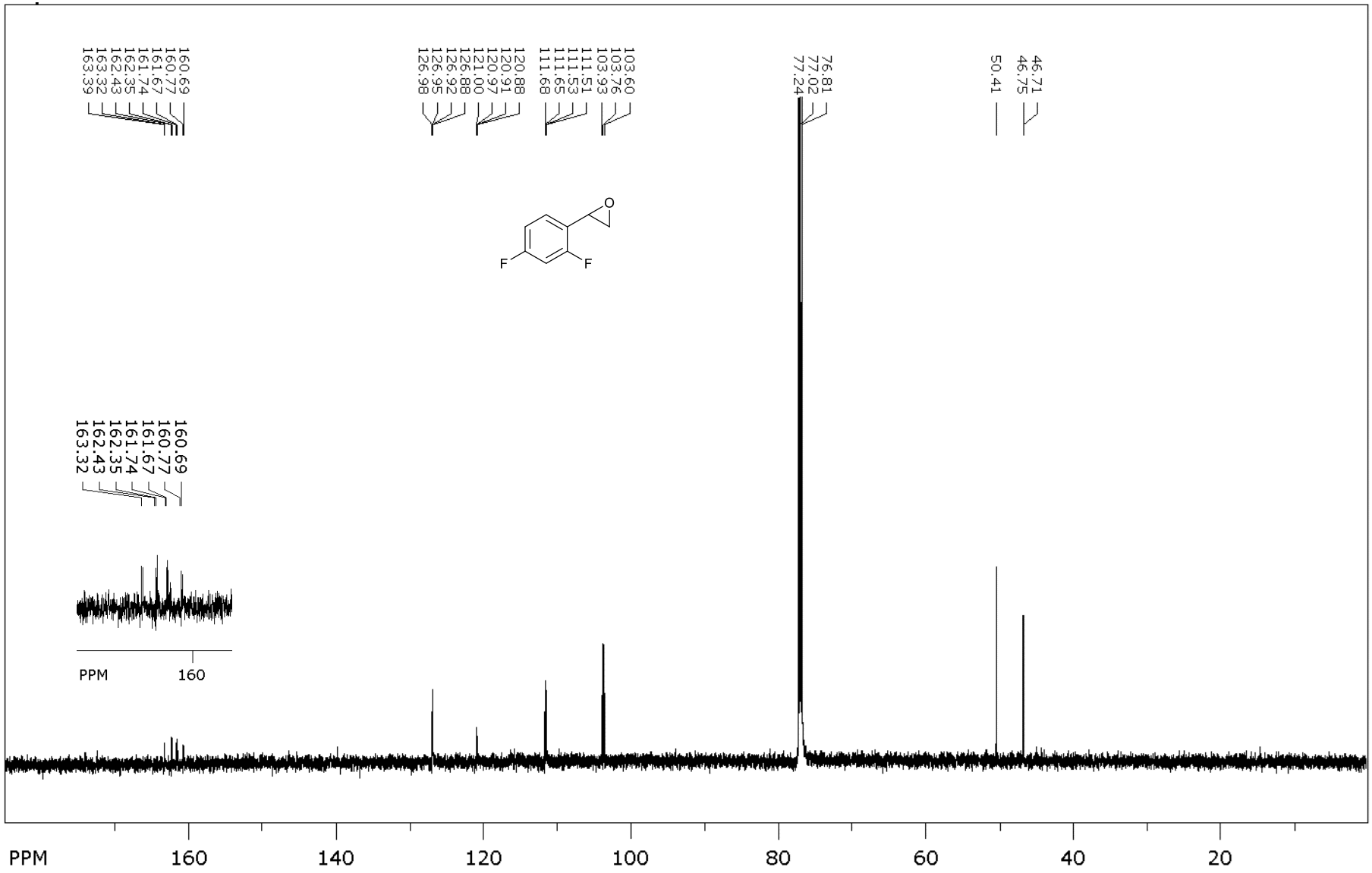
160.69
160.77
161.67
161.74
162.35
162.43
163.32
163.39
120.88
120.91
120.97
121.00
126.88
126.92
126.95
126.98
103.60
103.76
103.93
111.51
111.53
111.65
111.68
76.81
77.02
77.24
46.71
46.75
50.41
O
F
F
PPM
160
PPM
160
140
120
100
80
60
40
20

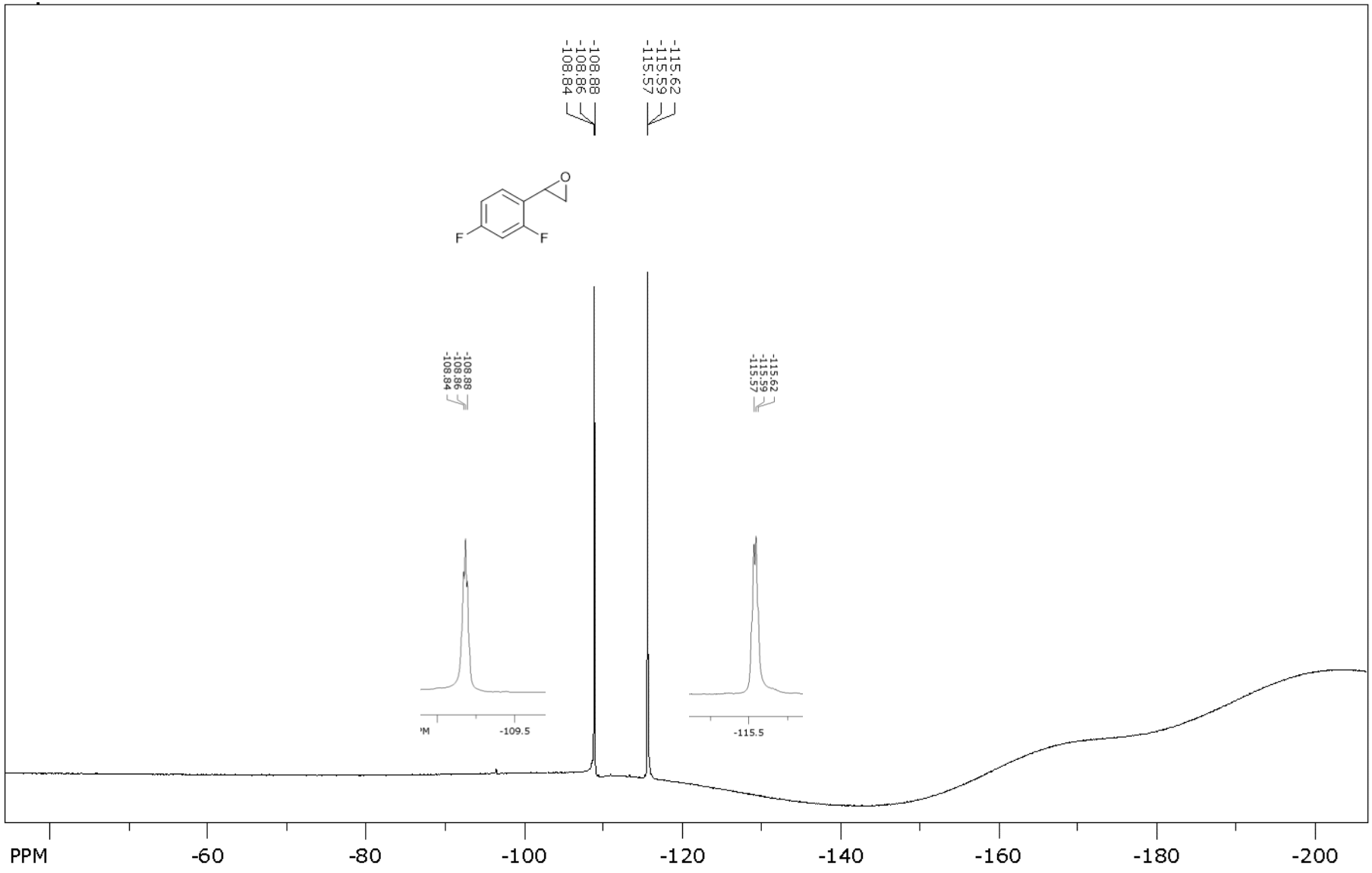
-108.88
-108.86
-108.84
-115.62
-115.59
-115.57
O
F
F
-109.5
-115.5
PPM
-60
-80
-100
-120
-140
-160
-180
-200

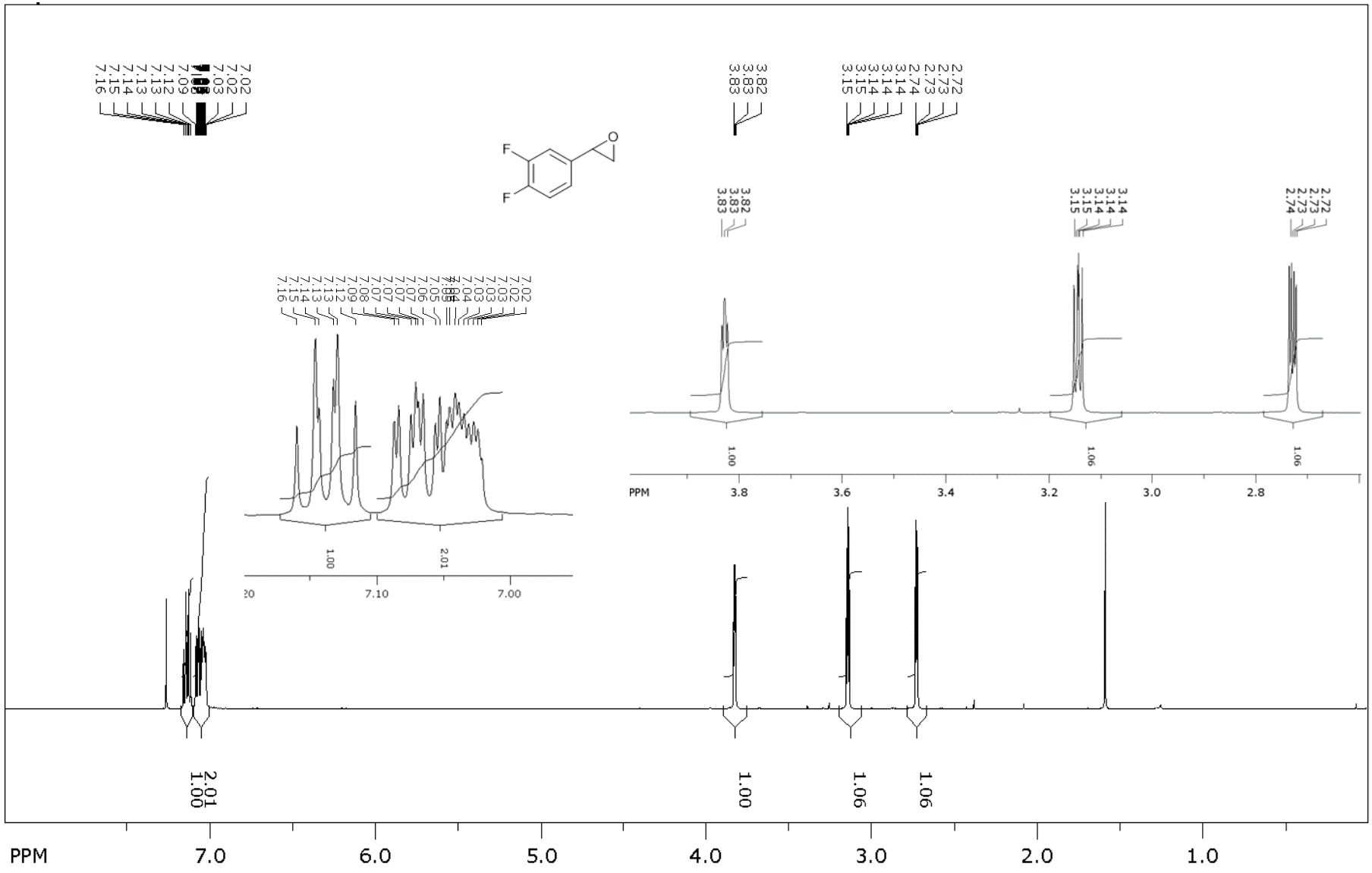
F
F
O
PPM
7.0
6.0
5.0
4.0
3.0
2.0
1.0
2.01
1.00
1.00
1.06
1.06
7.10
7.00
3.8
3.6
3.4
3.2
3.0
2.8

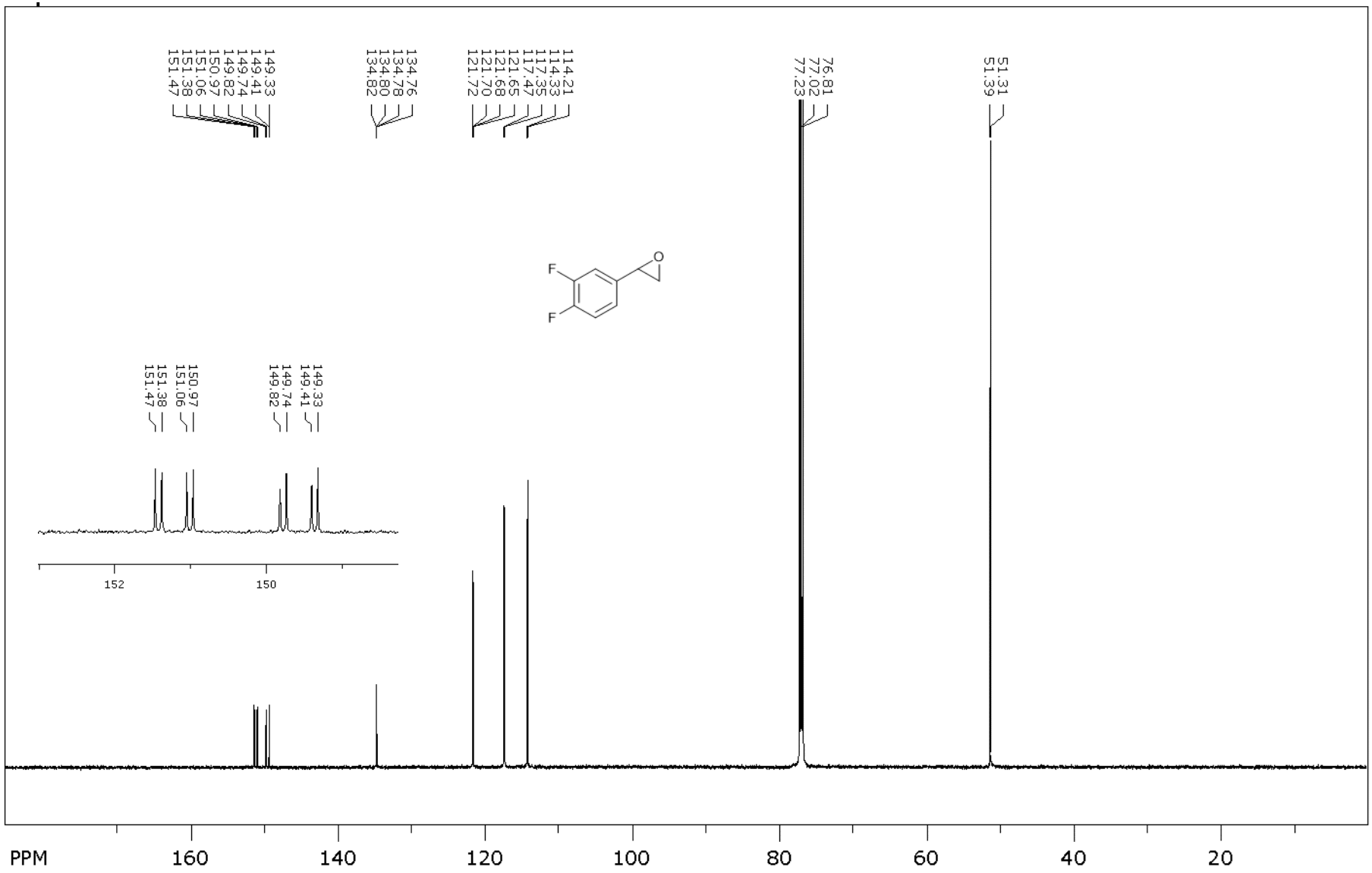
151.47
151.38
151.06
150.97
149.82
149.74
149.41
149.33
134.82
134.80
134.78
134.76
121.72
121.70
121.68
121.65
117.47
117.35
114.33
114.21
77.23
77.02
76.81
51.39
51.31
F
F
O
151.47
151.38
151.06
150.97
149.82
149.74
149.41
149.33
152
150
PPM
160
140
120
100
80
60
40
20

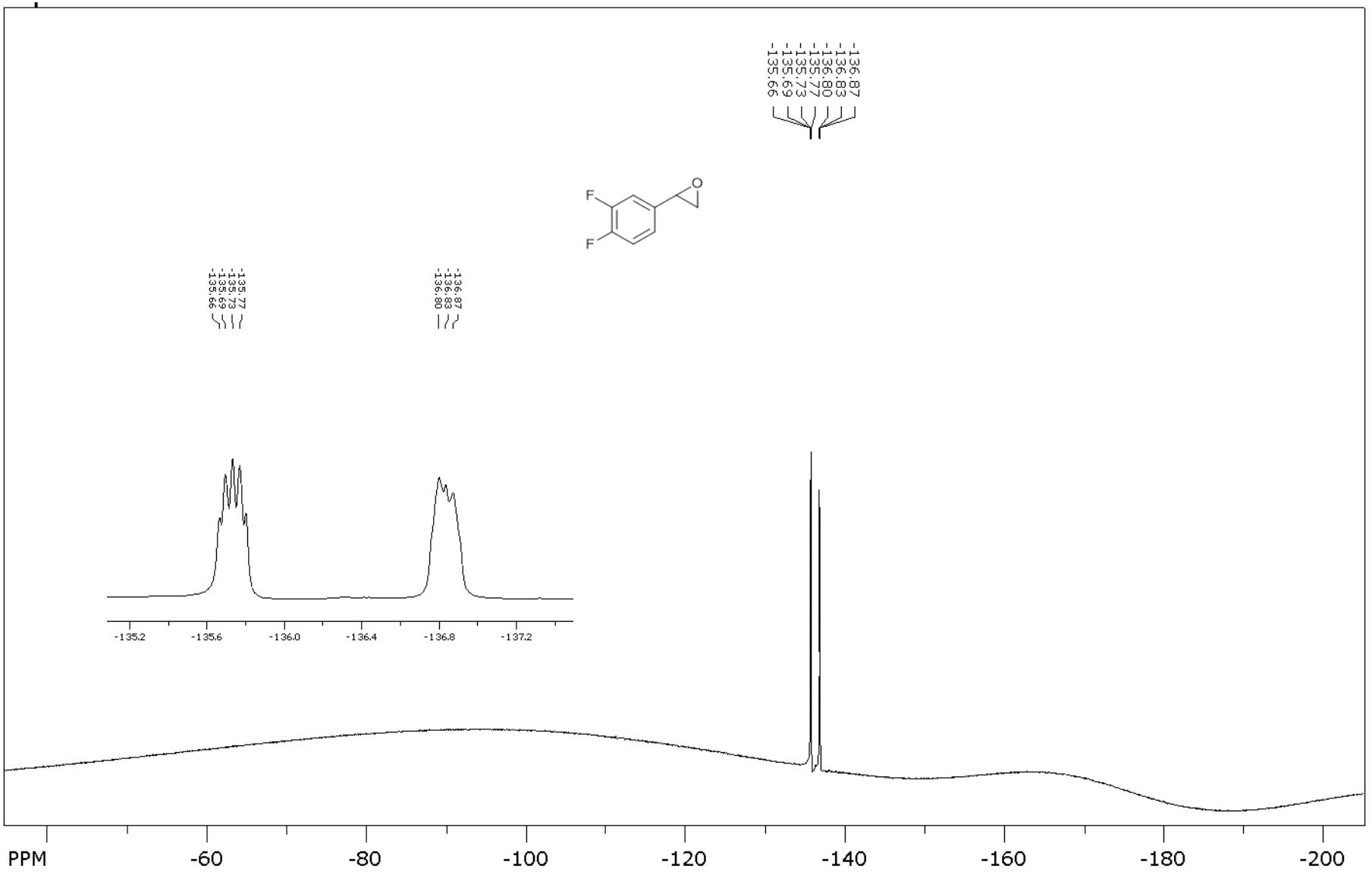
-135.66
-135.69
-135.73
-135.77
-135.80
-136.83
-136.87
F
F
O
-135.66
-135.69
-135.73
-135.77
-136.80
-136.83
-136.87
-135.2
-135.6
-136.0
-136.4
-136.8
-137.2
PPM
-60
-80
-100
-120
-140
-160
-180
-200

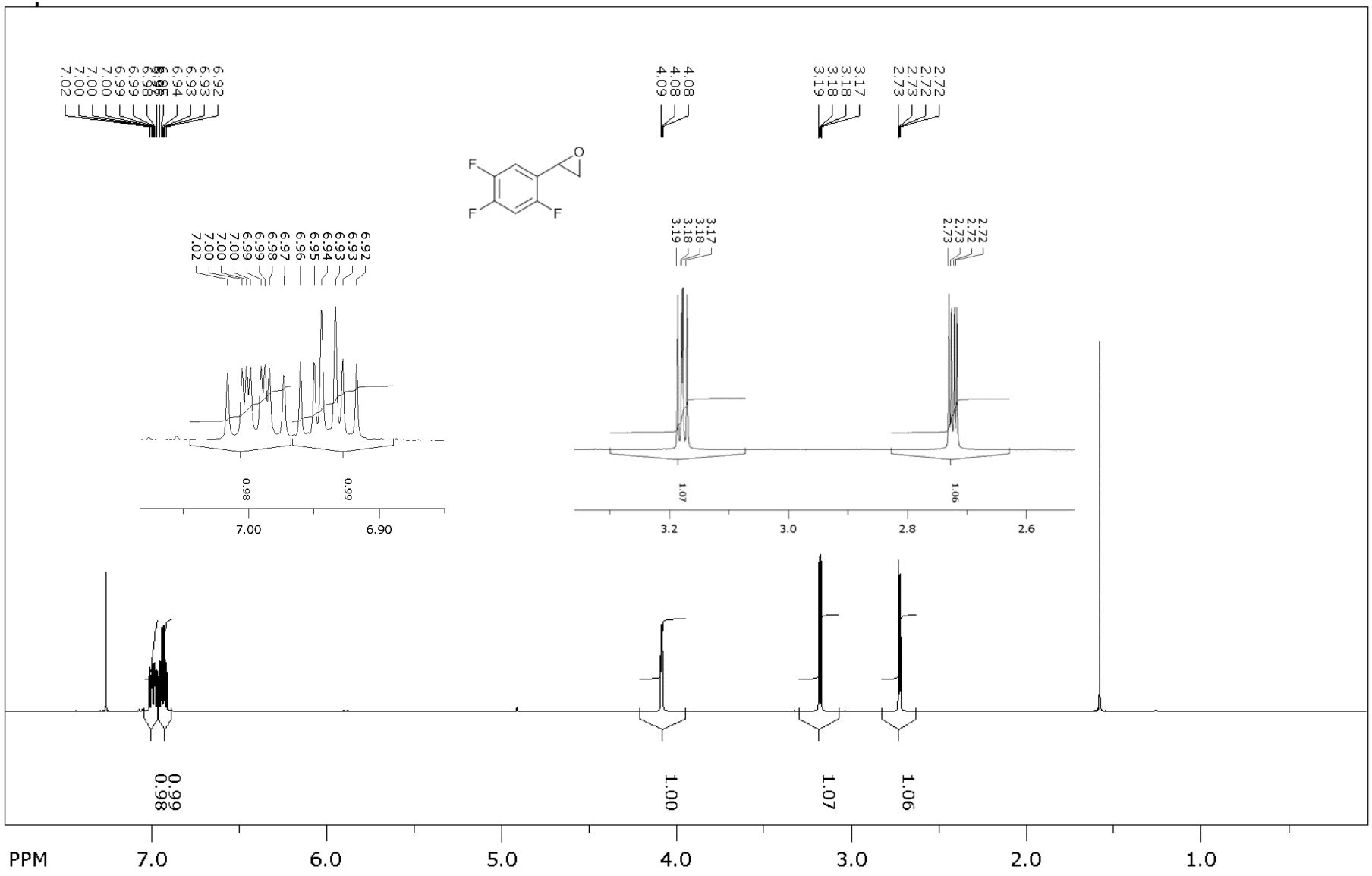
F
F
F
O
PPM
7.0
6.0
5.0
4.0
3.0
2.0
1.0
0.98
0.99
1.00
1.07
1.06
7.00
6.90
3.2
3.0
2.8
2.6

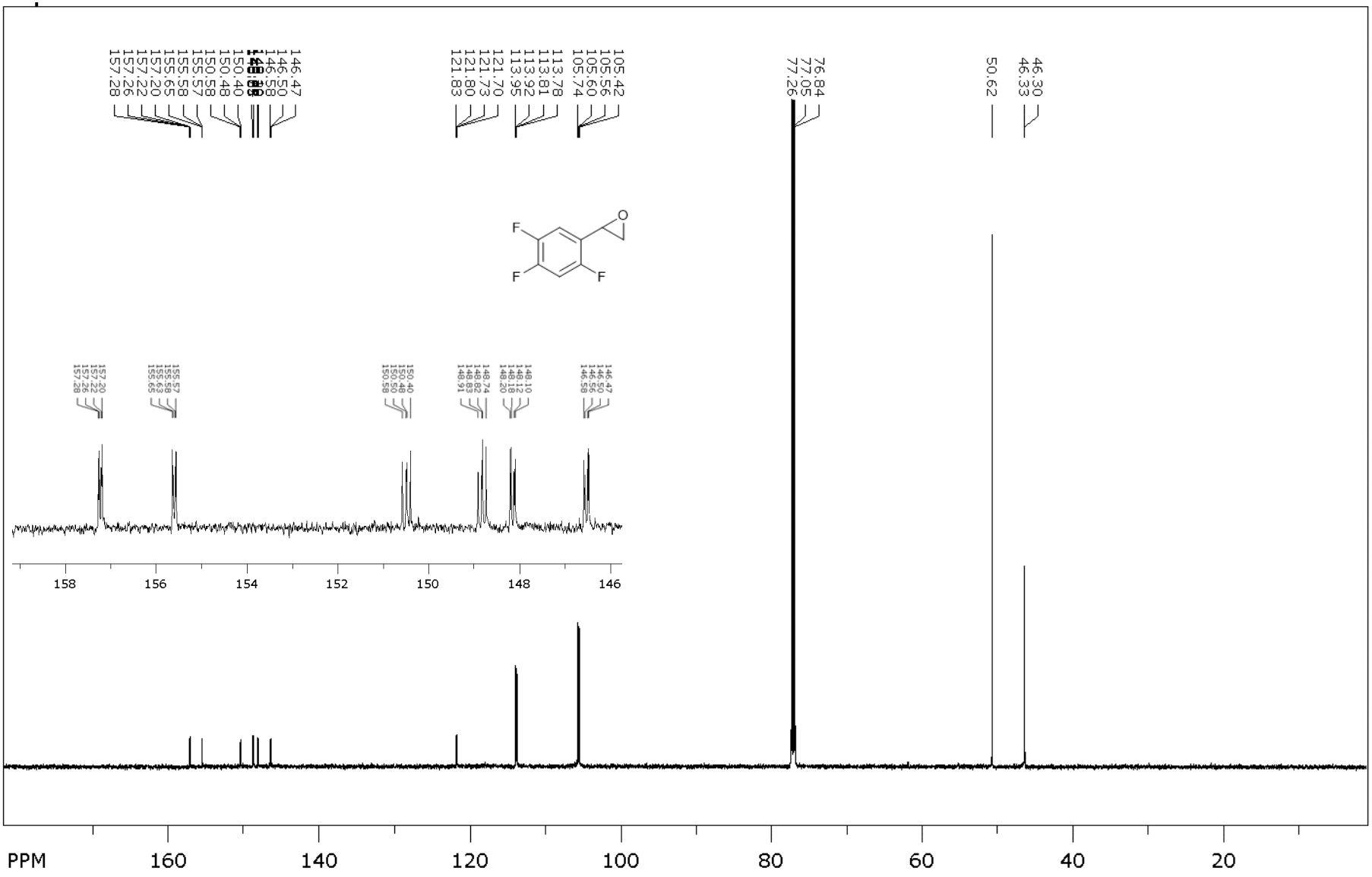
157.28
157.26
157.22
157.20
155.65
155.58
155.57
150.58
150.48
150.40
146.58
146.50
146.47
121.83
121.80
121.73
121.70
113.95
113.92
113.81
113.78
105.74
105.60
105.56
105.42
77.26
77.05
76.84
50.62
46.33
46.30
F
F
F
O
158
156
154
152
150
148
146
PPM
160
140
120
100
80
60
40
20

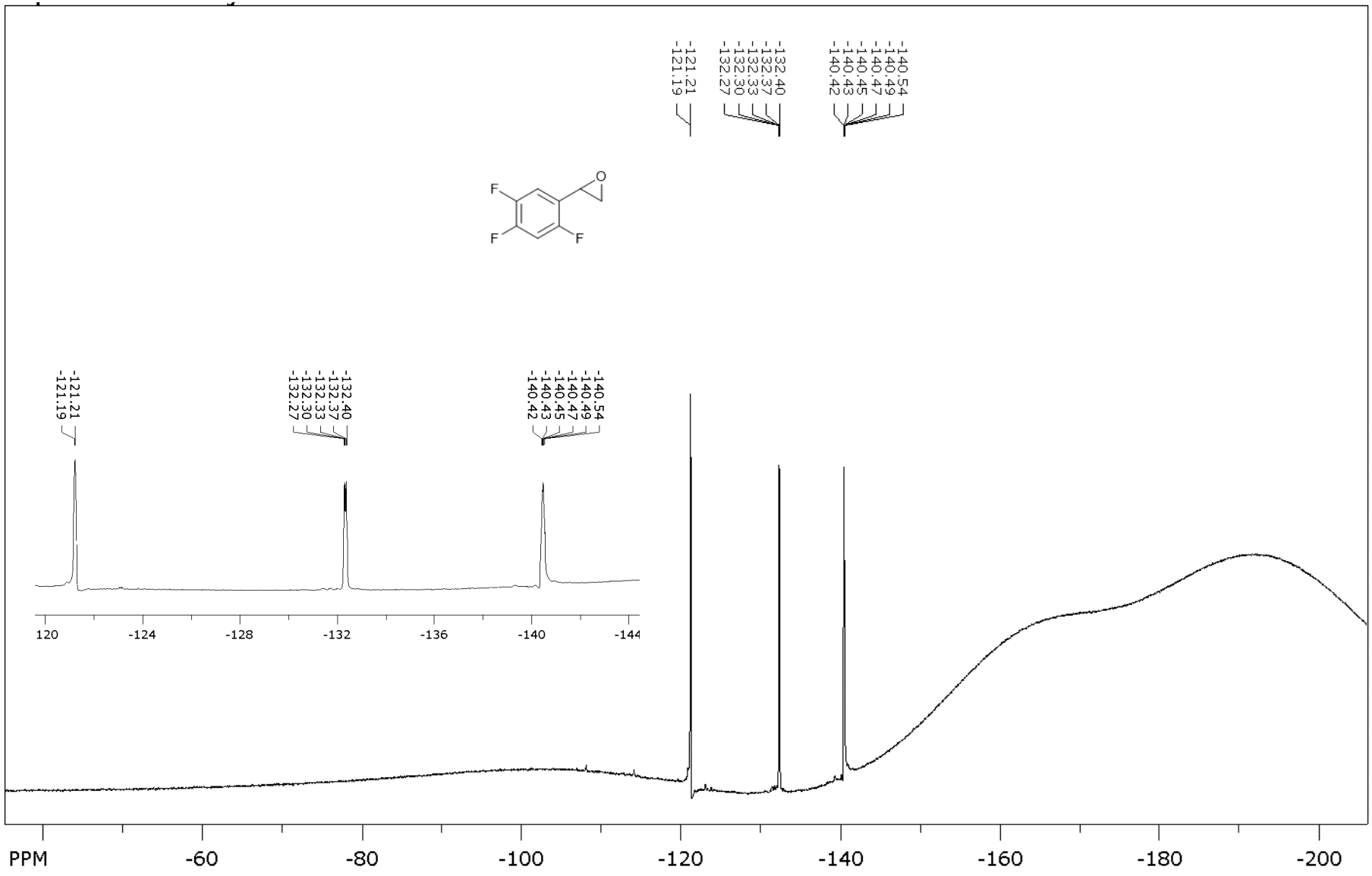
-121.21
-121.19
-132.40
-132.37
-132.33
-132.30
-132.27
-140.54
-140.49
-140.47
-140.45
-140.43
-140.42
F
F
F
O
120
-124
-128
-132
-136
-140
-144
PPM
-60
-80
-100
-120
-140
-160
-180
-200

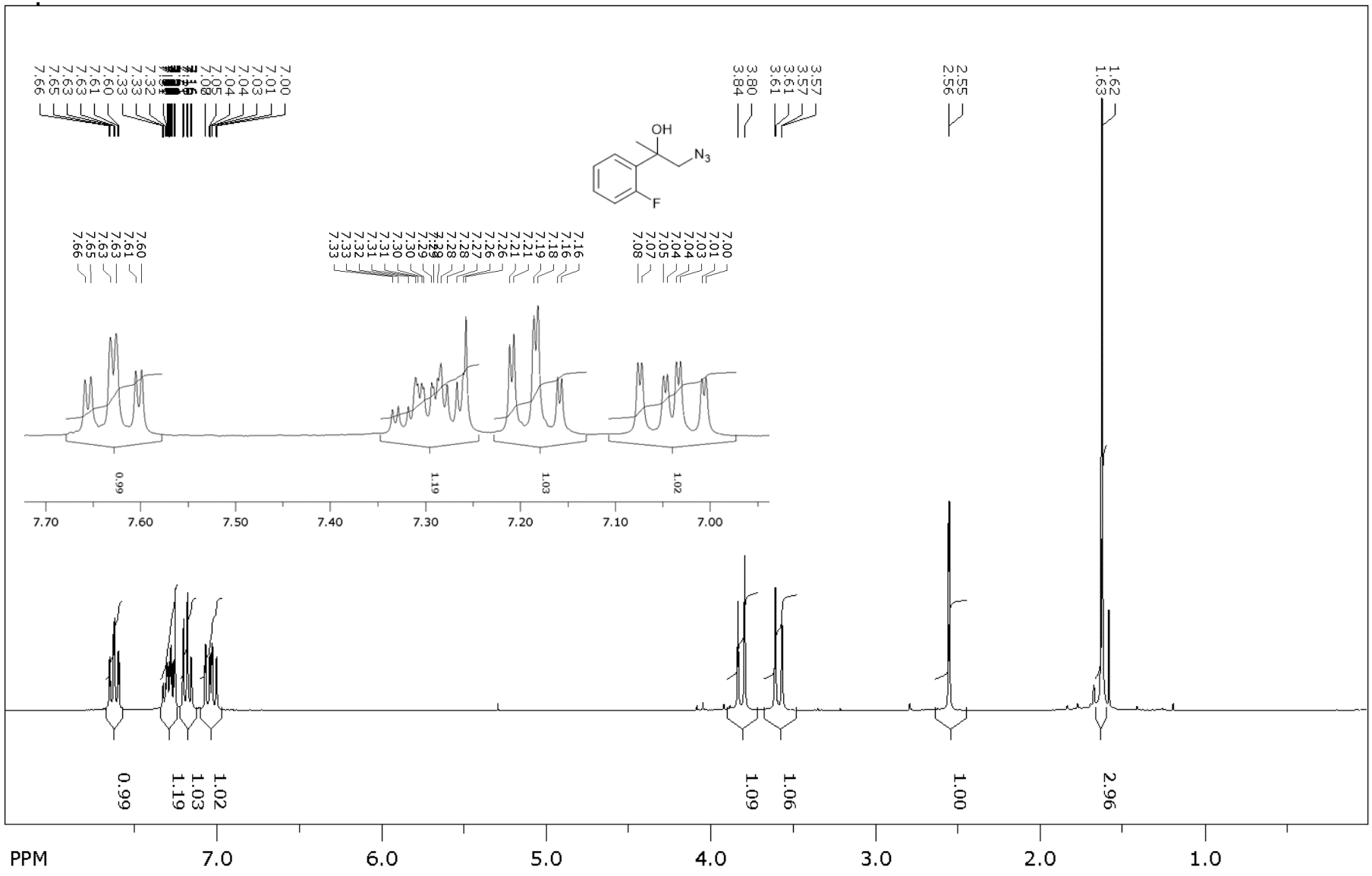
OH
N3
F
7.66
7.65
7.63
7.63
7.61
7.60
7.33
7.32
7.01
7.04
7.03
7.01
7.00
3.84
3.80
3.61
3.61
3.57
3.57
2.56
2.55
1.63
1.62
0.99
1.19
1.03
1.02
7.70
7.60
7.50
7.40
7.30
7.20
7.10
7.00
0.99
1.19
1.03
1.02
1.09
1.06
1.00
2.96
PPM
7.0
6.0
5.0
4.0
3.0
2.0
1.0

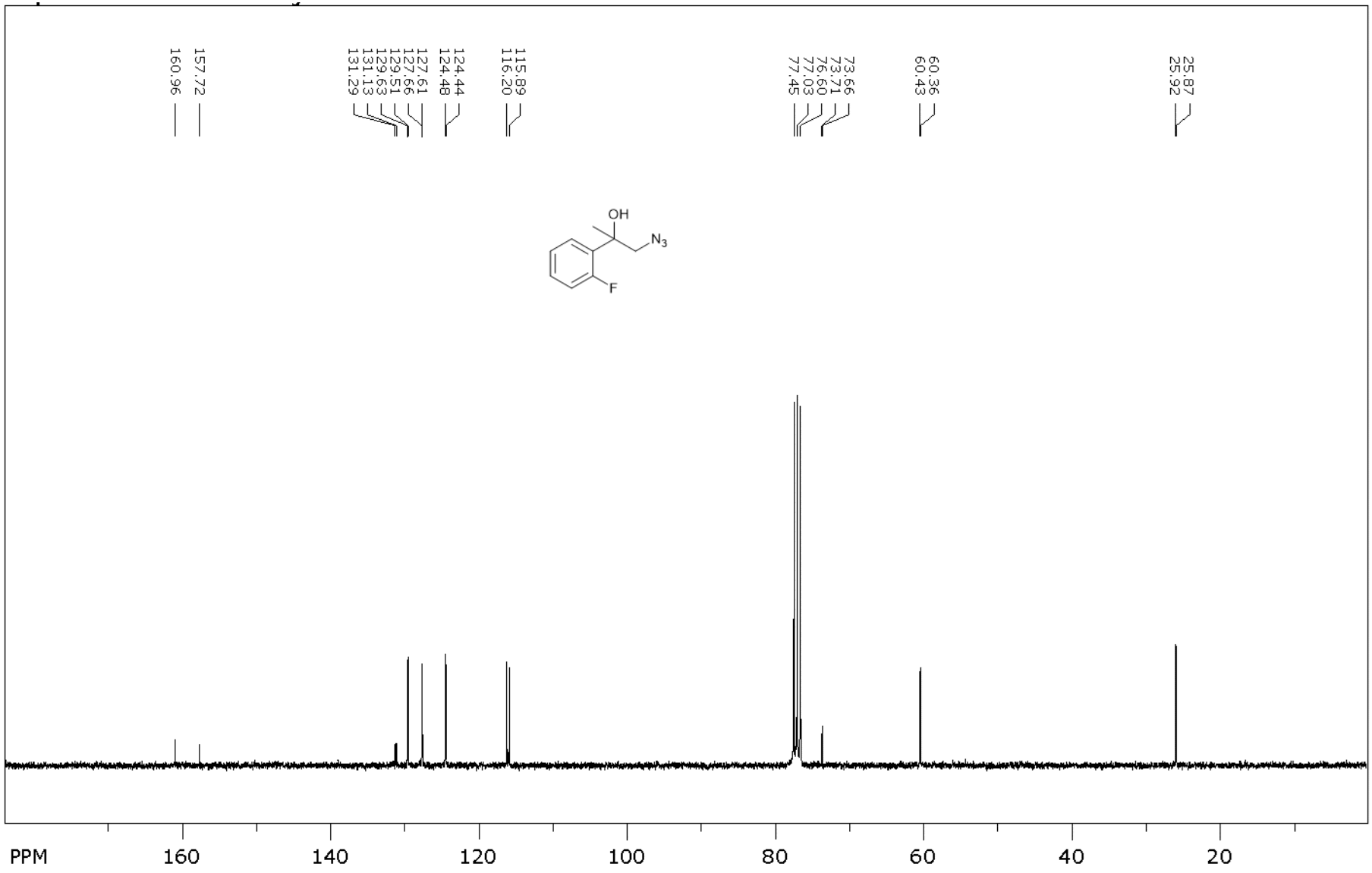
160.96
157.72
131.29
131.13
129.63
129.51
127.66
127.61
124.44
124.48
115.89
116.20
77.45
77.03
76.60
73.71
73.66
60.43
60.36
25.92
25.87
OH
N3
F
PPM
160
140
120
100
80
60
40
20

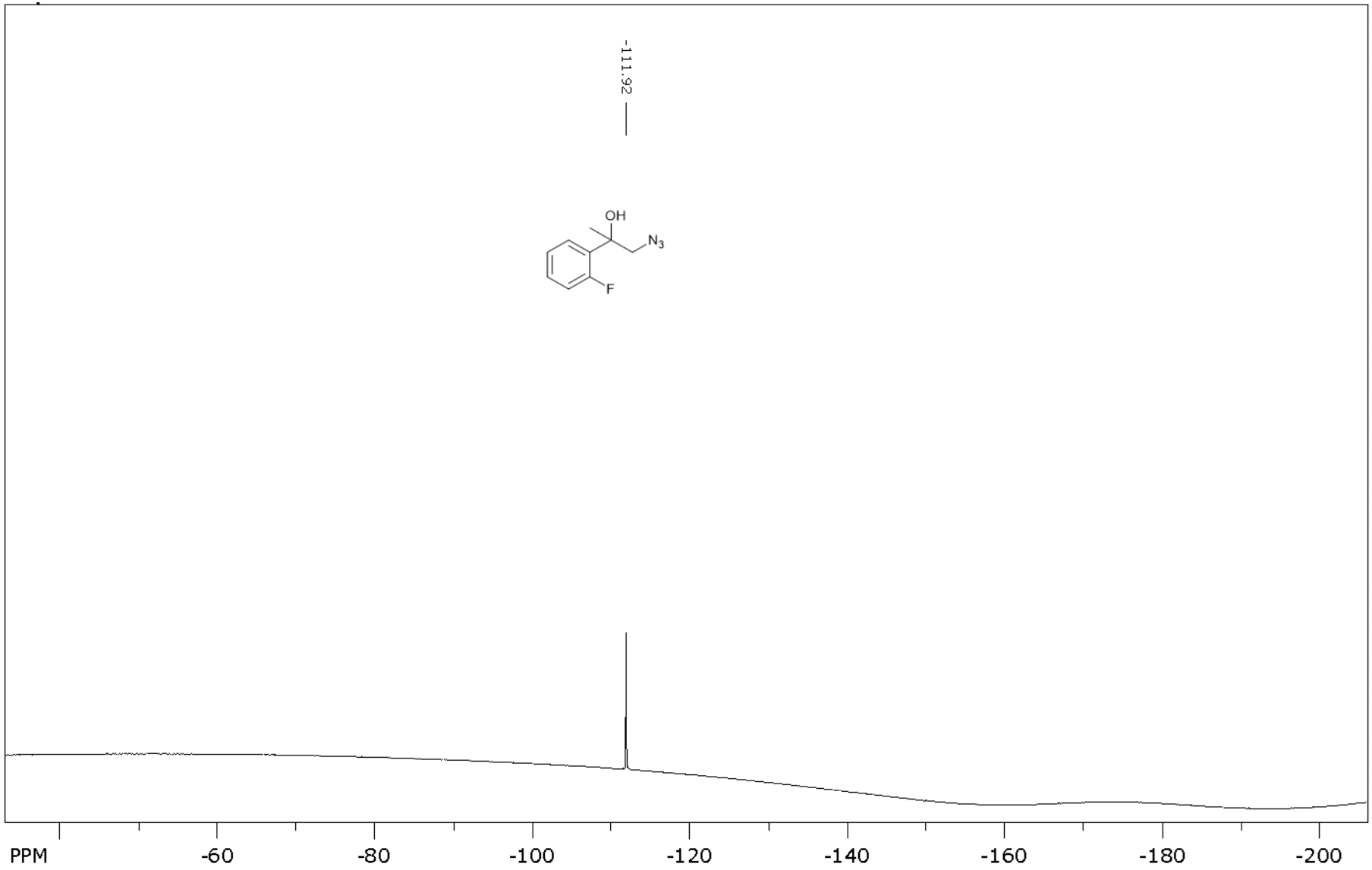
-111.92
OH
N3
F
PPM
-60
-80
-100
-120
-140
-160
-180
-200

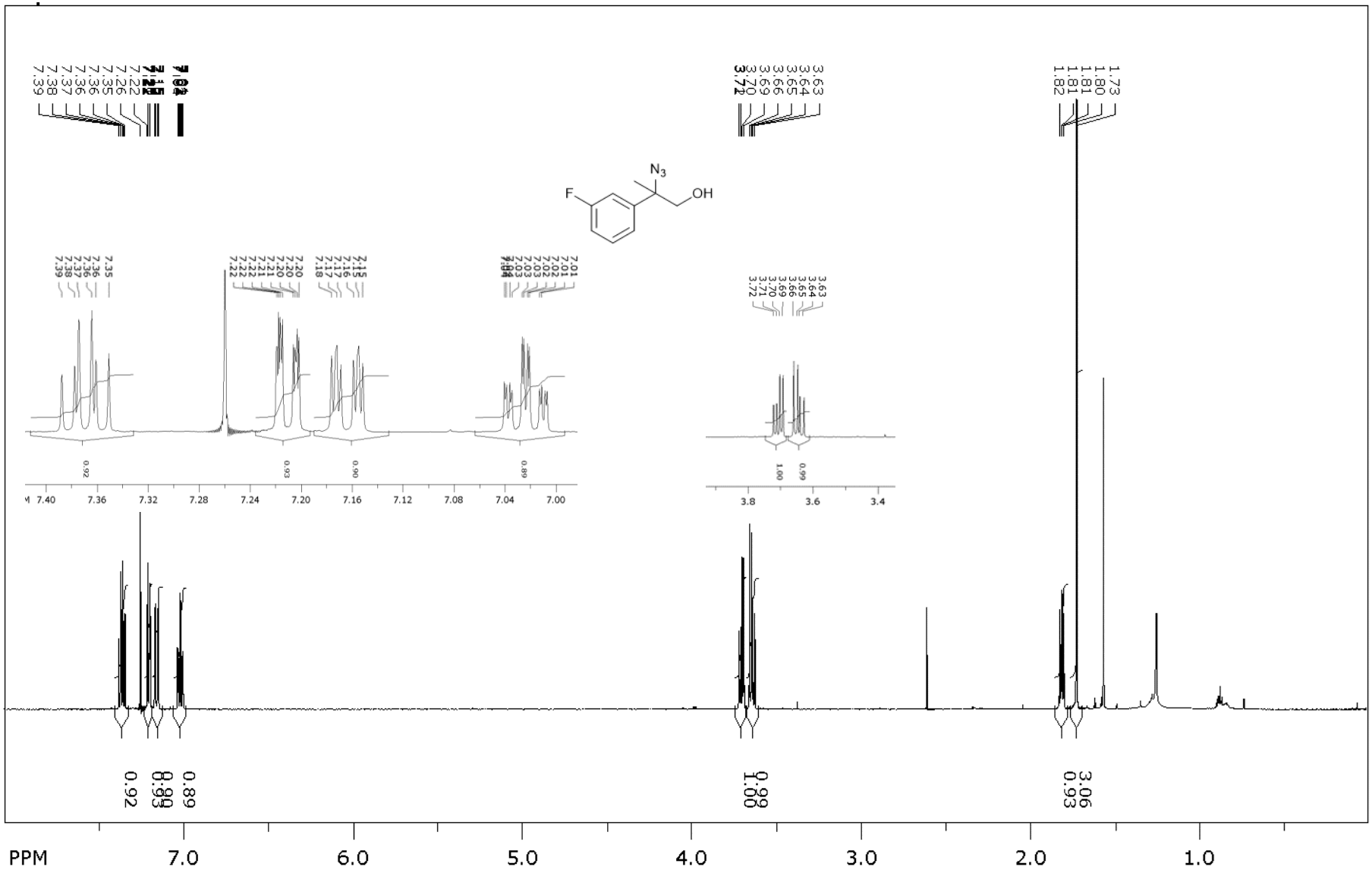
N3
F
OH
PPM
7.0
6.0
5.0
4.0
3.0
2.0
1.0
0.92
0.93
0.89
1.00
3.06
0.93

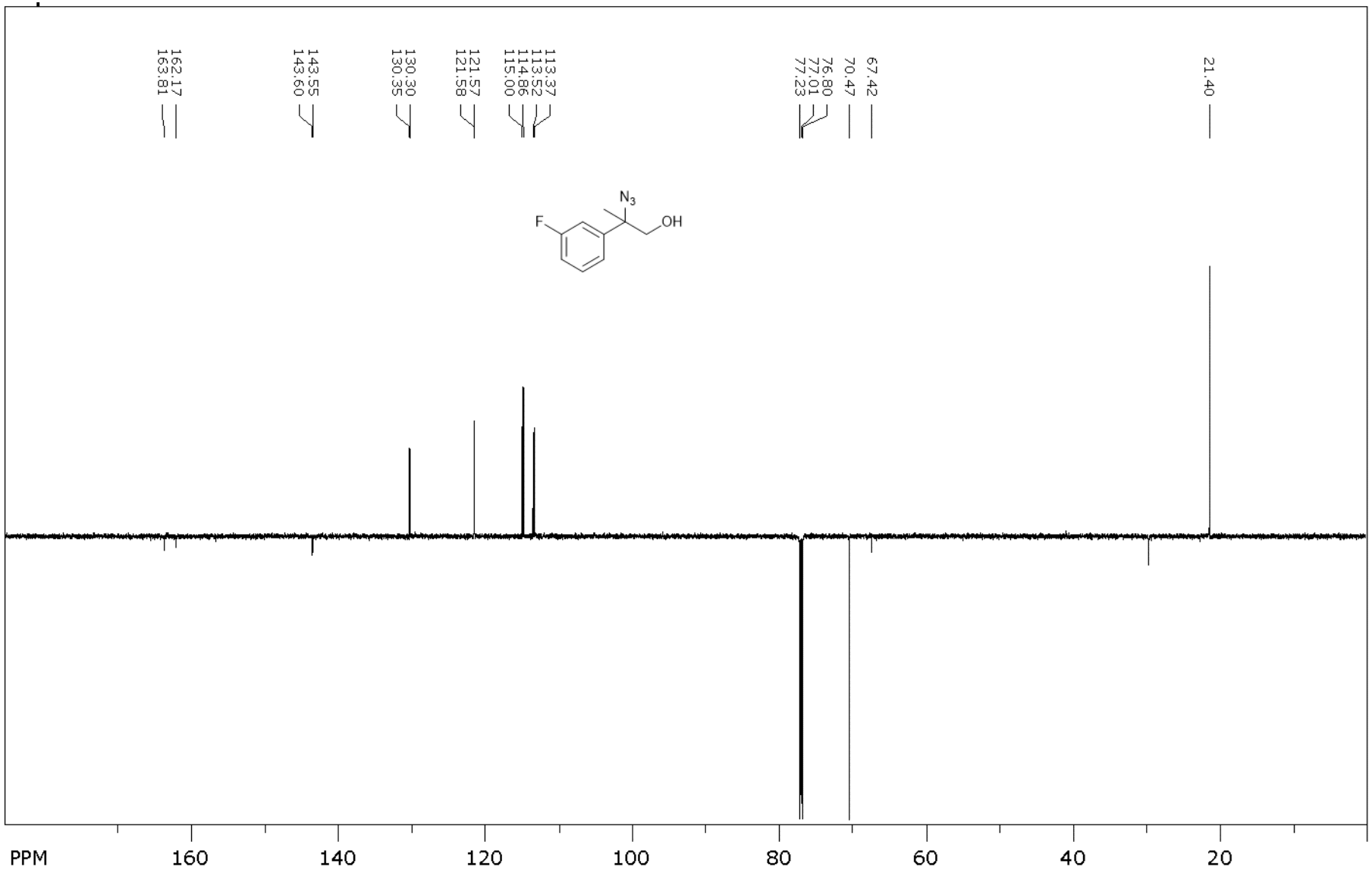
162.17
163.81
143.55
143.60
130.30
130.35
121.57
121.58
115.00
114.86
113.52
113.37
77.23
77.01
76.80
70.47
67.42
21.40
N3
F
OH
PPM
160
140
120
100
80
60
40
20

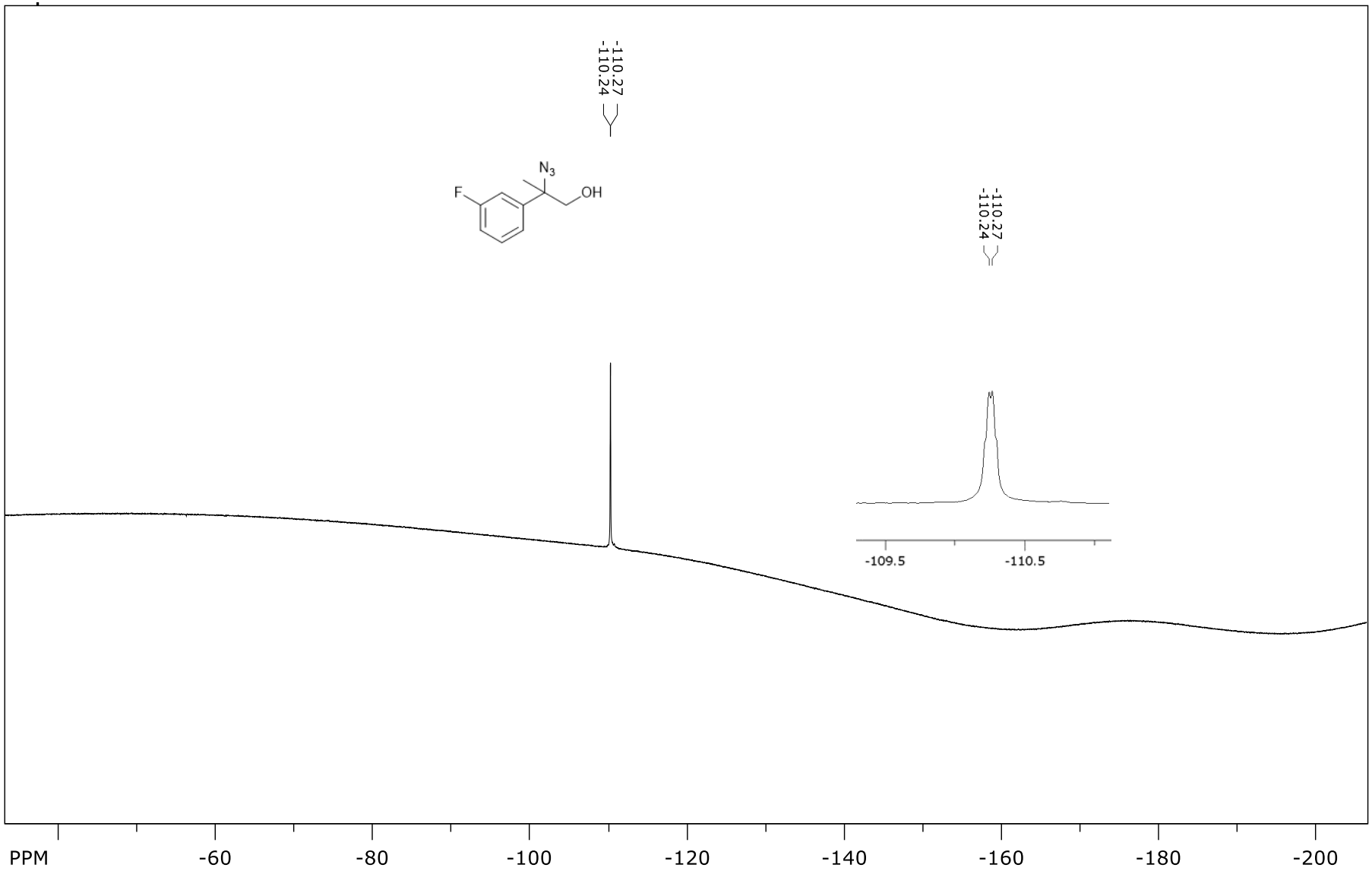
-110.27
-110.24
N3
F
OH
-110.27
-110.24
-109.5
-110.5
PPM
-60
-80
-100
-120
-140
-160
-180
-200

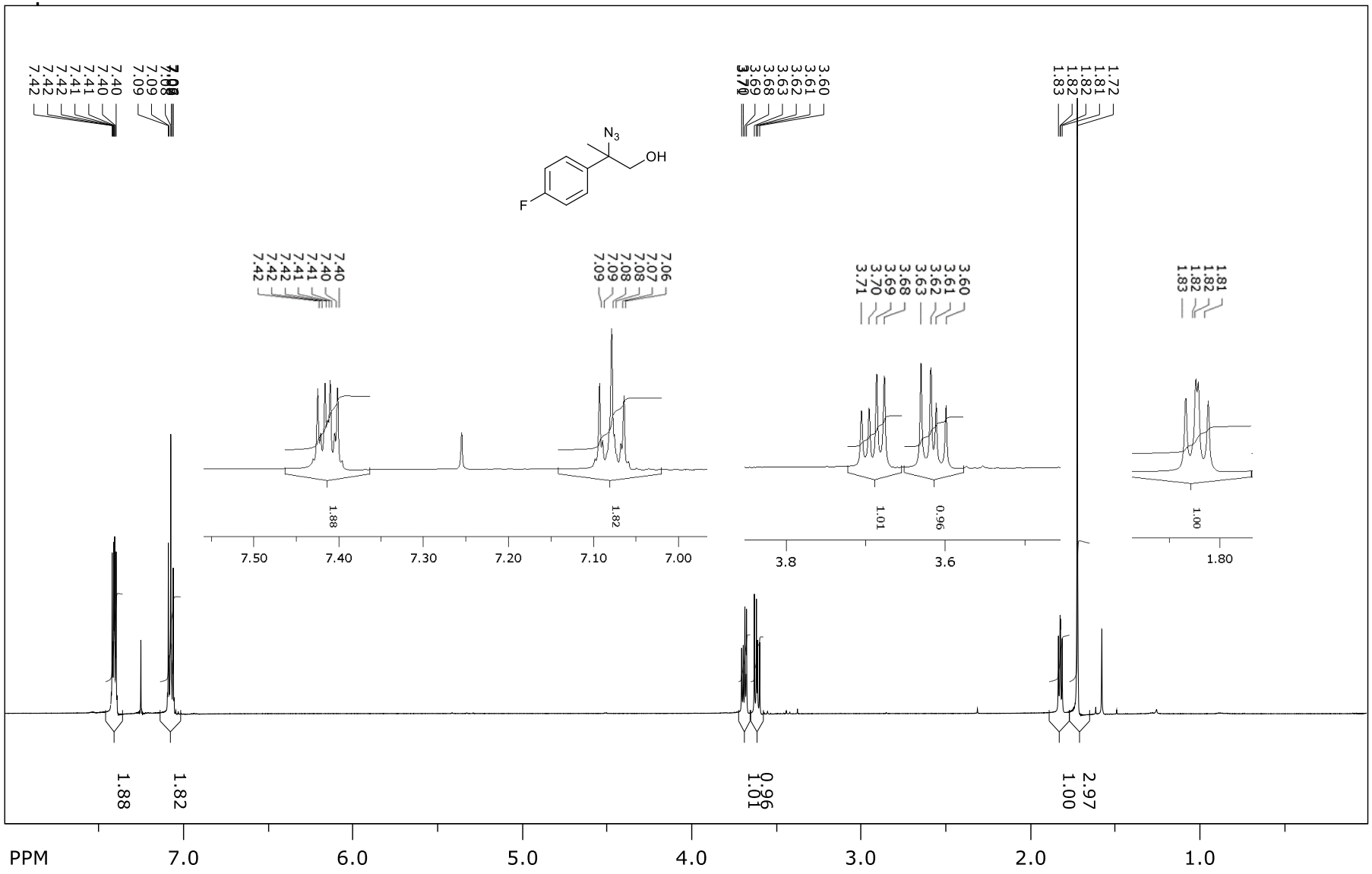
N3
OH
F
7.42
7.42
7.42
7.41
7.41
7.41
7.40
7.40
7.09
7.09
3.71
3.70
3.69
3.68
3.63
3.62
3.61
3.60
1.83
1.82
1.82
1.81
1.72
7.42
7.42
7.42
7.41
7.41
7.41
7.40
7.40
7.09
7.09
7.08
7.08
7.07
7.06
3.71
3.70
3.69
3.68
3.63
3.62
3.61
3.60
1.83
1.82
1.82
1.81
1.88
1.82
1.01
0.96
1.00
7.50
7.40
7.30
7.20
7.10
7.00
3.8
3.6
1.80
1.88
1.82
0.96
1.01
2.97
1.00
PPM
7.0
6.0
5.0
4.0
3.0
2.0
1.0

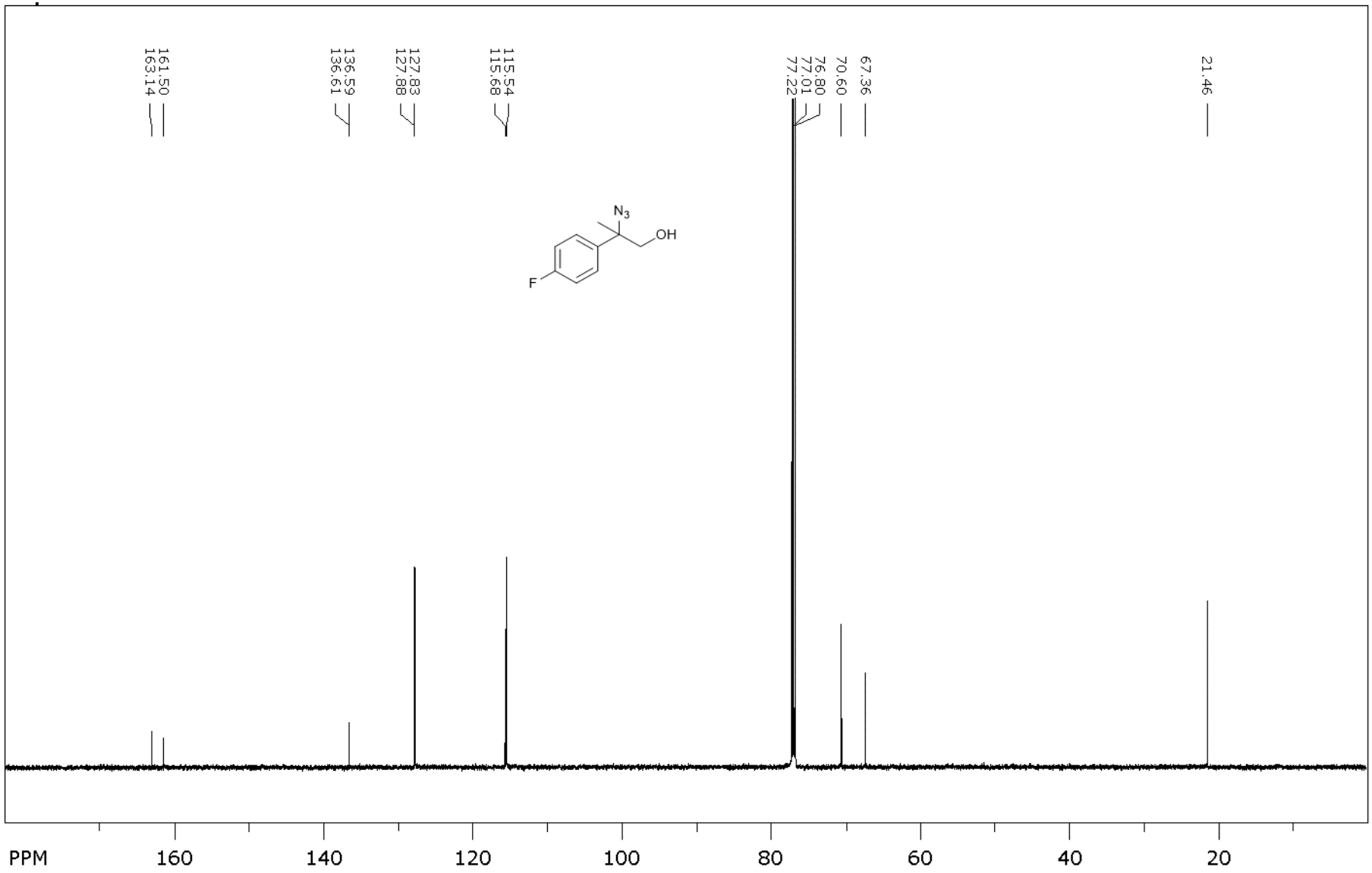
161.50
163.14
136.59
136.61
127.83
127.88
115.54
115.68
77.22
77.01
76.80
70.60
67.36
21.46
N3
OH
F
PPM
160
140
120
100
80
60
40
20

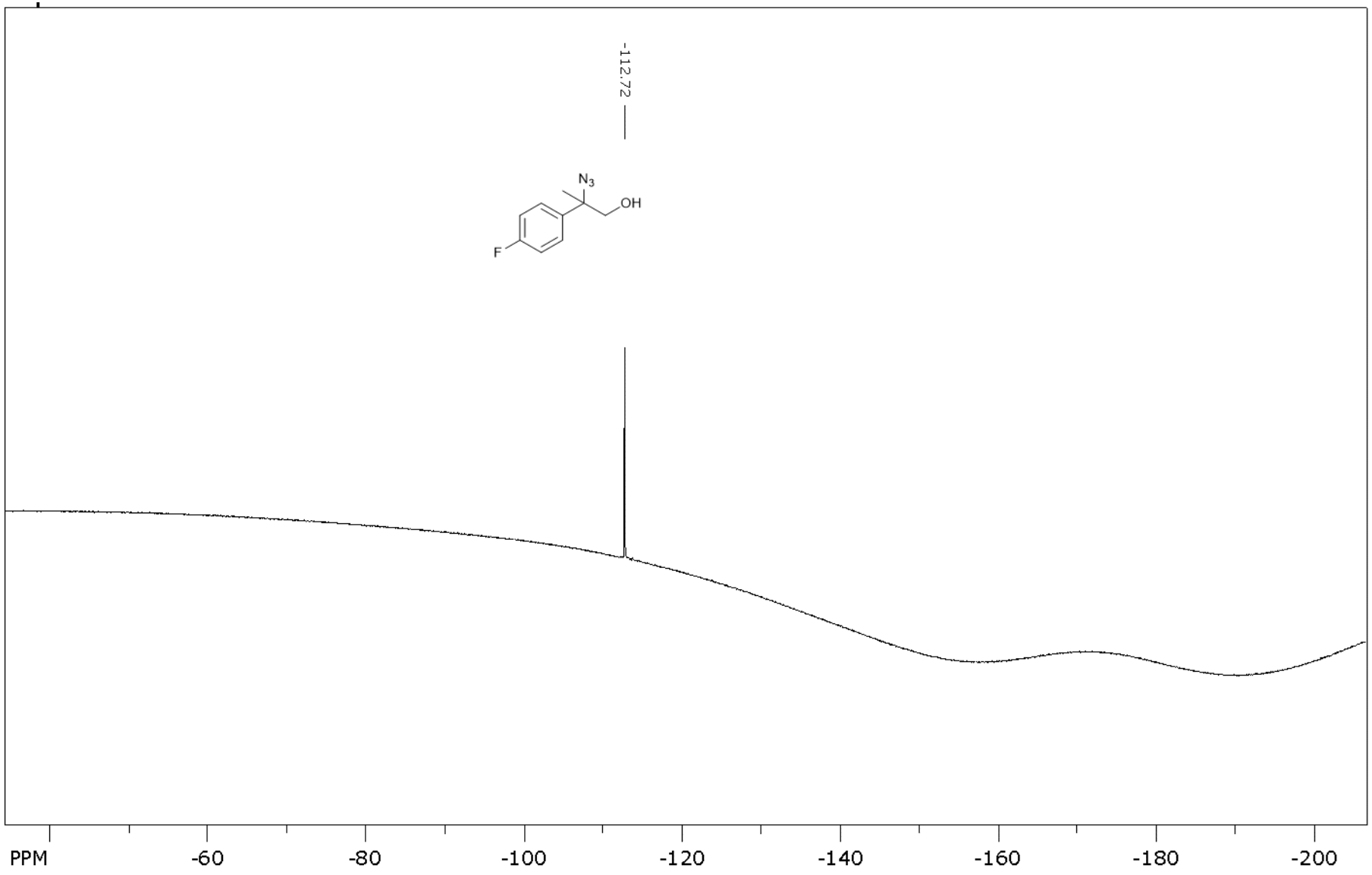
-112.72
N3
OH
F
PPM
-60
-80
-100
-120
-140
-160
-180
-200

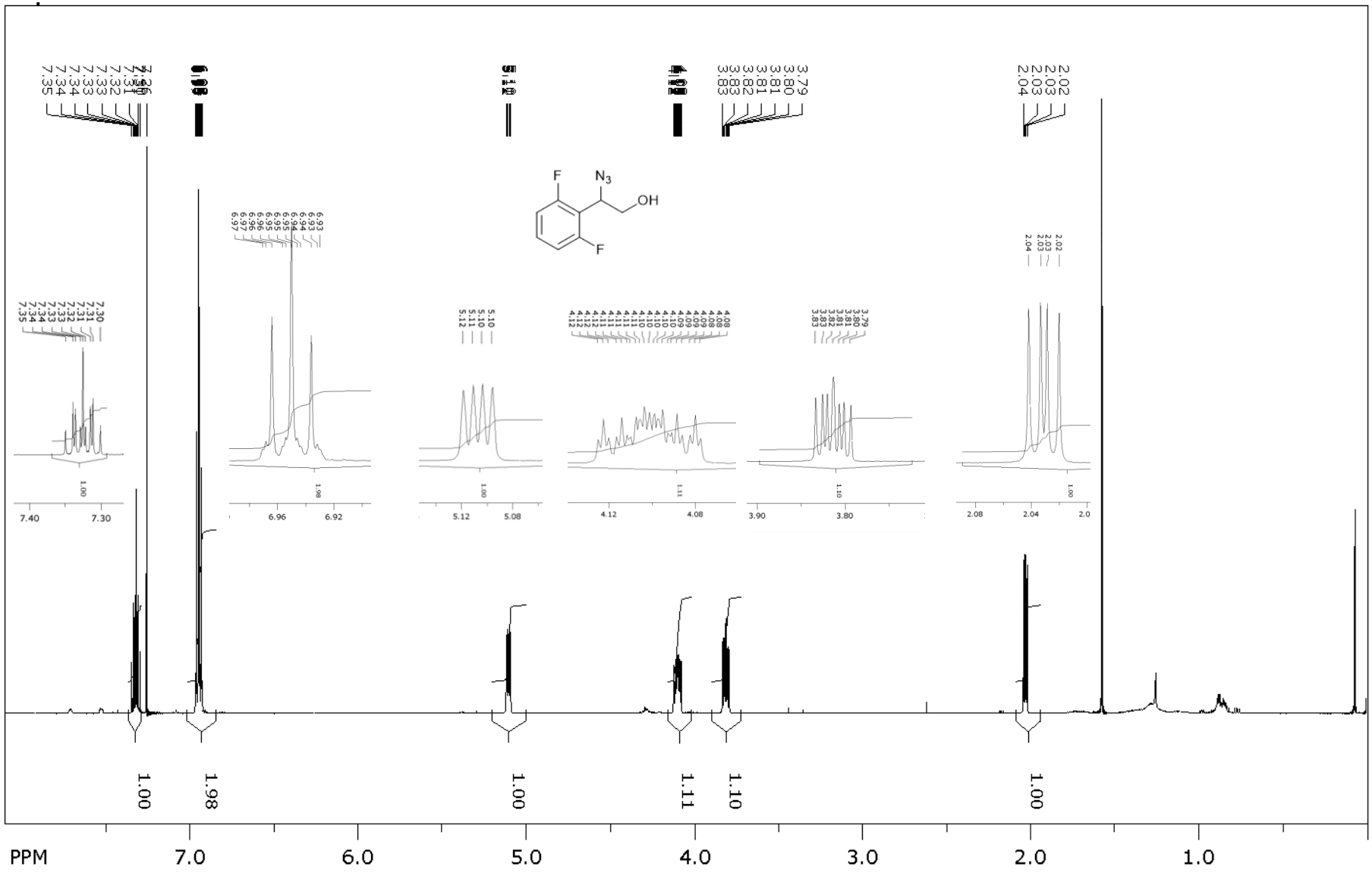
F
N3
OH
F
1.00
1.98
1.00
1.11
1.10
1.00
PPM
7.0
6.0
5.0
4.0
3.0
2.0
1.0

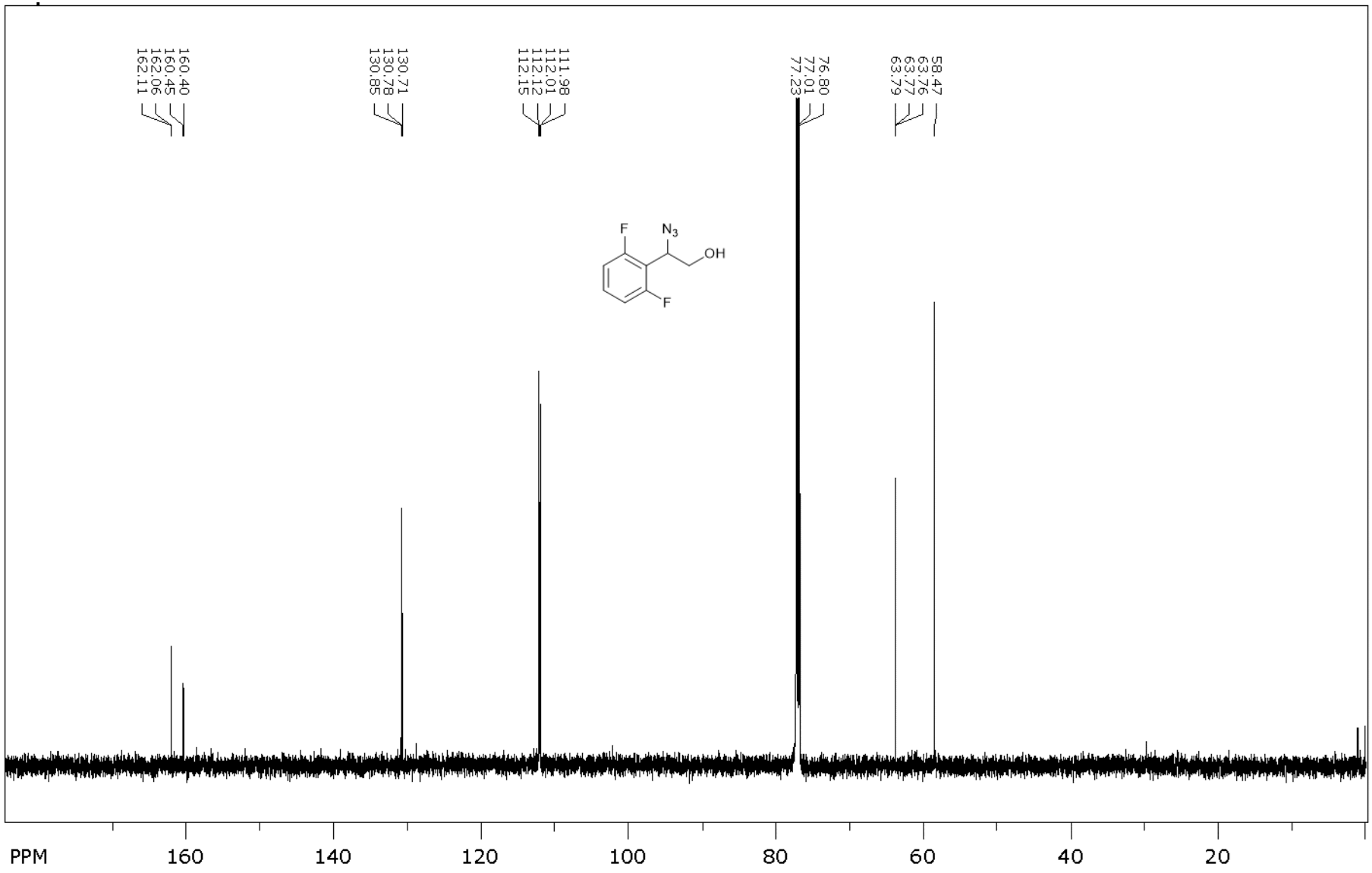
162.11
162.06
160.45
160.40
130.85
130.78
130.71
112.15
112.12
112.01
111.98
77.23
77.01
76.80
63.79
63.77
63.76
58.47
F
N3
OH
F
PPM
160
140
120
100
80
60
40
20

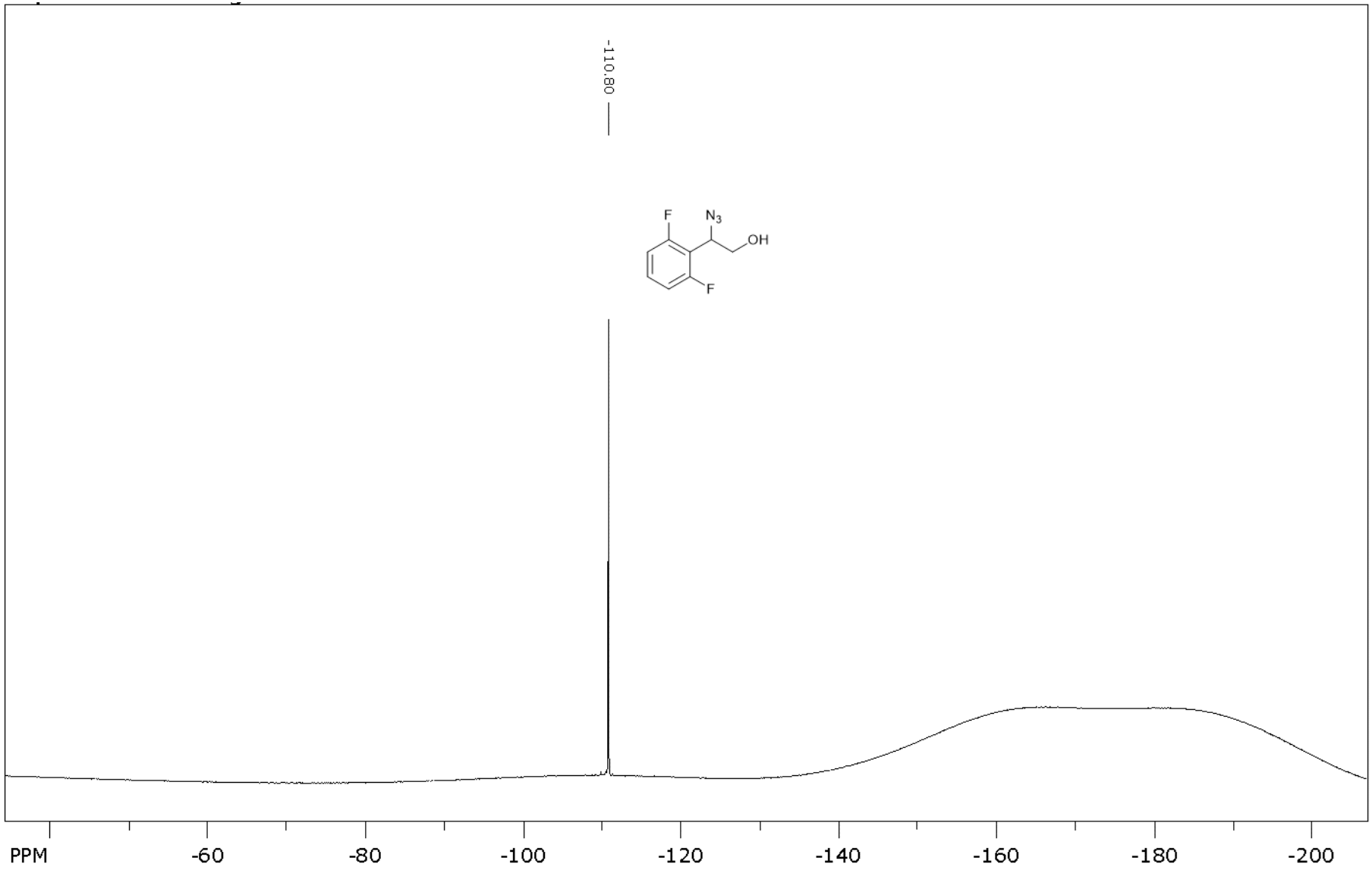
-110.80
F
N3
OH
F
PPM
-60
-80
-100
-120
-140
-160
-180
-200

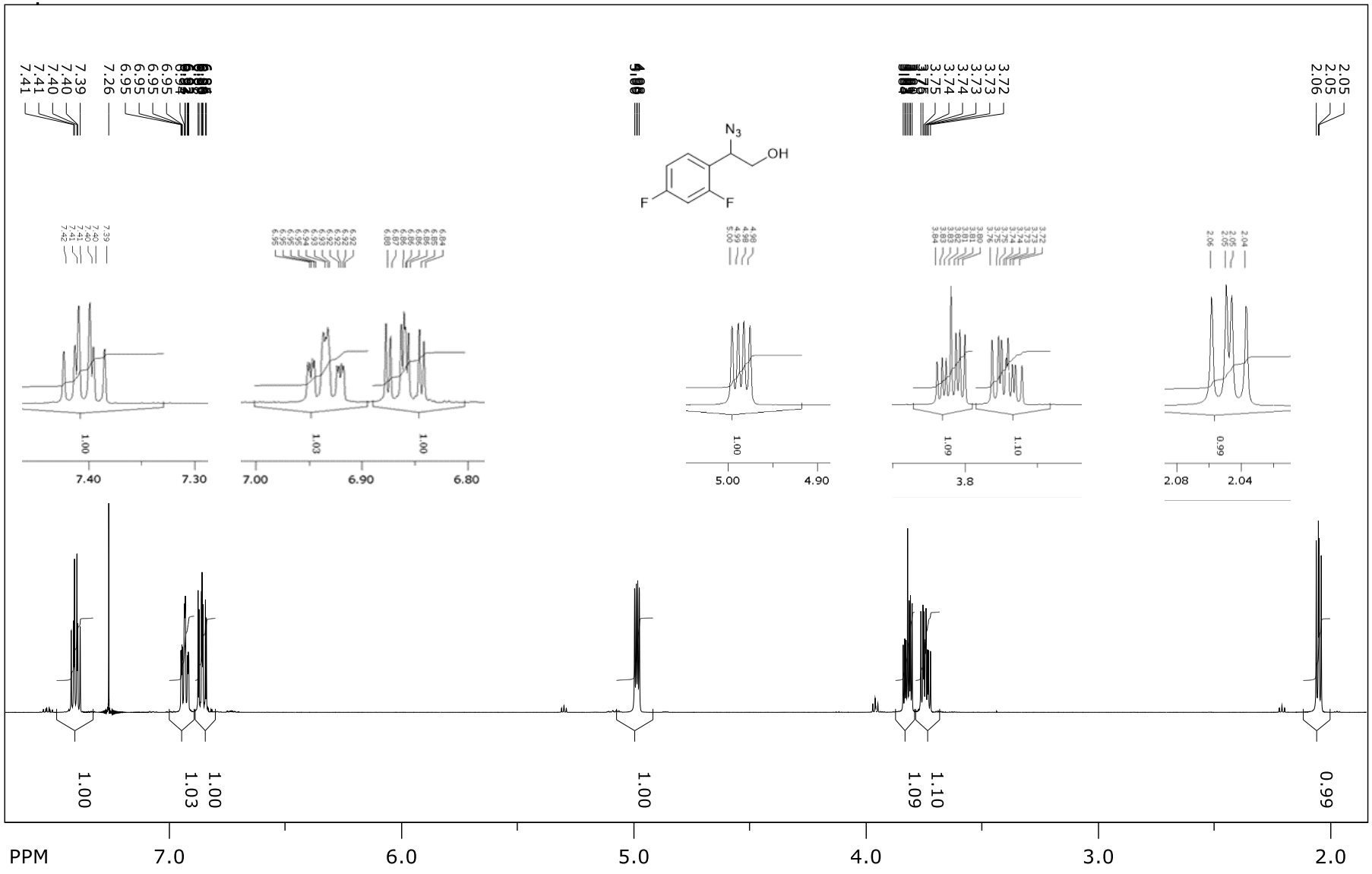
N3
OH
F
F
PPM
7.0
6.0
5.0
4.0
3.0
2.0
1.00
1.03
1.00
1.00
1.09
1.10
0.99

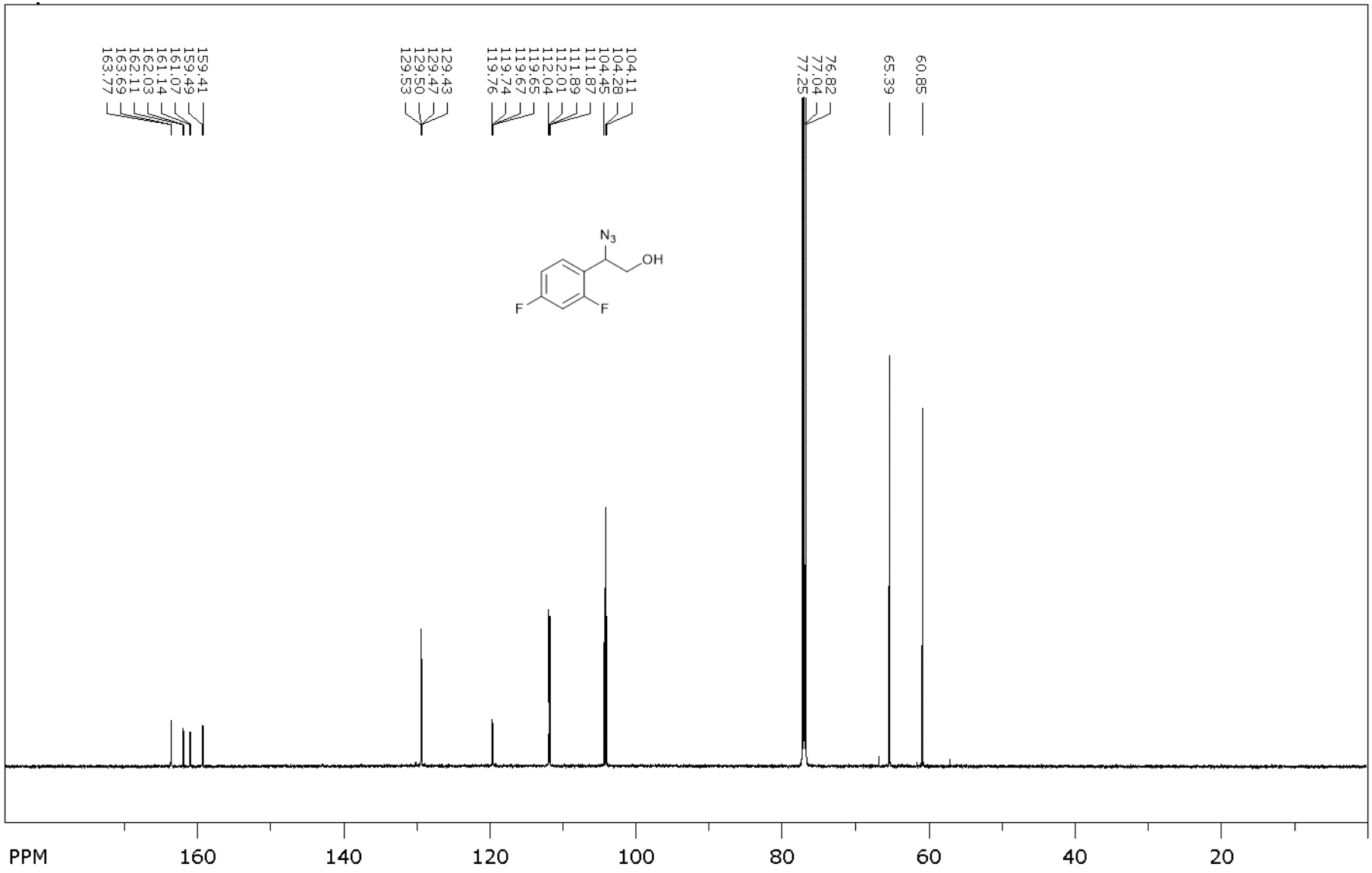
163.77
163.69
162.11
162.03
161.14
161.07
159.49
159.41
129.53
129.50
129.47
129.43
119.76
119.74
119.67
119.65
112.04
112.01
111.89
111.87
104.45
104.28
104.11
77.25
77.04
76.82
65.39
60.85
N3
OH
F
F
PPM
160
140
120
100
80
60
40
20

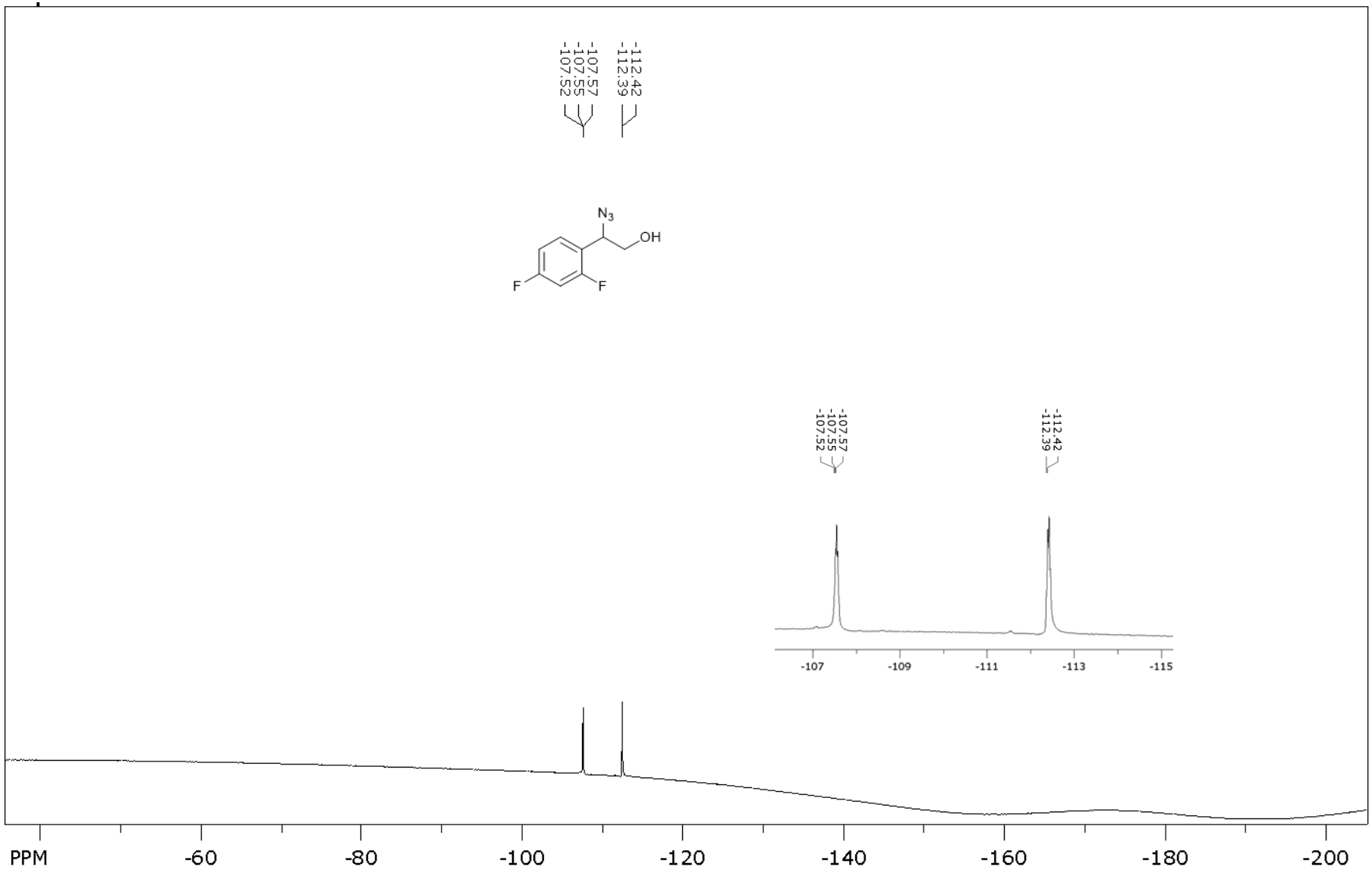
-107.52
-107.55
-107.57
-112.39
-112.42
N3
OH
F
F
-107
-109
-111
-113
-115
PPM
-60
-80
-100
-120
-140
-160
-180
-200

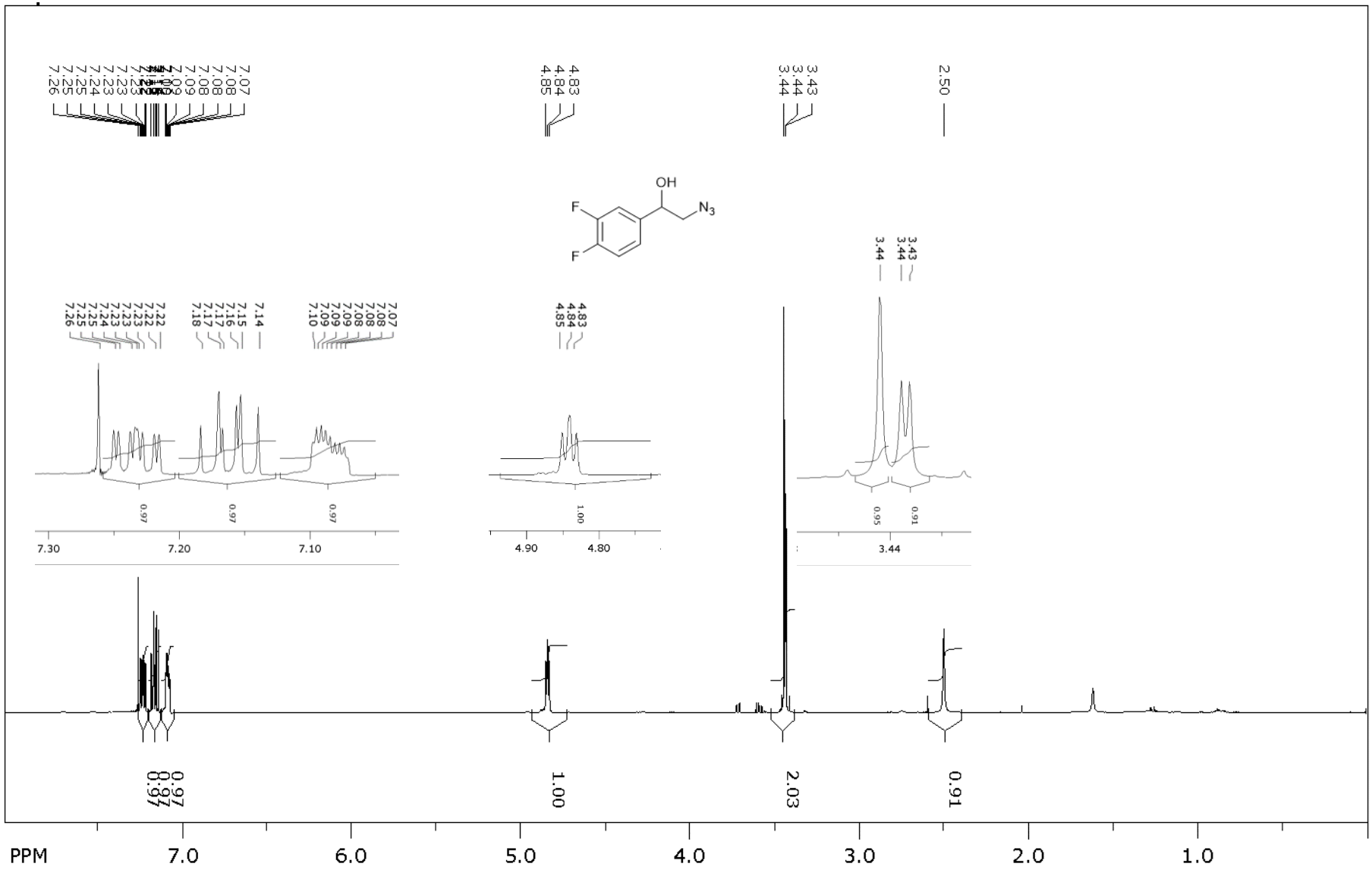
OH
F
F
N_3
7.30
7.20
7.10
4.90
4.80
3.44
PPM
7.0
6.0
5.0
4.0
3.0
2.0
1.0
0.97
0.97
1.00
2.03
0.91

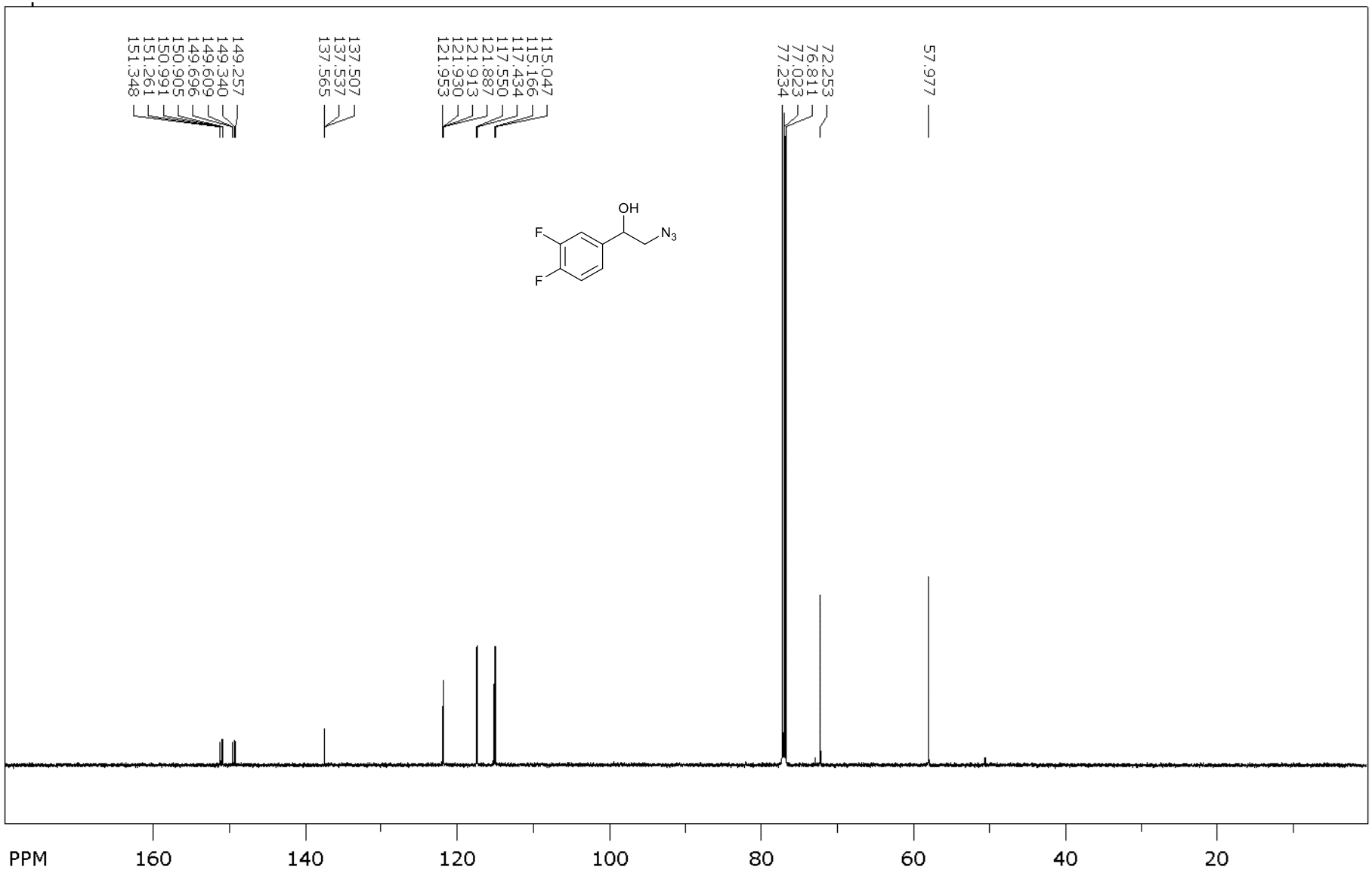
151.348
151.261
150.991
150.905
149.696
149.609
149.340
149.257
137.565
137.537
137.507
121.953
121.930
121.913
121.887
117.550
117.434
115.166
115.047
77.234
77.023
76.811
72.253
57.977
OH
F
F
N3
PPM
160
140
120
100
80
60
40
20

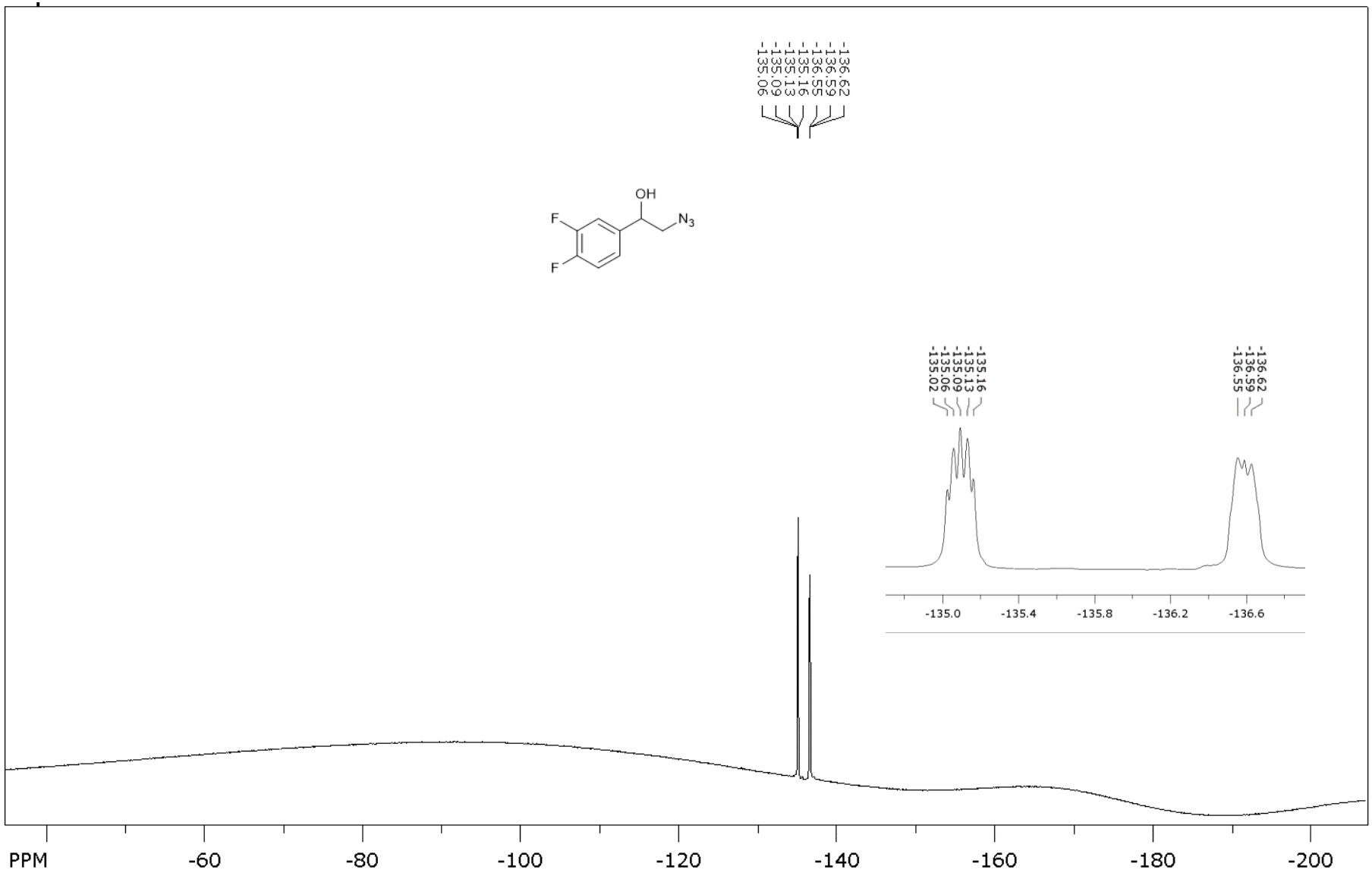
-135.06
-135.09
-135.13
-135.16
-136.55
-136.59
-136.62
OH
F
F
N_3
-135.02
-135.06
-135.09
-135.13
-135.16
-136.55
-136.59
-136.62
-135.0
-135.4
-135.8
-136.2
-136.6
PPM
-60
-80
-100
-120
-140
-160
-180
-200

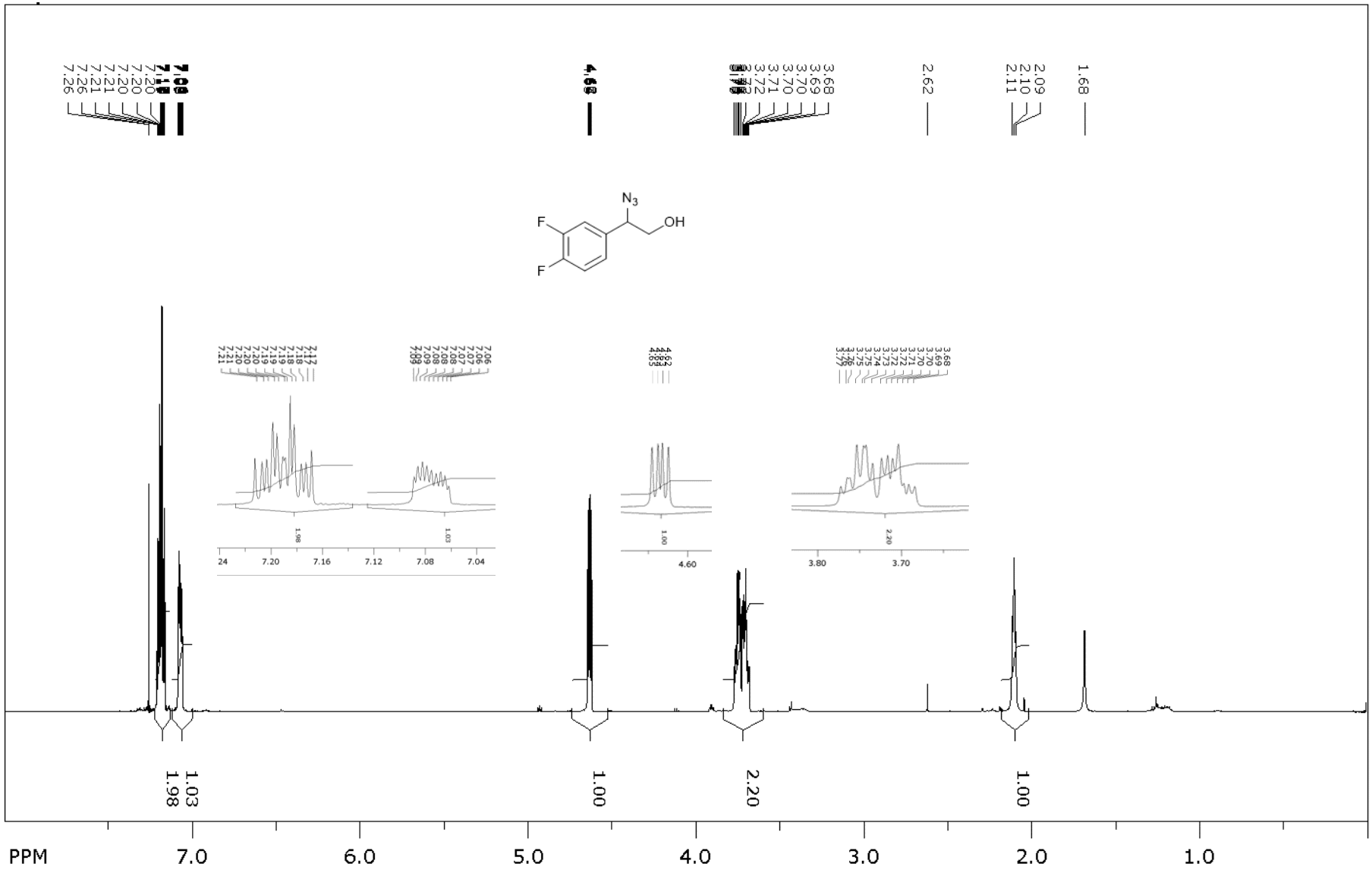
7.26
7.21
7.21
7.20
7.20
4.68
3.72
3.71
3.70
3.69
3.68
2.62
2.11
2.10
2.09
1.68
N3
OH
F
F
1.98
1.03
1.00
2.20
1.00
PPM
7.0
6.0
5.0
4.0
3.0
2.0
1.0

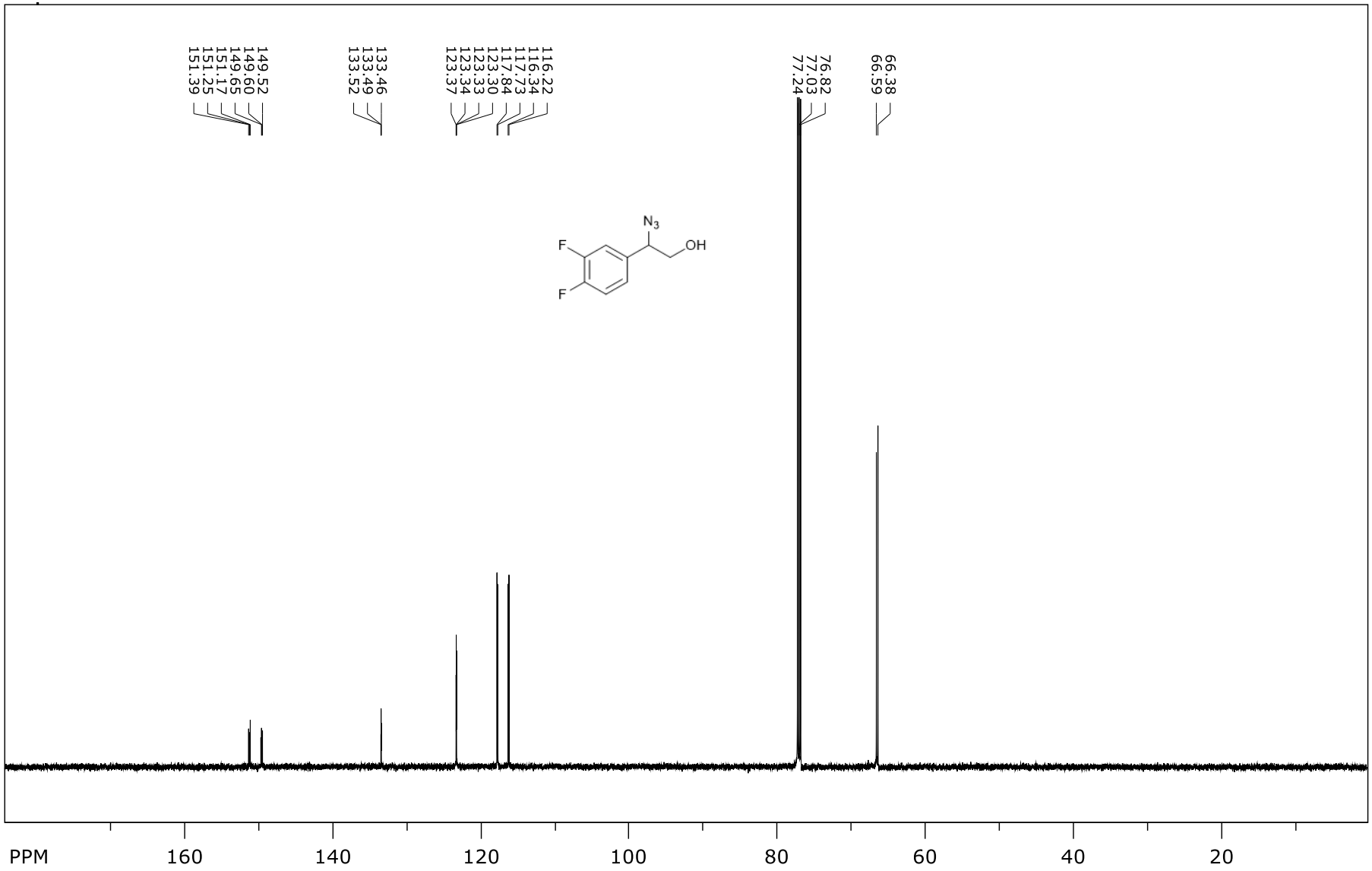
151.39
151.25
151.17
149.65
149.60
149.52
133.52
133.49
133.46
123.37
123.34
123.33
123.30
117.84
117.73
116.34
116.22
77.24
77.03
76.82
66.59
66.38
N3
OH
F
F
PPM
160
140
120
100
80
60
40
20

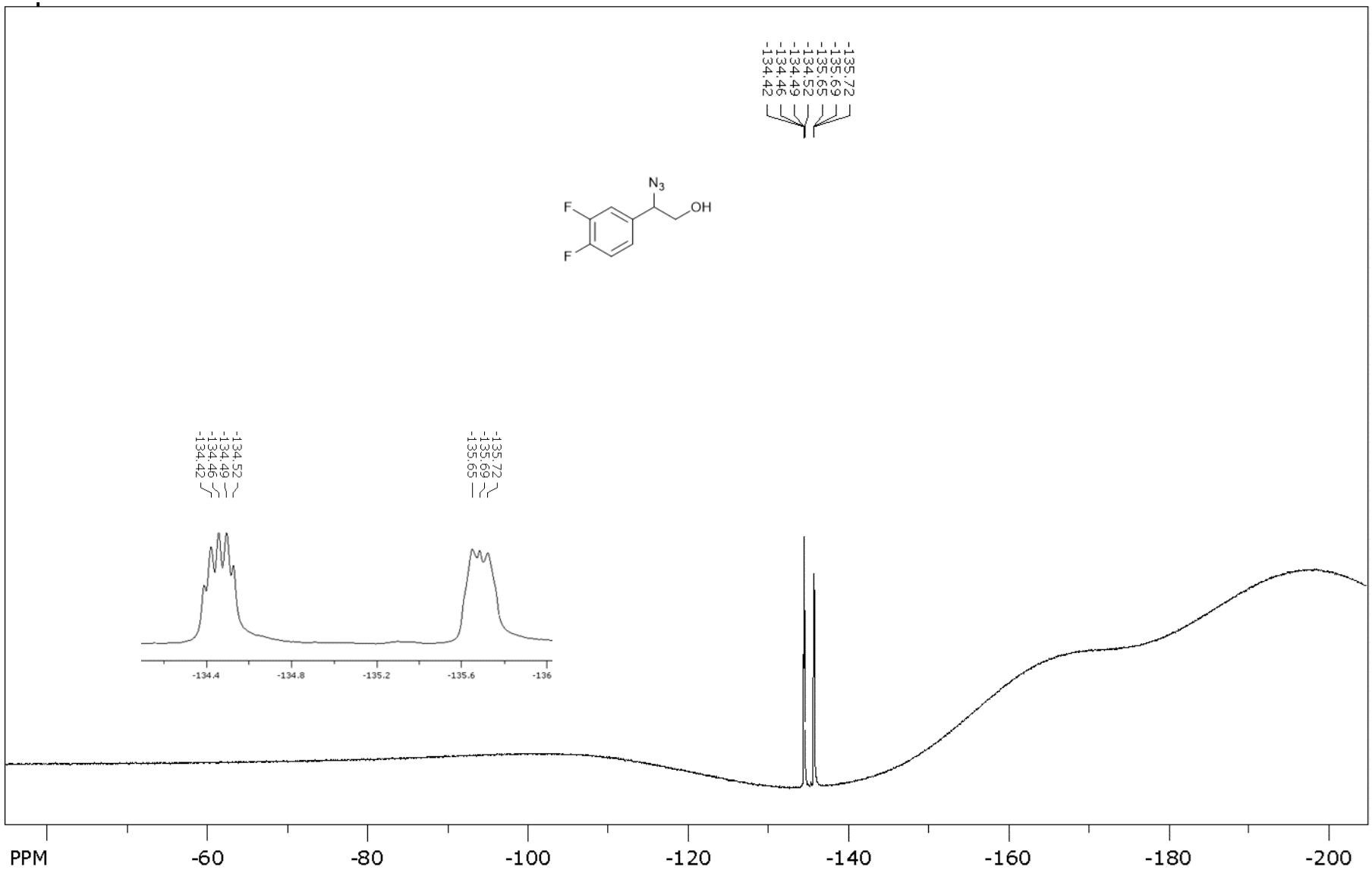
-134.42
-134.46
-134.49
-134.52
-135.65
-135.69
-135.72
N3
OH
F
F
-134.4
-134.8
-135.2
-135.6
-136
PPM
-60
-80
-100
-120
-140
-160
-180
-200

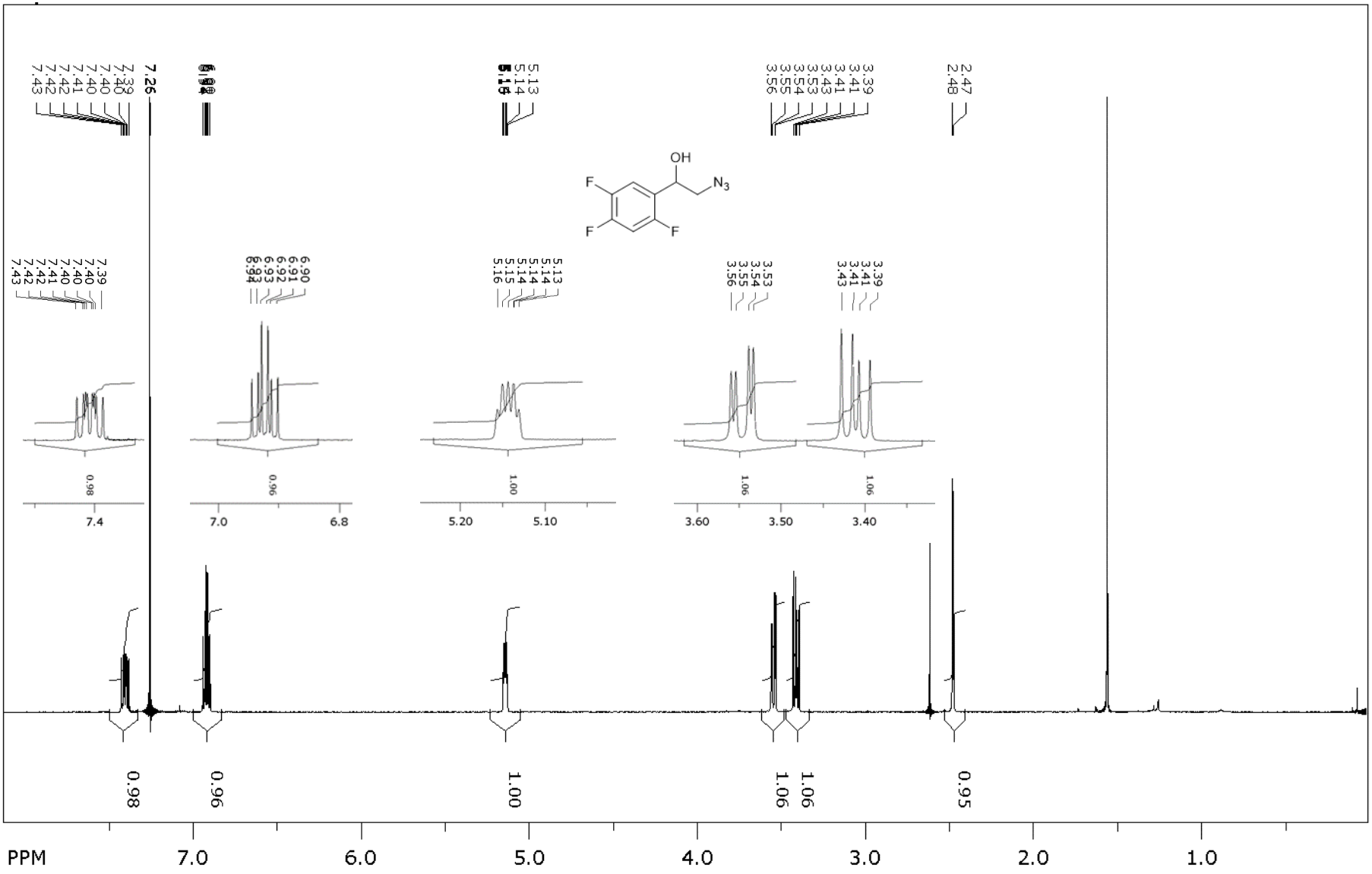
OH
F
F
F
N3
7.26
2.48
0.98
0.96
1.00
1.06
1.06
0.95
PPM
7.0
6.0
5.0
4.0
3.0
2.0
1.0

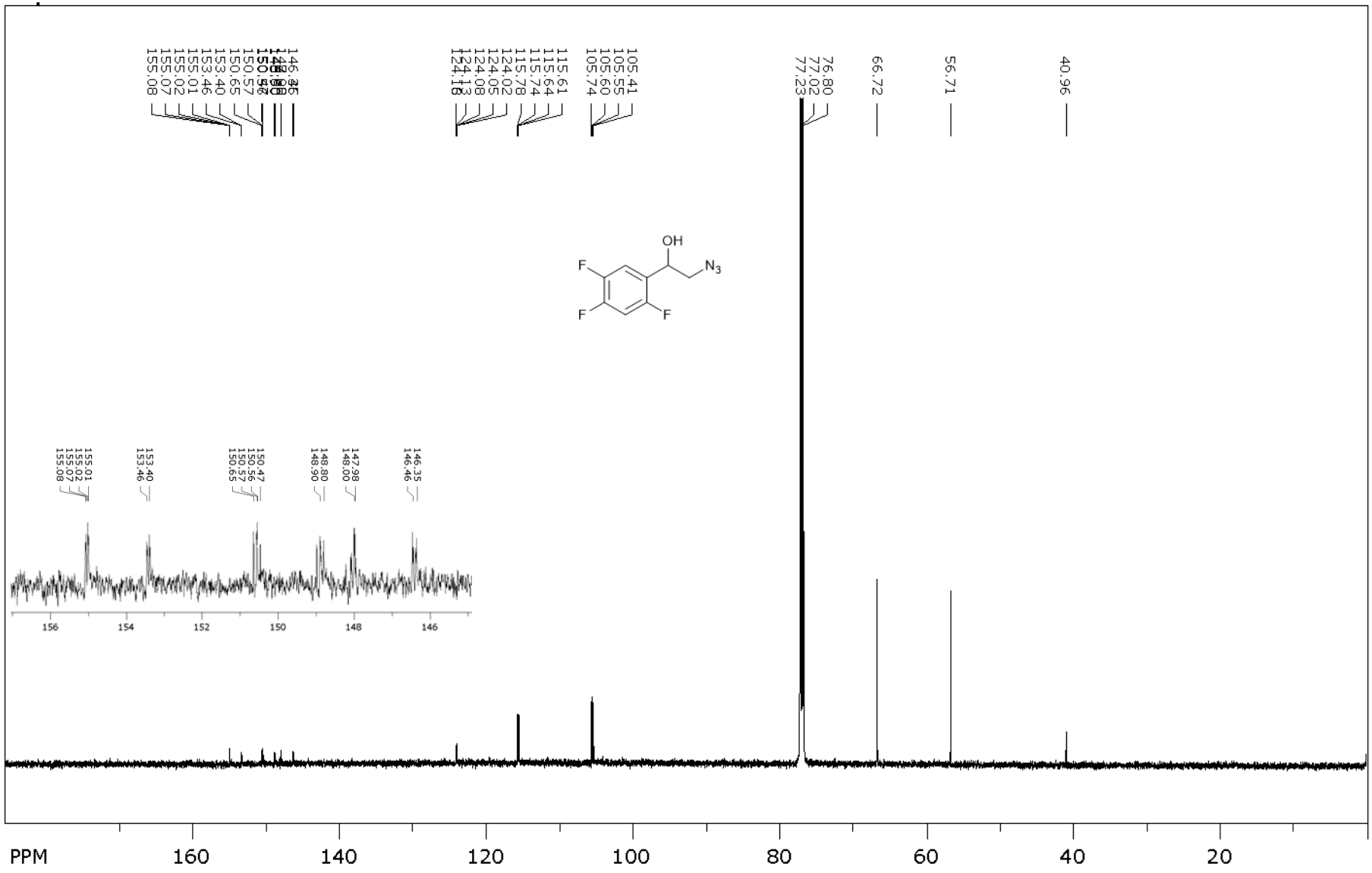
155.08
155.07
155.02
155.01
153.46
153.40
150.65
150.57
124.16
124.13
124.08
124.05
124.02
115.78
115.74
115.64
115.61
105.74
105.60
105.55
105.41
77.23
77.02
76.80
66.72
56.71
40.96
OH
N3
F
F
F
155.01
155.02
155.07
155.08
153.40
153.46
150.47
150.56
150.57
150.65
148.80
148.90
147.98
148.00
146.35
146.46
156
154
152
150
148
146
PPM
160
140
120
100
80
60
40
20

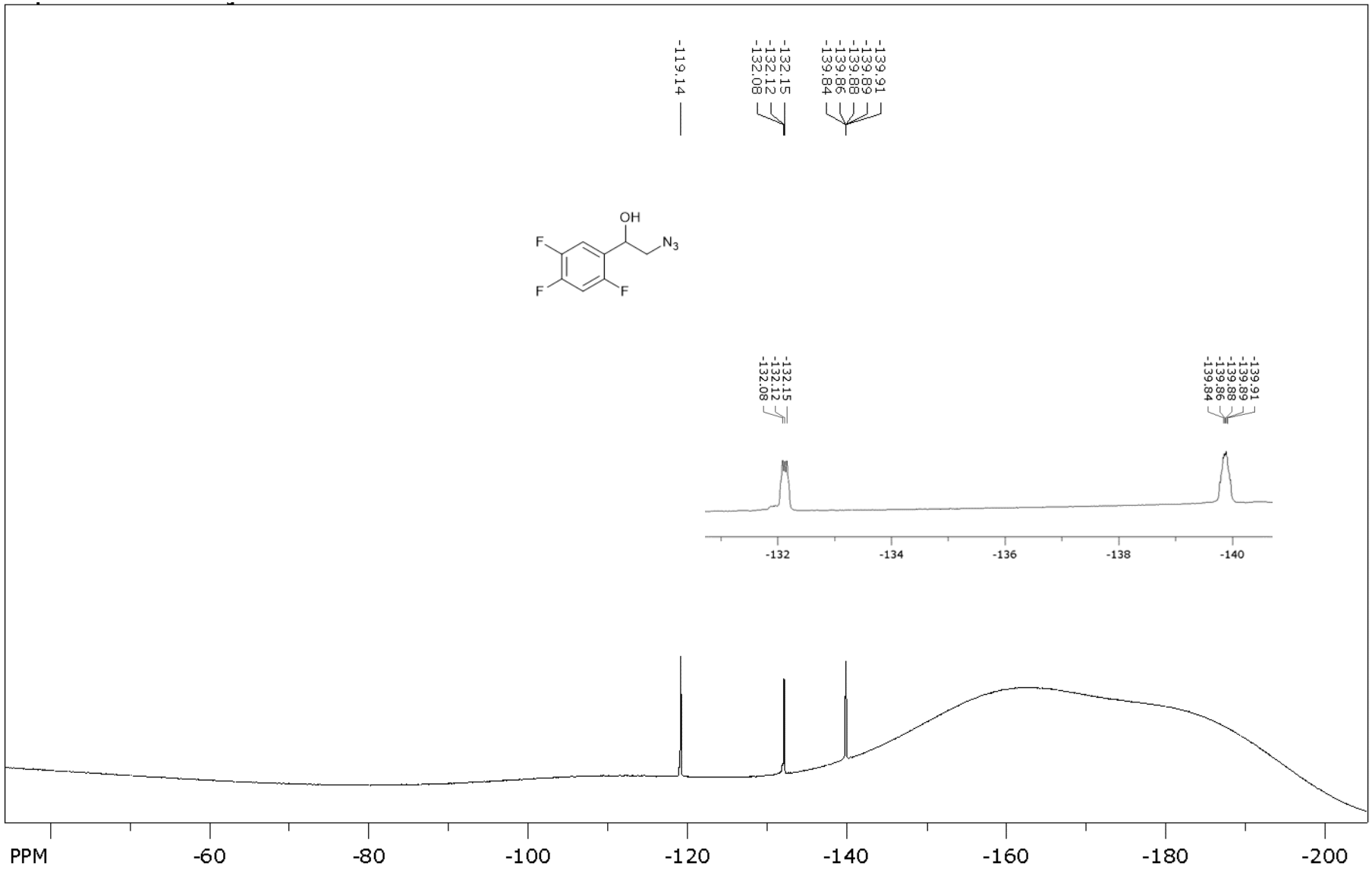
-119.14
-132.15
-132.12
-132.08
-139.91
-139.89
-139.88
-139.86
-139.84
OH
F
F
F
N_3
-132
-134
-136
-138
-140
PPM
-60
-80
-100
-120
-140
-160
-180
-200

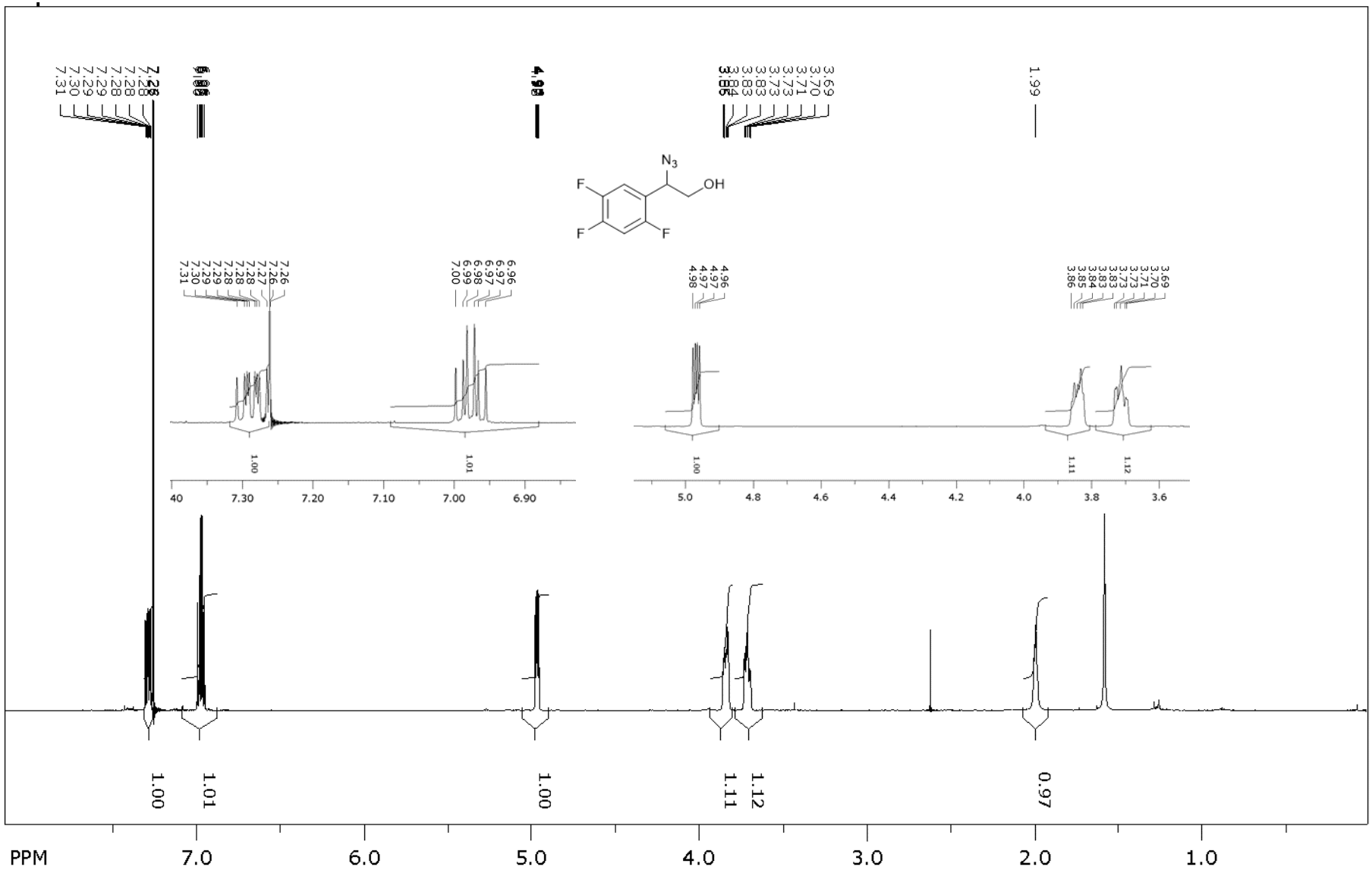
N3
OH
F
F
F
1.00
1.01
1.00
1.11
1.12
0.97
PPM
7.0
6.0
5.0
4.0
3.0
2.0
1.0

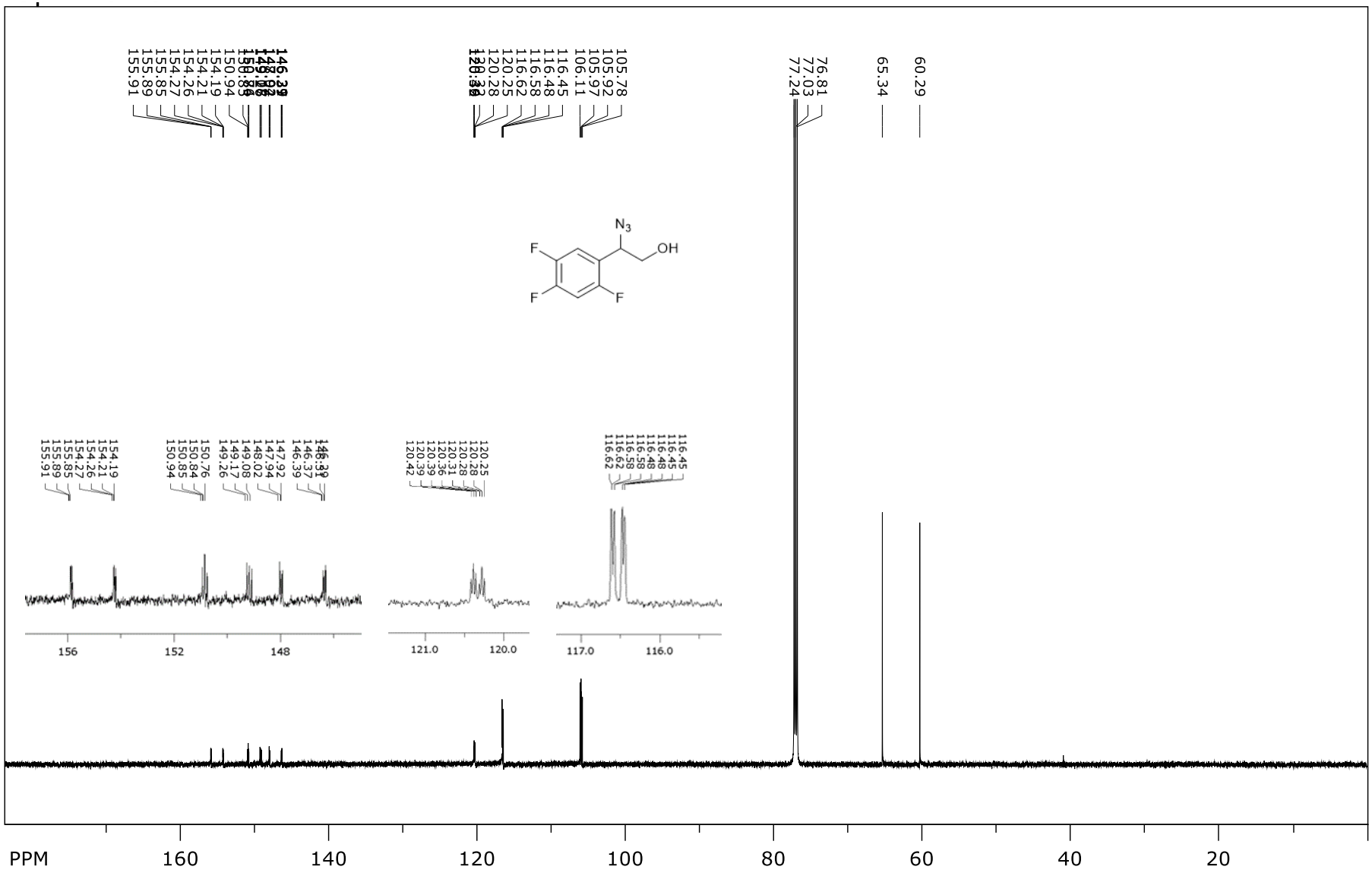
155.91
155.89
155.85
154.27
154.26
154.21
154.19
150.94
106.11
105.97
105.92
105.78
77.24
76.81
77.03
65.34
60.29
N3
OH
F
F
F
PPM
160
140
120
100
80
60
40
20

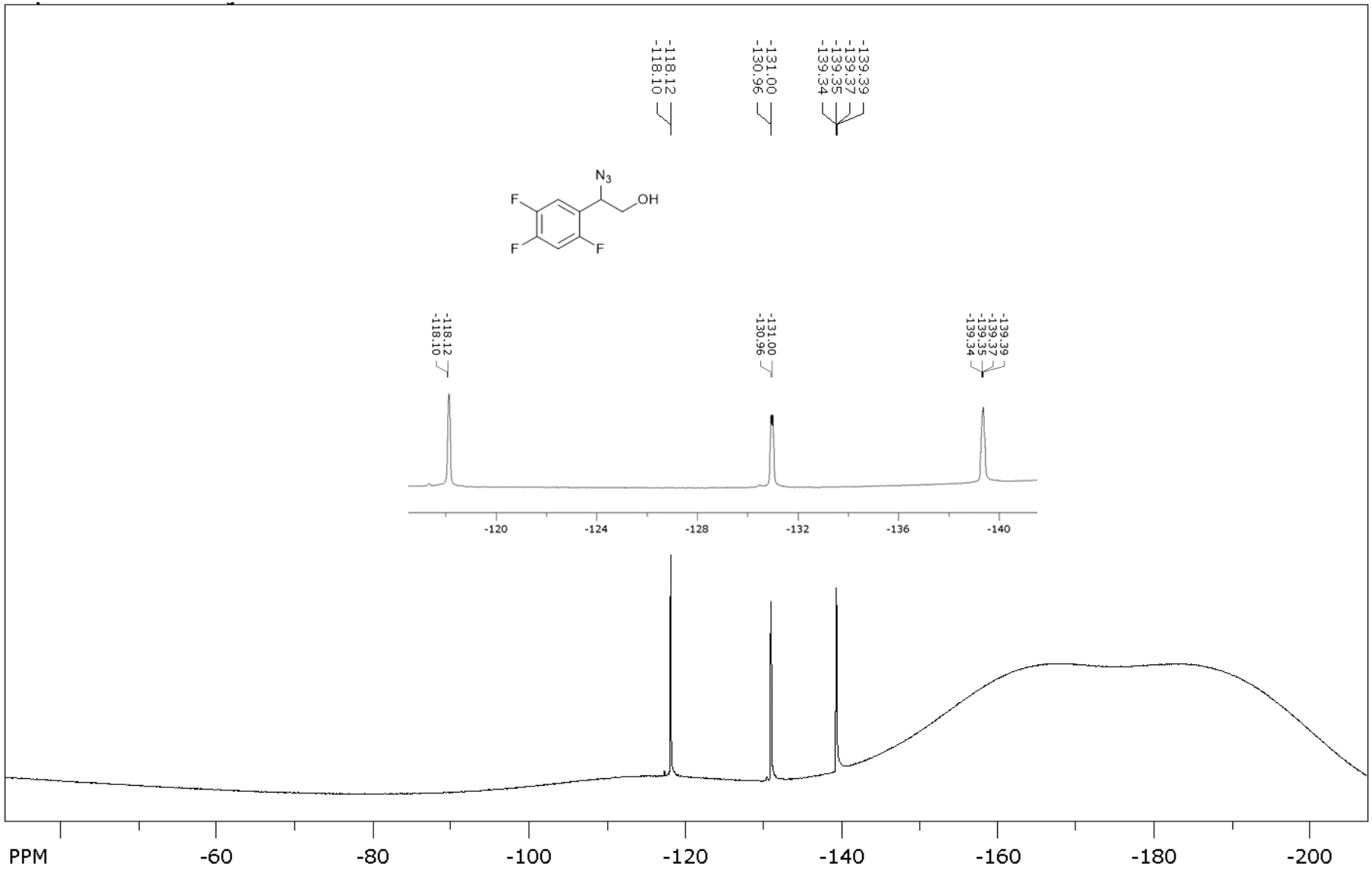
-118.12
-118.10
-131.00
-130.96
-139.39
-139.37
-139.35
-139.34
N3
OH
F
F
F
-120
-124
-128
-132
-136
-140
PPM
-60
-80
-100
-120
-140
-160
-180
-200

References

(1) Mehić, E.; Hok, L.; Wang, Q.; Dokli, I.; Miklenić, M. S.; Findrik Blažević, Z.; Tang, L.; Vianello, R.; Majerić Elenkov, M. Expanding the Scope of Enantioselective Halohydrin Dehalogenases – Group B. *Adv. Synth. Catal.* **2022**, (363), 388–410**.** https://doi.org/10.1002/adsc.202200342.

(2) Majerić Elenkov, M.; Primožič, I.; Hrenar, T.; Smolko, A.; Dokli, I.; Salopek-Sondi, B.; Tang, L. Catalytic Activity of Halohydrin Dehalogenases towards Spiroepoxides. *Org. Biomol. Chem.* **2012**, *10* (26), 5063–5072. https://doi.org/10.1039/c2ob25470k.

(3) Deregnaucourt, J.; Archelas, A.; Barbirato, F.; Paris, J. M.; Furstoss, R. Enzymatic Transformations 63. High-Concentration Two Liquid-Liquid Phase Aspergillus Niger Epoxide Hydrolase-Catalysed Resolution: Application to Trifluoromethyl-Substituted Aromatic Epoxides. *Adv. Synth. Catal.* **2007**, *349* (8–9), 1405–1417. https://doi.org/10.1002/adsc.200700085.

(4) Toda, H.; Imae, R.; Itoh, N. Efficient Biocatalysis for the Production of Enantiopure (*S*)-Epoxides Using a Styrene Monooxygenase (SMO) and Leifsonia Alcohol Dehydrogenase (LSADH) System. *Tetrahedron: Asymmetry* **2012**, *23* (22–23), 1542–1549. https://doi.org/10.1016/j.tetasy.2012.09.017.

(5) Tian, Y.; Jürgens, E.; Kunz, D. Regio- and Chemoselective Rearrangement of Terminal Epoxides into Methyl Alkyl and Aryl Ketones. *Chem. Commun.* **2018**, *54* (80), 11340–11343. https://doi.org/10.1039/C8CC06503A.

(6) Schirok, H. Microwave-Assisted Synthesis of N- *Sec* - and N- *Tert* -Alkylated Indoles. *Synthesis* **2008**, *2008* (9), 1404–1414. https://doi.org/10.1055/s-2008-1067005.

(7) Sone, T.; Yamaguchi, A.; Matsunaga, S.; Shibasaki, M. Catalytic Asymmetric Synthesis of 2,2-Disubstituted Terminal Epoxides via Dimethyloxosulfonium Methylide Addition to Ketones. *J. Am. Chem. Soc.* **2008**, *130* (31), 10078–10079. https://doi.org/10.1021/ja803864p.

(8) Dou, D.; He, G.; Li, Y.; Lai, Z.; Wei, L.; Alliston, K. R.; Lushington, G. H.; Eichhorn, D. M.; Groutas, W. C. Utilization of the 1,2,3,5-Thiatriazolidin-3-One 1,1-Dioxide Scaffold in the Design of Potential Inhibitors of Human Neutrophil Proteinase 3. *Bioorg. Med. Chem.* **2010**, *18* (3), 1093–1102. https://doi.org/10.1016/j.bmc.2009.12.057.

(9) Molinaro, C.; Guilbault, A. A.; Kosjek, B. Resolution of 2,2-Disubstituted Epoxides via Biocatalytic Azidolysis. *Org. Lett.* **2010**, *12* (17), 3772–3775. https://doi.org/10.1021/ol101406k.

(10) Wu, J.-F.; Wan, N.-W.; Li, Y.-N.; Wang, Q.-P.; Cui, B.-D.; Han, W.-Y.; Chen, Y.-Z. Regiodivergent and Stereoselective Hydroxyazidation of Alkenes by Biocatalytic Cascades. *iScience* **2021**, *24* (8), 102883. https://doi.org/10.1016/j.isci.2021.102883.

(11) Guy, A.; Doussot, J.; Garreau, R.; Godefroy-Falguieres, A. Selective Ring-Opening Reaction of Styrene Oxide with Lithium Azide in the Presence of Cyclodextrins in Aqueous Media. *Tetrahedron: Asymmetry* **1992**, *3* (2), 247–250. https://doi.org/10.1016/S0957-4166(00)80202-5.

(12) Wang, H.-Y.; Huang, K.; de Jesús, M.; Espinosa, S.; Piñero-Santiago, L. E.; Barnes, C. L.; Ortiz-Marciales, M. Synthesis of Enantiopure 1,2-Azido and 1,2-Amino Alcohols via Regio- and Stereoselective Ring-Opening of Enantiopure Epoxides by Sodium Azide in Hot Water. *Tetrahedron Asymmetry* **2016**, *27* (2–3), 91–100. https://doi.org/10.1016/j.tetasy.2015.12.002.

(13) Hsueh, N.-C.; Chan, C.-K.; Chang, M.-Y. BiI3 Mediated Difunctionalization of α-Methylstyrenes, Including Azidohydroxylation and Azidoiodination. *Tetrahedron* **2018**, *74* (9), 1002–1008. https://doi.org/10.1016/j.tet.2018.01.023.

(14) Ankati, H.; Yang, Y.; Zhu, D.; Biehl, E. R.; Hua, L. Synthesis of Optically Pure 2-Azido-1-Arylethanols with Isolated Enzymes and Conversion to Triazole-Containing β-Blocker Analogues Employing Click Chemistry. *J. Org. Chem.* **2008**, *73* (16), 6433–6436. https://doi.org/10.1021/jo8009616.

(15) Lebel, H.; Jacobsen, E. N. *Chromium Catalyzed Kinetic Resolution of 2,2-Disubstituted Epoxides*; *Tetrahedron Lett*., **1999**, (40), 7303–7306. https://doi.org/10.1016/S0040-4039(99)01502-6.

(16) Selectivity Program (Http://Biocatalysis.Uni-Graz.at/Enantio/Cgi-Bin/Enantio.Pl).

(17) Wang, H.-Y.; Huang, K.; de Jesús, M.; Espinosa, S.; Piñero-Santiago, L. E.; Barnes, C. L.; Ortiz-Marciales, M. Synthesis of Enantiopure 1,2-Azido and 1,2-Amino Alcohols via Regio- and Stereoselective Ring-Opening of Enantiopure Epoxides by Sodium Azide in Hot Water. *Tetrahedron: Asymmetry* **2016**, *27* (2–3), 91–100. https://doi.org/10.1016/j.tetasy.2015.12.002.

(18) Abraham, M. J.; Murtola, T.; Schulz, R.; Páll, S.; Smith, J. C.; Hess, B.; Lindahl, E. GROMACS: High Performance Molecular Simulations through Multi-Level Parallelism from Laptops to Supercomputers. *SoftwareX* **2015**, *1–2*, 19–25. https://doi.org/10.1016/j.softx.2015.06.001.

(19) Milčić, N.; Stepanić, V.; Crnolatac, I.; Findrik Blažević, Z.; Brkljača, Z.; Majerić Elenkov, M. Inhibitory Effect of DMSO on Halohydrin Dehalogenase: Experimental and Computational Insights into the Influence of an Organic Co-solvent on the Structural and Catalytic Properties of a Biocatalyst. *Chem. Eur. J.* **2022**, *28* (56) 28, e2022019. https://doi.org/10.1002/chem.202201923.

(20) de Jong, R. M.; Tiesinga, J. J. W.; Villa, A.; Tang, L.; Janssen, D. B.; Dijkstra, B. W. Structural Basis for the Enantioselectivity of an Epoxide Ring Opening Reaction Catalyzed by Halo Alcohol Dehalogenase HheC. *J. Am. Chem. Soc.* **2005**, *127* (38), 13338–13343. https://doi.org/10.1021/ja0531733.

(21) Maier, J. A.; Martinez, C.; Kasavajhala, K.; Wickstrom, L.; Hauser, K. E.; Simmerling, C. Ff14SB: Improving the Accuracy of Protein Side Chain and Backbone Parameters from Ff99SB. *J. Chem. Theory. Comput.* **2015**, *11* (8), 3696–3713. https://doi.org/10.1021/acs.jctc.5b00255.

(22) Joung, I. S.; Cheatham, T. E. Determination of Alkali and Halide Monovalent Ion Parameters for Use in Explicitly Solvated Biomolecular Simulations. *J. Phys. Chem. B* **2008**, *112* (30), 9020–9041. https://doi.org/10.1021/jp8001614.

(23) Darden, T.; York, D.; Pedersen, L. Particle Mesh Ewald: An *N*·log(*N*) Method for Ewald Sums in Large Systems. *J. Chem. Phys.* **1993**, *98* (12), 10089–10092. https://doi.org/10.1063/1.464397.

(24) Jones, G.; Willett, P.; Glen, R. C.; Leach, A. R.; Taylor, R. Development and Validation of a Genetic Algorithm for Flexible Docking. *J. Mol. Biol.* **1997**, *267* (3), 727–748. https://doi.org/10.1006/jmbi.1996.0897.

(25) Stank, A.; Kokh, D. B.; Fuller, J. C.; Wade, R. C. Protein Binding Pocket Dynamics. *Acc. Chem. Res.* **2016**, *49* (5), 809–815. https://doi.org/10.1021/acs.accounts.5b00516.

(26) PyMOL. L. Schrödinger, The {PyMOL} Molecular Graphics System, Version~2.3.2, 2015.

(27) Humphrey, W.; Dalke, A.; Schulten, K. VMD: Visual Molecular Dynamics. *J. Mol. Graph.* **1996**, *14* (1), 33–38. https://doi.org/10.1016/0263-7855(96)00018-5.

(28) Laskowski, R. A.; Swindells, M. B. LigPlot+: Multiple Ligand–Protein Interaction Diagrams for Drug Discovery. *J. Chem. Inf. Model.* **2011**, *51* (10), 2778–2786. https://doi.org/10.1021/ci200227u.